Fall 2020

Development of tools for water management in the Hatra watershed (Northwestern Iraq) using satellite technologies

Majid S. Mohamod

Department: Geosciences and Geological and Petroleum Engineering

DEVELOPMENT OF TOOLS FOR WATER MANAGEMENT IN THE HATRA

WATERSHED (NORTHWESTERN IRAQ) USING SATELLITE TECHNOLOGIES

by

MAJID SUEED MOHAMOD

A DISSERTATION

Presented to the Graduate Faculty of the

MISSOURI UNIVERSITY OF SCIENCE AND TECHNOLOGY

In Partial Fulfillment of the Requirements for the Degree

DOCTOR OF PHILOSOPHY

in

GEOLOGICAL ENGINEERING

2020

Approved by:

Katherine Grote, Advisor
David J. Rogers
David M. Borrok
Emitt C. Witt
Neil Anderson
Robert Tucker

PUBLICATION DISSERTATION OPTION

This dissertation consists of the following three articles, formatted in the style used by the Missouri University of Science and Technology:

Paper I: Pages 5-46, is intended for submission.

Paper II: Pages 47-77, is intended for submission.

Paper III: Pages 78-99, is intended for submission.

ABSTRACT

All around the world the demand for water is increasing, especially in arid and semi-arid regions, including Iraq which subject to continuous desertification that is worsening, more importantly the Jezira region in northwestern Iraq. Thus, it's crucial to have a better strategy for water management. One of these strategies is to promote groundwater recharge for restoring the aquifer depletion. The successful groundwater recharge is limited by some potential data such as the annual water budge and precipitation measurements. The atomospheric and hydrological observations are limited by sparse population which tends to be less in arid and semi-arid regions. Therefore, an alternative to the ground measurement of rainfall is needed. Satellite-based measurements limit the restriction of ground station. However, the satellite products have significant uncertainty. Therefore, seven precipitation estimates have tested against rain gauges in Orange County and Los Angeles County, California. In order to establish a water management strategy in Jezira region, annual water budget should be known, which could be measure through observational discharge station. Unfortunately, only few months of discharge was measured manually in the north Jezira, which Hatra subwatershed. Computer model was used to recover the streamflow measurement. The Soil and Water Assessment Tool (SWAT) was great candidate to overcome the problem. The observational data of stream discharge was used to calibrate the model. In conclusion, water management is possible in ungauged arid and semi-arid regions by using remote sensing data and computer modeling

ACKNOWLEDGMENTS

First, I would like to thank the Iraqi Ministry of Higher Education and Scientific Research (MOHESR) for giving me the opportunity to study in USA. I would like to express my deep gratitude and appreciation to my advisor, Dr. Katherine Grote for her tremendous support and guidance during my PhD. I also want to thank my co-advisor, Dr. J. David Rogers for providing his advice and insights. I would like to give my thanks to Dr. Norbert Maerz, my initial academic advisor at Missouri University S&T. A special thanks to my committee members; Dr. Neil Anderson, Dr. Emitt C. Witt, Dr. David Borrok, and Dr. Robert Tucker, for their valuable comments and suggestions. I would also like to express my love and gratitude for my parents and siblings in Iraq for their continuous support and to all my friends for their support.

TABLE OF CONTENTS

LIST OF ILLUSTRATIONS

LIST OF TABLES

1. INTRODUCTION

A lack of water resources has created challenges globally, which worsen in arid and semiarid regions. Arid and semiarid area characterize by having finite natural water resources, with surface runoff and precipitation varying greatly in time and space (Wheater, Mathias, & Li, 2010; Ribot, Magalhães, & Panagides, 2005; Watson & Zinyowera, 1996.).

Despite the need for hydrological data to improve water management, such data in arid and semiarid areas has been limited such as precipitation and watershed discharge data (Wheater, Sorooshian, & Sharma, 2007). (Jezira region). The lack of such hydroclimatic measurements limits the success of hydrological models (Kavetski, Kuczera, & Franks, 2006). To improve models of poorly or ungauged catchments, remote sensing data have been the alternative of in situ measurements (Tang, Gao, Lu, & Lettenmaier, 2009; Schmugge, Kustas, Ritchie, Jackson, & Rango, 2002; Pietroniro, & Prowse, n.d.).

Satellite-based precipitation methods overcome many of the limitations associated with ground-based data and are widely used in the scientific community (Adler et al., 2003; Ebert, 2005; Huffman et al., 2006; Ebert et al., 2007; Artan et al., 2007; Sawunyama and Hughes, 2008; Stisen and Sandholt, 2010). Although satellite-based precipitation estimates have significant advantages over ground-based techniques, they are not as accurate as rain gauge data (Tian and Peters-Lidard, 2010; Behrangi et al., 2011; Carrey, 2011; Sharifi, E, et. al. 2016). The error in satellite-based estimates of precipitation leads to the need for calibration, as this error adds significant uncertainty to hydrological models (Nijssen and Lettenmaier, 1997; Tian et al., 2010). Several studies have explained that the source of error could come from the sensor itself, while other errors could be generated by the algorithm used to estimate precipitation (Hong et al., 2007; Aghakouchak et. al., 2012). Many researchers have investigated the uncertainty in satellite-based precipitation (Bellerby and Sun 2005; Turk et al.,., 2008; Ebert et al.,., 2007; Habib et al.,., 2012; Bharti et al.,., 2015), and numerous studies have suggested improvements to the algorithms to enhance the satellite-based precipitation accuracy (Taylor 1997).

There is no ground-based or direct method to estimate water budget rather than the computer modeling to obtain the water balance in a watershed. As there are numerous hydrological models, choosing the right one is critical to making accurate hydrological predictions. Devia, Ganasri, and Dwarakish (2015) have examined the performance of various hydrological models (i.e. SWAT model). They concluded that the SWAT model could obtain good hydrological predictions with little direct calibration. In addition, several studies have proven the capability of SWAT to predict hydrological information in tropical regions with sparse data (Nyeko, 2015; Näschen et al., 2018, Suliman et. al., 2015; Wagner et. al., 2013; Srinivasan et. al., 2010; Noori & Kalin, 2016; Rafiei Emam et al., 2017). In this study, remotely sensed datasets were input into the SWAT model to estimate the historical surface runoff in poorly gauged Hatra sub-watersheds. Within the region of study, local runoff during the wet season is the main source of surface water, which contributes to small, local floods. In the absence of continuous in situ observations in the area, the SWAT model was calibrated against three months of observational data. After the volume of the possible water supply is determined, the model must estimate how much of this water can be stored for future use.

Given the arid climate in the study site, promoting groundwater recharge during the wet season for later extraction during the growing season may be one method limiting evaporative losses and providing a longer-term groundwater supply (Gale 2005, Dillon et al. 2009; Maliva and Missimer 2012; O'Leary et al. 2012, Russo, Fisher, and Lockwood 2015, Das and Pardeshi 2018),) One of the advantages of ground storage is limiting water losses by evaporation as well as improve groundwater quality (Russo, Fisher, and Lockwood 2015) (Ma and Spalding 1997). Understanding the infiltration rates for groundwater recharge will also help determine the need for supplemental water storage using surface impoundments. better water management in such regions are crucial and have been improving constantly,one of these practices is to promote groundwater recharge during the wet season for later extraction during the drought time.

Success groundwater recharge project is depending totally on how accurate the groundwater potential delineation (Ahmadi, Mahdavirad, and Bakhtiari 2017). Indicating suitable zones for groundwater recharge through traditional methods by using field testing is difficult and time consuming as groundwater is subsurface flow, it will require numerous field measurements in this matter. For these reasons, using the indirect method to locate groundwater potential zones is more efficient, which relies on analysis several satellite-derived surface features data such as soil texture, drainage pattern and density, lineament features, landuse and land cover, surficial lithology, and some satellite-based precipitation measurements (Sander et al. 1996; Nag 2005; Sener et al. 2005; Solomon and Quiel 2006;Ahmed, Jayakumar, and Salih 2008 ; Ganapuram et al. 2009; Singh et al.

2011b; Magesh et al. 2012; Mukherjee et al. 2012; Russo, Fisher, and Lockwood 2015; Russo, Fisher, and Lockwood 2015; Ahmadi, Mahdavirad, and Bakhtiari 2017;Das et al. 2017, 2018; Das and Pardeshi 2018b). Many hydrogeomorphology features can be processed and integrated into variety hydrogeomorphology thematic layers, to identify groundwater potential zones with accuracy and time-consuming efficiency, (Tiwari et al. 2017). (Bhowmick, Mukhopadhyay, and Sivakumar 2014) (Tiwari et al. 2017) (Bhowmick, Mukhopadhyay, and Sivakumar 2014). Several studies have applied remote sensing and GIS techniques to delineate groundwater potential zones all over the world (Raj and Sinha, 1989; Champati et al., 1993; Krishnamurththyet al., 1996; Saraf and Chaudhary, 1998; Shahid et al., 2000). , Jaiswal, 2003) Solomon and Quiel 2006; Agarwal, P. K. Garg and R. D. Garg.

PAPER

I. EVALUATION OF THE ACCURACY OF DIFFERENT SATELLITE-BASED ESTIMATES OF PRECIPITATION IN A SEMI-ARID CLIMATE

Majid S. Mohamod1, 2 and Katherine Grote1

Department of Geosciences and Geological and Petroleum Engineering, Missouri University of Science and Technology, McNutt Hall, 1400 N. Bishop Ave, Rolla, MO 65401, USA,

College of Science, University of Tikrit, Salahdin, Iraq

ABSTRACT

Satellite data play a significant role in hydrological studies and provide an important source of continuous precipitation data that can be used to study regions without ground-based precipitation measurements. The high temporal resolution, comprehensive spatial coverage, and availability of satellite data are significant advantages of satellite-based precipitation estimates. However, there is still significant uncertainty about the accuracy of these data, and calibration for specific climates and latitudes is often needed. This study explores the accuracy of different satellite-based estimates of precipitation in a semi-arid environment that is very similar to that in much of the Middle East, which is a region where satellite data are especially important for hydrologic studies. In this study, precipitation estimates from Global Precipitation Measurement (GPM), Multi-satellite Precipitation Analysis (TRMM 3B42), Global Satellite Mapping of Precipitation (GsMaP MVK), Climate Forecast System Reanalysis (CFSR), and Estimation from Remotely Sensed Information using Artificial Neural

Networks (PERSIANN, PERSIANN-CCS and PERSIANN-CDR) were compared to ground-based measurements on daily, bi-weekly, and monthly scales over a time period ranging from 2012 to 2016. The study area is located within Orange County and Los Angeles County, California, and has 15 ground-based weather stations that have daily data over this time period. Statistical analyses between ground-based and satellite-based precipitation data show that daily correlations between the two data types were typically poor. As expected, both bi-weekly and monthly satellite-based data showed higher correlations with ground-based measurements than did daily data. Of the different precipitation estimate techniques, TRMM data were the most accurate for all time intervals when different types of error or correlation were considered, while the CFSR and GsMaP were the least accurate.

1. INTRODUCTION

Measurements of precipitation are vital to understanding and solving important societal problems, especially in arid climates. Precipitation measurements are core to a variety of scientific applications including climate change modeling, hydrological modeling, and drought and flood forecasting. The timing and intensity of precipitation are also critical for water budget analyses, including partitioning precipitation into groundwater recharge or surface runoff (Blacutt, et. al., 2015; Sikorska and Seibert, 2015). The accuracy of the precipitation estimates used in these models and analyses is important for obtaining reliable results (Meng et al., 2002; Sorooshian et al., 2005).

Precipitation has historically been measured using ground-based methods such as rain gauges. Rain gauges are one of the most accurate methods for precipitation measurement, but the scarcity of ground stations, particularly in areas with sparse populations or political unrest, limits the availability of rain gauge data in some locations. It is also difficult to place rain gauges in complex terrain such as mountainous regions or in areas with large surface water bodies. These limitations restrict the use of rain gauges for obtaining precipitation measurements with high spatial and temporal resolution in some regions. Satellite-based precipitation methods overcome many of the limitations associated with ground-based data and are widely used in the scientific community (Adler et al., 2003; Ebert, 2005; Huffman et al., 2005; Ebert et al., 2007; Artan et al., 2007; Sawunyama and Hughes, 2008; Stisen and Sandholt, 2010). Satellite-based precipitation measurements are based on statistical analyses of cloud characteristics obtained from visible and thermal IR imagery at different elevations (Arkin, 1979; Arkin, et. al. 1987; Arkin, et. al. 1989). Some satellite-based precipitation products (e.g. CFSR) also use ground-based measurements to calibrate the satellite estimates. Global satellite coverage is obtained through the combination of several satellites monitoring simultaneously at different places around the globe. The coarsest spatial resolution from satellite data is approximately 0.5 degrees, and data are typically recorded every hour (Tian et. al., 2009).

Although satellite-based precipitation estimates have significant advantages over ground-based techniques, they are not as accurate as rain gauge data (Tian and Peters-Lidard, 2010; Behrangi et al., 2010; Carrey, 2011; Sharifi, E, et. al. 2016). The error in satellite-based estimates of precipitation leads to the need for calibration, as this error adds significant uncertainty to hydrological models (Nijssen and Lettenmaier, 2004; Tian et al., 2010). Several studies have explained that the source of error could come from the sensor itself, while other errors could be generated by the algorithm used to estimate precipitation (Hong et al., 2006; Aghakouchak et. al., 2012). Many researchers have investigated the uncertainty in satellite-based precipitation (Bellerby and Sun 2005; Turk et al.,., 2008; Ebert et al.,., 2007; Habib et al.,., 2012; Bharti et al.,., 2015), and numerous studies have suggested improvements to the algorithms to enhance the satellite-based precipitation accuracy (Taylor 1999). As satellite data are collected and aggregated at different temporal and spatial resolutions, these studies can be broadly classified by resolution. As upscaling and interpolation techniques are often used to address the differences in spatial resolution, we have considered studies based on their temporal resolution. Although there is a wide range of studies and satellite data used, note that most of these studies were performed in subtropical, tropical, temperate, or alpine climates, so an analysis focusing on arid regions is still needed.

Several studies have analyzed satellite-based precipitation estimates with daily temporal resolution. Tang et. al. (2016) investigated the accuracy of the satellite-based Global Precipitation Measurement (GPM) mission Integrated Multi-Satellite Retrievals for GPM (IMERG), Multi-satellite Precipitation Analysis (TMPA 3B42V7), and the Tropical Rainfall Measuring Mission (TRMM 3B42RT) over the Ganjiang River basin in southeast China, which has a subtropical, humid monsoon climate. The analysis was conducted on daily basis with 0.25° spatial resolution, from May to September 2014. A standard bilinear interpolation method was used to grid 0.1° x 0.1° satellite weather stations. The results show that the three products have approximately the same correlation coefficient against the rain gauges; these coefficients range between 0.63 and 0.87. TRMM Multi-Satellite Precipitation Analysis (TMPA) was analyzed on a daily scale with a spatial resolution of 0.25° by Scheel et al., (2011) to evaluate its ability to estimate the rainfall rates in the Central Andes, which have a warm temperate climate with dry winters and wet summers. In this study, contingency and statistical analyses (bias, root mean square error (RMSE), and Pearson's correlation coefficient) methods were used to evaluate the TMPA data. The results show that TMPA has large biases within the daily scale, but the bias decreases significantly at the monthly scale. Duan et al., (2016) evaluated eight high resolution precipitation products, including TRMM, CMORPH (the Climate Prediction Center MORPHing technique), CMORPH_RAW, CMORPH_CRT and CMORPH_BLD, PGF (Global Meteorological Forcing Dataset for land surface modelling), PCDR (Precipitation Estimation from Remotely Sensed Information using Artificial Neural Networks-Climate Data Record), CHIRPS (Climate Hazards Group InfraRed Precipitation with Station data) and GSMaP_MVK (Global Satellite Mapping of Precipitation) over complex topography in Adige Basin (Italy) on a daily scale. This study area also has wet summers and dry winters. They concluded that CMORPH_BLD and TRMM had better correlation coefficients with rain gage data than did PGF data. Liu, et al., (2016) used the Soil and Water Assessment Tool (SWAT) to evaluate PERSIANN-CDR and Global Land Data Assimilation System (GLDAS) precipitation in the northern Tibetan Plateau, China. This region has a climate of summer monsoons. The simulated streamflow from SWAT indicates that both products have the high-level capability for hydrological predications. A similar study was conducted by Fuka, et al., (2014) to evaluate CFSR data to predicate historical streamflow of five watersheds using the SWAT model. These watersheds are located within a variety of climate types and ground elevations. They concluded in this study that simulated streamflow accurate as the rainfall gauges. CFSR and TRMM 3B42V7 were also used in a hydrological model Hydrologiska Byråns Vattenbalansavdelning (HBV) and Parameter Efficient Distributed (PED) in Upper Blue Nile Beles, (Worqlul et al., 2017), and they found that both data types were able to predicate streamflow in both locations.

Many studies have also been performed using total precipitation received each month. On a monthly time scale, Fengrui and Xi (2016) have concluded in a study within several climate zones (tropical, subarctic, and alpine) over China's mainland that GPM data have better estimations of rainfall than TRMM; however, GPM had a poor performance during winter time. Another study conducted by Pfeifroth et al.,., (2013) examined four satellite-based weather precipitation products: European Centre for Medium-Range Weather Forecasts (ERA-Interim), Global Precipitation Climatology Centre (GPCP), NASA's Modern-Era Retrospective Analysis for Research and Applications (MERRA), and Hamburg Ocean Atmosphere Parameters and Fluxes from Satellite Data (HOAPS) against ground-based measurements acquired in the tropical Pacific Database (PACRAIN) by dividing the study area into gridded boxes of 2.58° latitude-longitude resolution. The results show that GPCP data have the best correlation and lowest bias on a monthly scale.

Some studies have been performed using a variety of time scales. A study was applied over mountainous terrain in the western Black Sea area of Turkey by Derin and Yilmaz (2014). Two types of climate exist in this region, depending on the orographic location. The windward side of the mountains is classified as a mid-latitude humid temperate climate, while the leeward side is classified as a dry/sub-humid continental climate. Four satellite-based products were examined: TRMM-3B42v7, TMPA near-real-time (7RT) and post-real-time (7A), CMORPH, and the Multi-Sensor Precipitation Estimate (MPE) of the European Organization for the Exploitation of Meteorological Satellites (EUMETSAT). The study was conducted using daily, monthly, seasonal, and annual scales for the period 2007-2011. The authors concluded that the satellite-based precipitation estimates have different levels of accuracy based on the region of the mountain and the season. TMPA-7A, TMPA-7RT products typical under-forecast along the region of windward slopes and over-forecast within leeward regions, especially during the periods of colder weather. CMORPH data always under-forecast in windward and leeward slopes during all seasons. TRMM shows better performance among other satellite estimates on monthly scales for both regions and seasons. Overall, all satellite estimates products tend to overestimate monthly precipitation except CMORPH. Satellite daily estimates were less accurate than those taken on a monthly time scale. In another study, Zambrano-Bigiarini et al., (2016) evaluated seven satellite-based precipitation measurements (CHIRPSv2, TMPA 3B42v7, PERSIAN-CCS, MSWEPv1.1, CMORPH, PERSIANN-CDR, and PGFv3) acquired over 11 climates types ranging from polar/tundra to hot desert in Chile and compared them to measurements recorded at 366 ground stations on a daily, monthly, seasonal, and annual basis. Point-based rain gauge comparison was applied using the bilinear interpolation method by upscaling the satellite-based pixel to 0.25° (Hijmans, 2016). Results show that the satellite-based precipitation estimates predict rainfall within the humid climate regions better than they do in the arid regions of the study area, and all techniques were better at determining whether precipitation occurred than in estimating precipitation intensity. Overall, PGFv3 data were the most accurate, followed by CHIRPSv2, 3B42v7, and MSWEPv1.1, for all time scales except the annual scale. The least accurate precipitation estimates were generated by CMORPH, PERSIANN-CCS-Adj, and PERSIANN-CDR. Zhu et al.,(2016) was analyzed three satellite-based rainfall products: PERSIANN-CDR, TRMM 3B42v7, and CFSR on daily and monthly scales over humid climate in China. SWAT was used to test their performance in hydrological predication. The results indicate that TRMM 3B42V7 has better performance on monthly scales, meanwhile, the other two products showed better hydrological predication on daily basis.

In the studies identified in this literature review, estimates of precipitation from GPM IMERG and TRMM 3B42V7 were typically the most accurate. However, problems have been noted with GPM-based precipitation estimates during winter months in tropical, subarctic, and alpine climate zones. TRMM data tend to have more bias on a daily scale than do GPM data, although these bias decreases noticeably on a monthly scale. In the studies cited, TRMM products typically under-forecast in mid-latitude humid climate zones and over-forecast within dry/sub-humid continental climate regions, especially during the winter. PERSIANN-CCS and PERSIANN-CDR data did not perform as well as GPM or TRMM techniques, and the accuracy of TRMM data within arid climates was notably poorer than in humid climate zones.

In this study, we seek to better understand the accuracy and the uncertainties of satellite-based precipitation products in mid-latitude arid regions over a range of time scales. We compare satellite data with ground-based rainfall measurements on a daily, bi-weekly, and monthly basis to understand the limitations of each data set. Several techniques have been used in this study to investigate the bias and uncertainty of satellite-based precipitation estimates as a function of temporal resolution in an arid climate.

2. STUDY AREA LOCATION AND CLIMATE

The study area is located in southeastern California (Figure 1), in Los Angeles and Orange Counties. This study area was chosen because it has a similar climate (arid to semi-arid) to north-western Iraq (Peel et al., 2007), which is a future study area. This area in Iraq is similar to many other areas in the Middle East, and it is of critical importance for water management studies. Like many locations in this region, accurate ground-based measurements of precipitation are not available, so satellite data are the only method of constructing the water budgets needed for water management planning. The study area in California was chosen as the location that best replicated climatic and topographic conditions in the Middle East, but also had accurate ground-based measurements available, and thus may be most useful for understanding the accuracy of different types of satellite-based data in the Middle East. In general, satellite-based precipitation estimates in the Middle East are expected to have relatively low error, based on the conclusions of a study performed by Tian and Peters-Lidard (2010), which attempts to quantify the global uncertainty of satellite-based rainfall measurements by classifying the world into zones based on the probability of error in satellite data in each zone. However, understanding the magnitude of the expected error and bias is important for predicting uncertainties in model outputs that use these satellite data as inputs.

The climate of southern California is classified as Mediterranean, which is characterized by warm, wet winters and hot, dry summers (Kottek et. al., 2006). The average low and high monthly temperatures are 3.6°C and 12.2°C, which occur during December and August, respectively. The driest month is August, with an average rainfall of 0.21 mm, and the wettest month is February, with an average of 91.16 mm (National Centers for Environmental Information, 2015). Average monthly temperature and precipitation data are given in Figures 2 and 3.

3. DATA ACQUISITION

In this study, we used seven satellite-based weather products. A short description of the technique used by each product to estimate precipitation is given below.

3.1. CLIMATE FORECAST SYSTEM REANALYSIS (CFSR)

The National Centers for Environmental Prediction (NCEP) has designed CFSR to provide data of the coupled atmosphere–ocean–land surface–sea ice system with the best possible weather measurements. Reanalysis of weather data was generated based on high quality observational data using a model calibrated over very short periods until the results of the weather data matched the ground measurements. CFSR data are produced on a daily basis with a resolution of ~38 km (Saha et al., 2014).

3.2. PRECIPITATION ESTIMATION FROM REMOTELY SENSED INFORMATION USING ARTIFICIAL NEURAL NETWORKS (PERSIANN)

PERSIANN systems estimate rainfall based on infrared brightness and temperature images provided by geostationary satellites in addition to daytime visible imagery. These are used as inputs in neural network function calculations/approximations. PERSIANN has a spatial resolution of 0.25° with 50°S to 50°N global coverage. The model updates through supervised classification of adaptive training features from ground rainfall measurements when updates become available (Hsu et. al. 1997; Hsu et. al. 1999;

Sorooshian et. al. 2000; Hsu et. al. 2000; Sorooshian et. al. 2002; Hsu et. al. 2002; Sorooshian et. al. 2014).

3.3. PERSIANN-CLOUD CLASSIFICATION SYSTEM (PERSIANN-CCS)

The PERSIANN-CCS model was developed by the Center for Hydrometeorology and Remote Sensing (CHRS), University of California, Irvine (UCI). PERSIANN-CCS has a real-time global resolution of 0.04°. The PERSIANN-CCS model is based on the variable threshold cloud segmentation algorithm by categorizing clouds based on their features obtained from satellite imagery (cloud height, aerial extent and texture variability).Thus, each individual cloud patch would give a rainfall value (Hsu, et. al.1997; Hsuet, et. al. 1999; Sorooshian, et. 2000; Hsu, et. al. 2000; Sorooshian, et. al. 2002; Hsu, et. al. 2002; Hong, Y., Hsu, K., Sorooshian, et. al. 2004; Nguyen, et. al. 2014; Sorooshian, et. al. 2014; Nguyen, et. al. 2015).

3.4. PERSIANN-CLIMATE DATA RECORD (PERSIANN-CDR)

PERSIANN-CDR data were also founded by CHRS. CDR spatial resolution is 0.25° with near-global coverage (60N-60S), and these data have a daily temporal resolution. The PERSIANN-CDR Artificial Neural Networks model uses monthly rainfall data from the Global Precipitation Climatology project (GPCP) and GridSat-B1 infrared data. They are typically adjusted with GPCP data to produce rainfall data with a high spatial resolution (Hsu, et. al. 1997; Hsu, et. al. 1999; Sorooshian, et. al. 2000; Hsu, et. al. 2000; Sorooshian, et. al. 2002; Hsu, et. al. 2002; Ashouri, et. al. 2015; Miao, et. al. 2015).

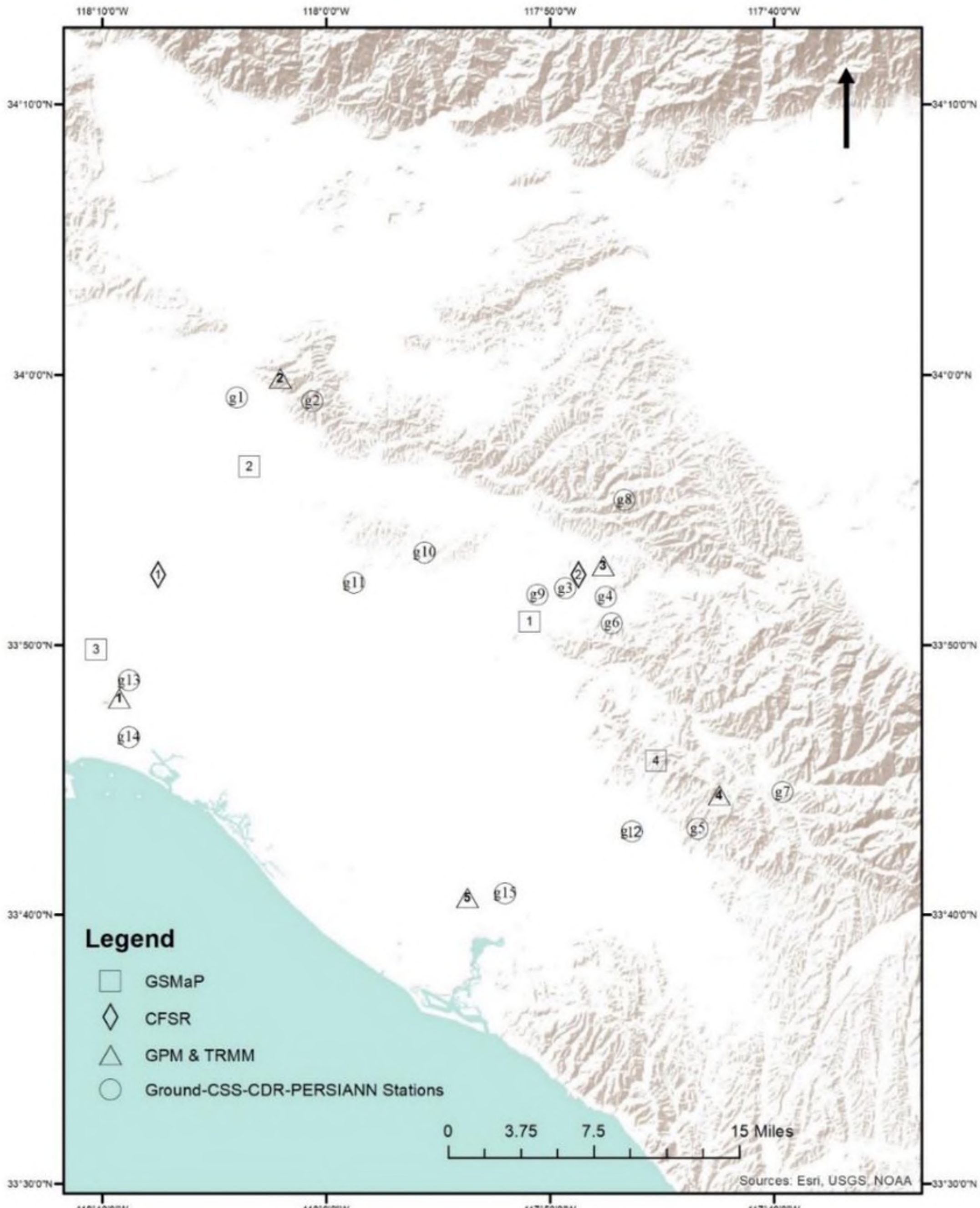

Figure 1. Ground-based weather stations and center of satellite-based measurements within the study area.

3.5. TROPICAL RAINFALL MEASURING MISSION (TRMM 3B42 V7)

TRMM is a joint mission between NASA and the Japan Aerospace Exploration Agency for climate research. TRMM was launched in 1998 and employs the TRMM Microwave Imager (TMI), Precipitation Radar (PR) and microwave MW sources to increase the swath width of scanning (Huffman et al., 2007). The spatial resolution of TRMM 3B42 V7, which was used in this study, is 0.25° with daily temporal resolution.

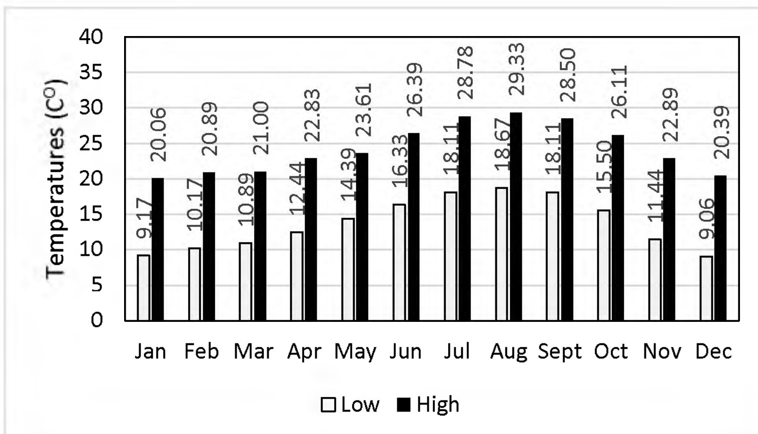

Figure 2. Average monthly temperatures (1989-2019) (National Centers for Environmental Information, 2015).

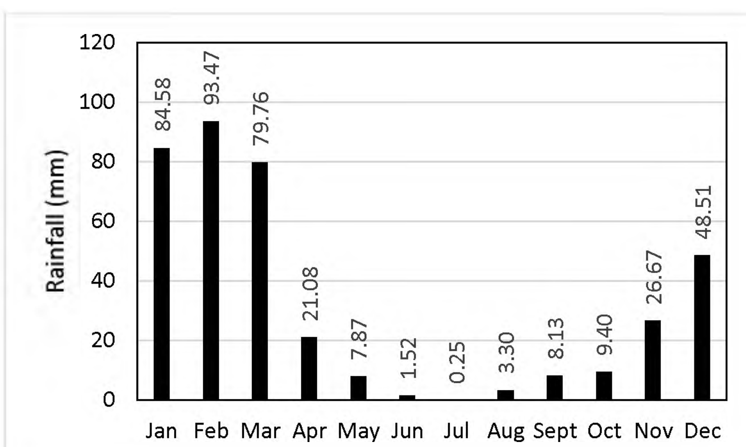

Figure 3. The average of monthly rainfall (1989-2015) (National Centers for Environmental Information, 2015).

3.6. GLOBAL PRECIPITATION MEASUREMENT (GPM 3IMERGDL V4)

GPM is a satellite mission that was developed in cooperation with NASA and the Japanese Aerospace Exploration Agency (JAXA). GPM launched the space in February of 2014. GPM is supported by very advanced instruments which provide high quality precipitation data (Jenner, 2015). GPM 3IMERGDL V4 was used in this study with a spatial resolution of 0.1° with a daily temporal scale.

3.7. GLOBAL SATELLITE MAPPING OF PRECIPITATION (GSMAP MVK)

This project was funded by the Core Research for Evolutional Science and Technology (CREST) of the Japan Science and Technology Agency (JST) from 2002-2007. GSMaP provides high spatiotemporal resolution with global coverage; the spatial resolution is 0.1° and has an hourly temporal resolution. GSMaP relies on two types of data to produce GSMaP MVK data. The first is "infrared data from multiple geostationary satellites" from the CPC archive. The second is passive microwave-based precipitation data. These two types of data are integrated together to produce precipitation data using a Kalman algorithm (Duan et. al., 2016).

4. METHODS

Satellite data have different temporal and spatial resolutions, so a comparison of satellite data with ground-based measurements requires spatial upscaling and occasional temporal averaging. First, satellite-based precipitation data were extracted from various sources and over varying time periods (Table 1) (Figure 4). TRMM 3B42 v07 and GPM 3IMERGDL v04 data were extracted through Giovanni, which is an online tool that allows one to download several NASA products. CFSR was extracted from the Global Weather Data for SWAT. For PERSIANN, PERSIANN-CSS and PERSIANN-CDR, the data were requested through the CHRS Data Portal online tool. GSMaP MVK v7 data were extracted through a G-Portal. After extraction, all data were converted and combined into a uniform file format.

Table 1. Summary of satellite-based data.

Product name	Spatial Resolution	Data Period	Data source
TRMM 3B42 v07	0.25 degree	Dec.1997 - Present	https://giovanni.gsfc.nasa.gov/giovanni/
GPM 3IMERGDL v04	0.1 degree	Mar. 2014 - Present	https://giovanni.gsfc.nasa.gov/giovanni/
CFSR	0.25 degree	Jan. 1979 – Jul. 2014	https://globalweather.tamu.edu/

Precipitation information was compiled from 35 ground-based weather stations for a period from 2010 to 2016. Ground-based data are sometimes incomplete, so 15 stations were identified that had data for almost all of the study time period (Figure 4 and

Table 2). This time period was chosen because most of the ground-based weather stations had records for much of the time. After 2016, significantly fewer ground-based weather

Table 1. Summary of satellite-based data (Cont.).

PERSIANN	0.25 degree	Mar. 2000 - Present	https://chrsdata.eng.uci.edu/
PERSIANN-CDR	0.25 degree	Jan. 1983 – Apr. 2017	https://chrsdata.eng.uci.edu/
PERSIANN-CSS	0.04 degree	Jan. 2003 - Present	https://chrsdata.eng.uci.edu/
GSMaP MVK v7	0.1 degree	Mar. 2014 - present	https://gportal.jaxa.jp/gpr/

stations were available, so the validity of comparing satellite-based estimates and ground-based measurements decreases. If any of the ground-based stations had temporal gaps in coverage between 2010 to 2016, data for these time periods were interpolated using neighboring stations and the inverse distance weighting (IDW) method. The criterion for the neighboring stations to be used in interpolation was that each station was within 3 miles of the station with missing data. After all the ground stations had a complete temporal record for the study period, ground-based precipitation measurements were compared to precipitation estimates from the satellite data. Since each satellite pixel is much larger than a ground-based station measurement, the ground-based station measurements were averaged within each satellite pixel. The resolution of different satellite-based techniques differs, so the number of ground-based measurements used varied for different satellite-based estimates depending upon the satellite pixel dimensions.

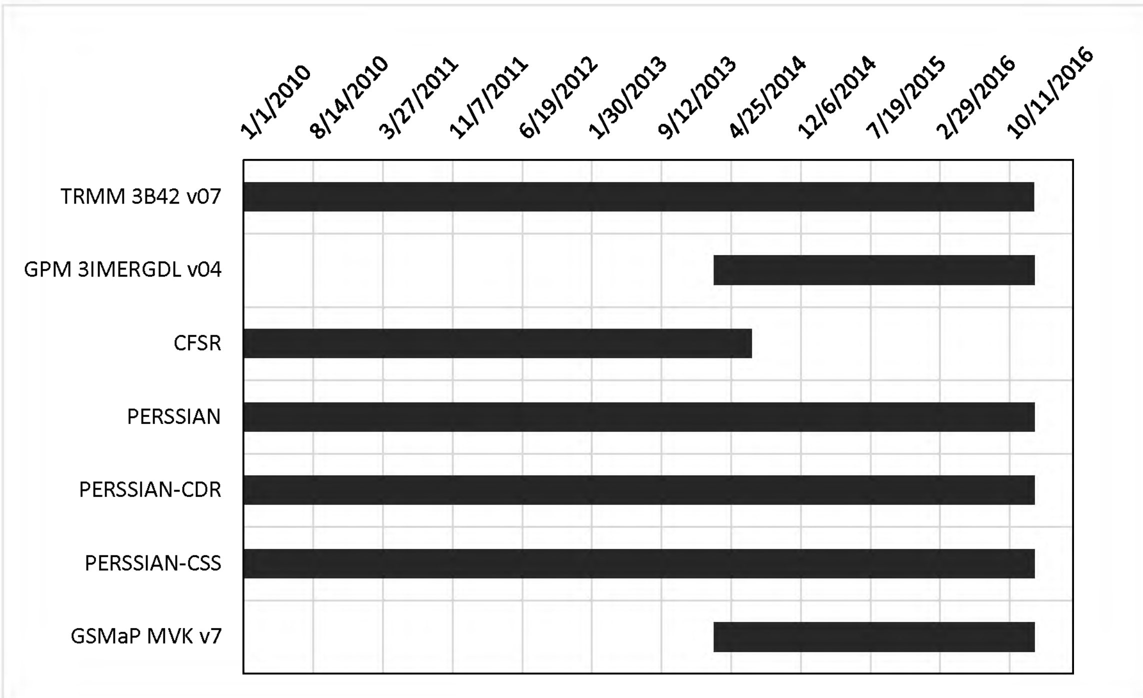

Figure 4. Satellite-based weather data for the time period of this study.

4.1. DATA ANALYSIS

Data were analyzed using several different approaches. First, a contingency analysis was applied to determine how accurately different techniques predicted the occurrence of precipitation. Next, simple regression of ground- and satellite-based precipitation was performed. Third, the slope and intercepts of these regression equations were used to predict whether different satellite data would over- or under-predict precipitation (forecasting). Finally, the RMSE and average error between satellite- and ground-based measurements were calculated. The correlation and error analyses are standard and require no explanation, but further explanation of the contingency analysis and forecasting analyses are provided below.

Table 2. Ground stations location and elevation.

ID	Name	Latitude	Longitude	Elevation (m)
1	US1CALA0010	33.986	-118.07	52.1
2	USR0000CWHH	33.984	-118.01	290
3	US1CAOR0013	33.869	-117.82	75
4	US1CAOR0021	33.863	-117.79	90.8
5	USC00044303	33.72	-117.72	165
6	US1CAOR0029	33.847	-117.79	114
7	USC00048243	33.743	-117.66	334
8	USC00041518	33.923	-117.78	493
9	USC00040192	33.865	-117.84	102
10	USC00041057	33.891	-117.93	83.8
11	USW00003166	33.872	-117.98	29.3
12	USW00023129	33.812	-118.15	9.4
13	US1CALA0038	33.777	-118.15	14.6
14	USW00093184	33.68	-117.87	16.5
15	US1CAOR0027	33.718	-117.77	46.3

Contingency analysis is a common method of analyzing the accuracy of satellite-based estimates of precipitation that focuses on determining whether satellite data accurately predict the occurrence of precipitation but does not evaluate the magnitude of precipitation events. A satellite method is considered accurate if it correctly predicts when precipitation occurs ("hit" in Table 3) and does not predict precipitation when it has not occurred ("correct negative" in Table 3).

Table 3. Contingency analysis shows the different conditions of event forecasting.

	Storm event occurrence:			
Ground measurement:	Yes	No	Yes	No
Satellite forecasting:	Yes	No	No	Yes
Condition:	Hit "H"	Correct negative "C"	Miss "M"	False alarm "F"

There are several parameters that can be computed using contingency methods. The forecasting accuracy parameter was calculated in this study, where forecasting accuracy is defined as the fraction of the total number of days which score hits and correct negatives to the total number of days of the analysis. The perfect score is 1 (Equation 1).

$$Accuracy = \frac{H+C}{H+C+M+F} \quad \text{Equation (1)}$$

Another way in which the accuracy of satellite data was investigated was to focus on the magnitude of precipitation events. Satellite-based estimates of precipitation tend to either over- or under-estimate precipitation when compared to ground measurements; the trend and magnitude of over- or under-estimation are related to the type of satellite data. To analyze whether different satellite data sets over- or under-estimated precipitation, we developed simple empirical equations, which rely on the slope (m) and the intercept (b) of a linear relationship between precipitation estimates from ground stations (P_G) and from precipitation from satellite data (P_S).

$$P_S = mP_G + b \qquad \text{Equation (2)}$$

The relationships between ground-based and satellite-based data were classified into four categories. The first category was under-forecasting, in which the satellite-based estimates were always less than the ground-based measurements. The second category was over-forecasting, where the satellite-based estimates were always greater than the ground-based measurements. The third category was extreme-biased variable-forecasting, in which the satellite data over-estimated precipitation when a large volume of rainfall had occurred and underestimated precipitation when only light rainfall occurred. The last category was average-biased variable-forecasting, in which the satellite data under-estimated precipitation when a large volume of rainfall had occurred and over-estimated precipitation when only light rainfall occurred (Figure 5).

To assist in classifying satellite data into these categories, the ground-based precipitation value at which the satellite – and ground-based data agreed (point at which the satellite regression line crossed the 1:1 line) was calculated. This point is referred to as the 1:1 intercept ($I_{1:1}$) (Equation 3) and was calculated as:

$$I_{1:1} = b/(1 - m) \qquad \text{Equation (3)}$$

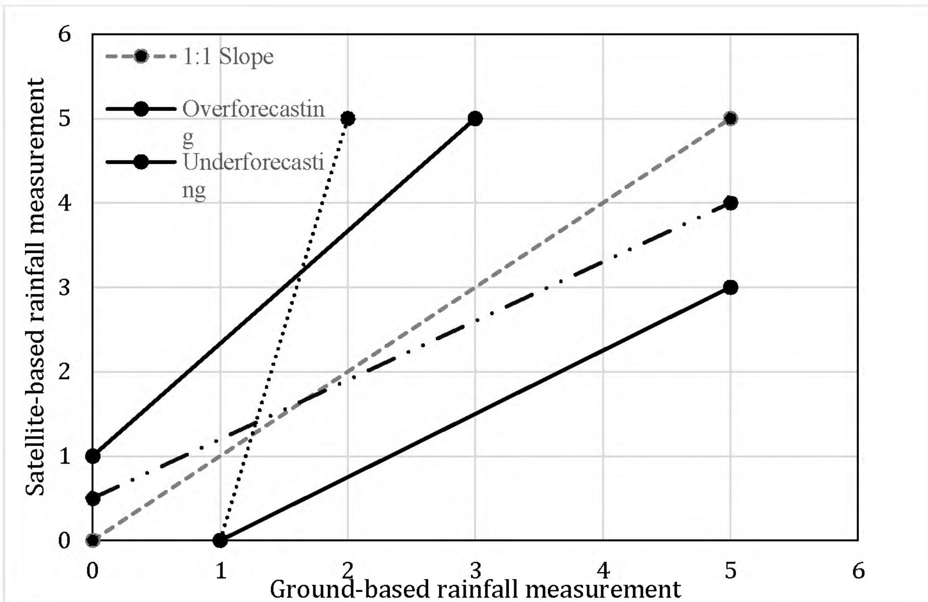

Figure 5. Categories of forecasting for prediction analysis.

5. RESULTS

Using contingency analysis for daily rainfall data, the satellite data that were the least accurate when compared to ground-based measurements were the CFSR (accuracy about 62%), and the most accurate satellite data sets were the GSMaP, which were accurate almost 90% of the time. With the exception of CFSR data, all data types had fairly similar accuracy, and the average accuracy of all methods was about 84%, (Figure 6). The high average forecasting accuracy shows that most types of satellite data were fairly accurate at detecting whether precipitation occurred or not.

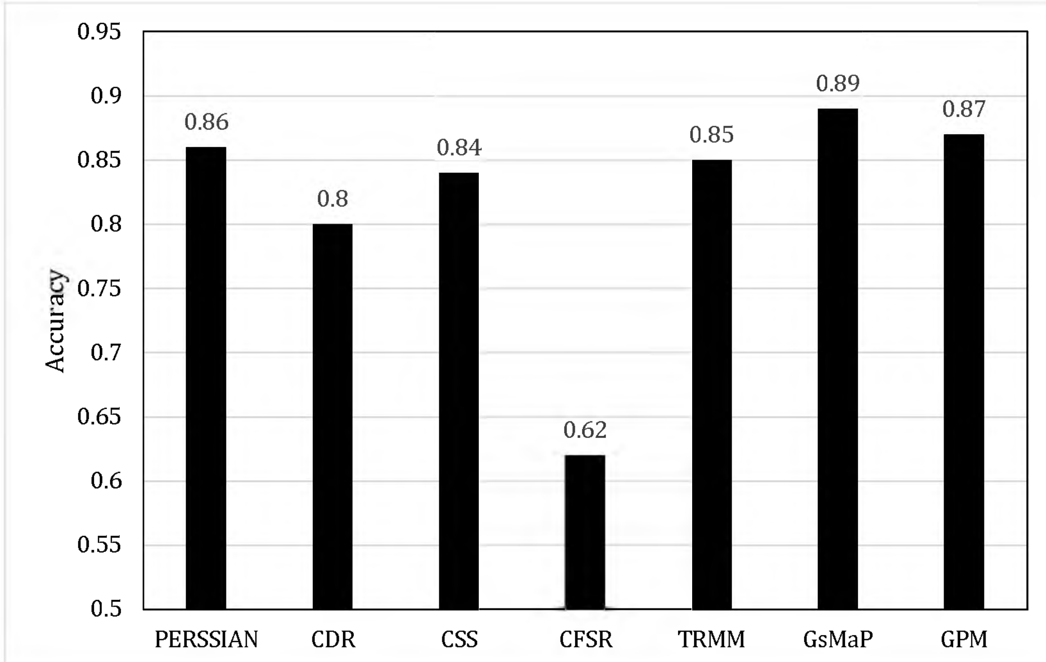

Figure 6. Forecasting accuracy parameter results of contingency table method.

The Pearson correlation coefficients between satellite-based estimates and ground-based measurements show that TRMM data were the most accurate and CDR data were the least accurate for the monthly, bi-weekly, and daily scales (Figure 7). CSS and CFSR are similar and are the next more accurate after TRMM. GSMaP, PERSIANN, and GPM estimates have similar degrees of correlation and are less accurate than the CSS and CFSR data. Temporally, most data types follow the expected trends of having higher correlation when the lowest temporal resolution is applied; monthly data usually have the highest correlation, while the bi-weekly data are slightly less accurate. For all data types, the daily data have the lowest correlation. These results are expected, since summing the precipitation over larger time periods (monthly and bi-weekly) reduces the need for exact temporal accuracy, but also reduces the impact of outlying measurements, which can increase the Pearson correlation coefficient if extreme events are well correlated. When data are considered on a daily basis, outlying individual measurements may have a disproportionate impact on the correlation coefficient.

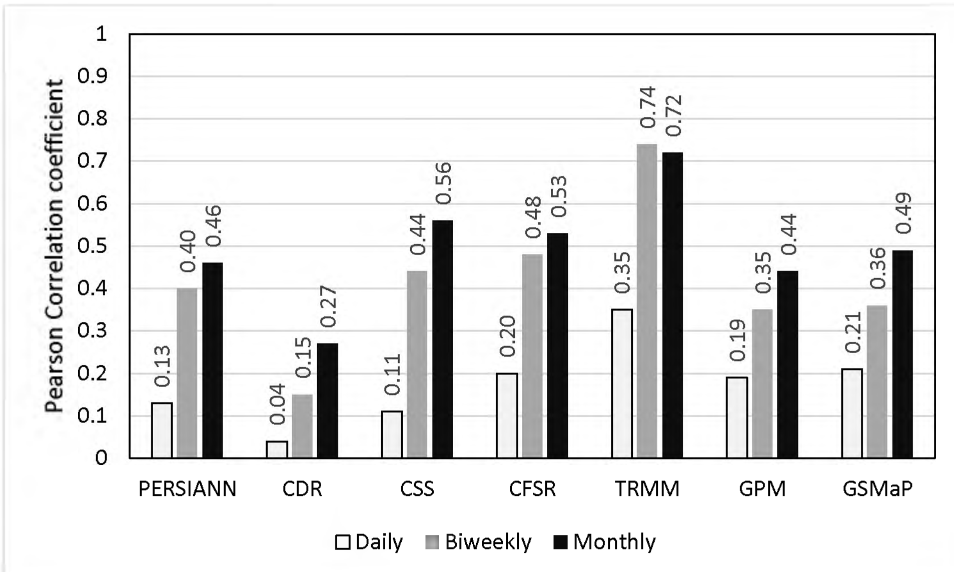

Figure 7. Pearson correlation coefficient for satellite estimates.

The regression equations were used to determine if different satellite-based techniques generally over- or under-forecast relative to ground-based measurements. In this study, CFSR, CSS, CDR and PERSIANN over-forecast for all time intervals considered (Figures 8, 9, and 10), while GSMaP closely matched the ground-based data for each time interval. TRMM and GPM under-forecast somewhat for all time intervals, but the under-forecasting was very slight for the bi-weekly and monthly time intervals.

Corrections can be made to account for under- and over-forecasting if the relationships between the satellite-based estimates and ground-based measurements is known (Figure 8, 9 and 10). Table 4 shows the slope, intercept, and $I_{1:1}$ values derived from using the ground-based measurements as the independent variable and the precipitation estimates as the dependent variable. These relationships can be used to improve the accuracy of satellite-based estimates of rainfall by relating them to the ground-based measurements (Equation 4). A linear correction is given by:

$$P_{S,cor} = \frac{P_S - b}{m} \qquad \text{Equation (4)}$$

where $P_{S,cor}$ is the corrected satellite-based estimate and P_S is the original satellite-based precipitation estimate. The reliability of each relationship can be assessed by considering the associated Pearson's correlation coefficient (Table 4).

When considering Table 4, it is helpful to note that if the $I_{1:1}$ value is negative and the slope is greater than 1, the satellite-based data are over-forecasting and are extreme-biased. If the $I_{1:1}$ value is negative and the slope is less than 1, the satellite-based data are over-forecasting and are average-biased. Similarly, if the $I_{1:1}$ value is positive and the slope is greater than 1, the satellite-based data are under-forecasting and are extreme-biased, while a positive $I_{1:1}$ value and slope less than one are under-forecasting and average-biased. Analysis of Table 4 shows that all data types that over-forecast are extreme-biased except for the daily GSMaP data, while all data types that under-forecast are average-biased. To consider error, both the RMSE and the "average" error were calculated. The RMSE is a standard method of calculating error but can be misleading when data sets of very different sizes are considered. For this study, the sample size for the daily data was much larger than the sample sizes for bi-weekly and monthly data, so the RMSE values for the daily data were much smaller than for other time intervals, although the true accuracy of satellite-based estimates of precipitations diminishes as more precise time intervals are required.

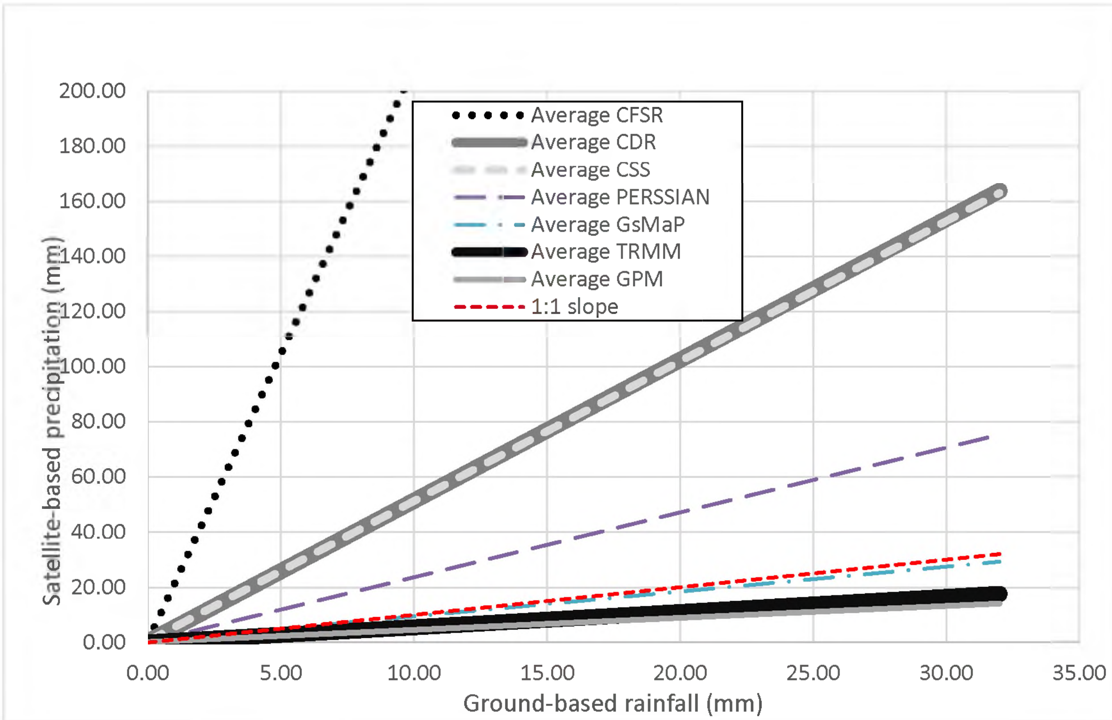

Figure 8. Categories of satellite daily forecasting for prediction analysis.

For this reason, we also calculated the "average" error, which takes the time interval into account; the average error is the average of the differences between the rain gauge measurements and the satellite-based estimates divided by the number of days over which precipitation was summed (the number of days in the interval). Thus, for daily data, the average error is simply the average difference between the rain gauge and satellite data, while the average errors for biweekly and monthly data are the average differences divided by 14 and 30, respectively. The average error may be a more intuitive method of evaluating the accuracy of different remote sensing data types when multiple time intervals are used. For the RMSE, satellite estimates of precipitation are fairly accurate at the daily scale, but the error increases significantly for longer time intervals (Figure 11). As explained above, the higher RMSE for longer time periods is a function of the smaller sample size for these intervals. The RMSE analysis is therefore most useful for comparing different types of satellite-based data rather than comparing temporal intervals. In this study, the PERSIANN data had the lowest RMSE, while CFSR had the highest. TRMM and GPM had the lowest error after the PERSIANN data, while the CSS error was only slightly higher than the error for these data types. The average error is more intuitive than RMSE for evaluating error when multiple time intervals (and thus differing sample sizes) are considered. Figure 12 shows the average error for all data types and time intervals when all data are considered.

This figure shows that when the error is normalized by the number of days in the sample (removing the effect of the time interval), the error for temporal intervals follow the expected pattern of having the lowest error for the monthly data and the highest error for the daily data. In the same figure, TRMM data were the most accurate for this data set, followed by the PERSIANN data. The CFSR data were the least accurate, followed by GSMaP. It also shows that the absolute value of the average error for each data set was relatively small, with an average absolute value of error of 2.2 mm for the daily data, 0.4 mm for the biweekly data, and 0.2 mm for the monthly data. Although the average error shown usually low, this number may be somewhat misleading, since days with no

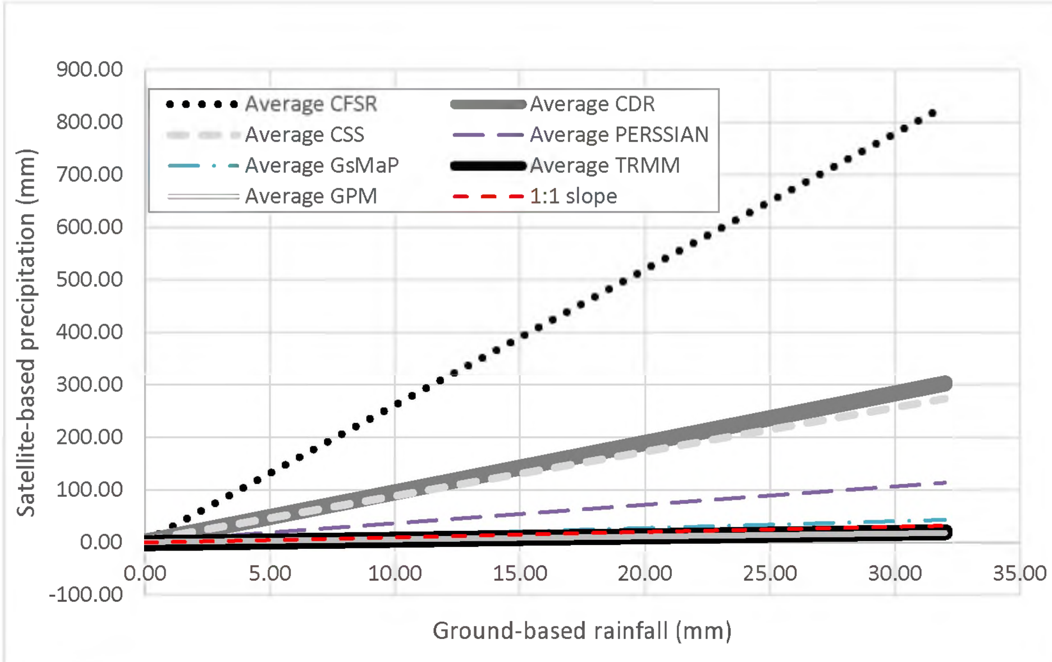

Figure 9. Categories of satellite biweekly forecasting for prediction analysis.

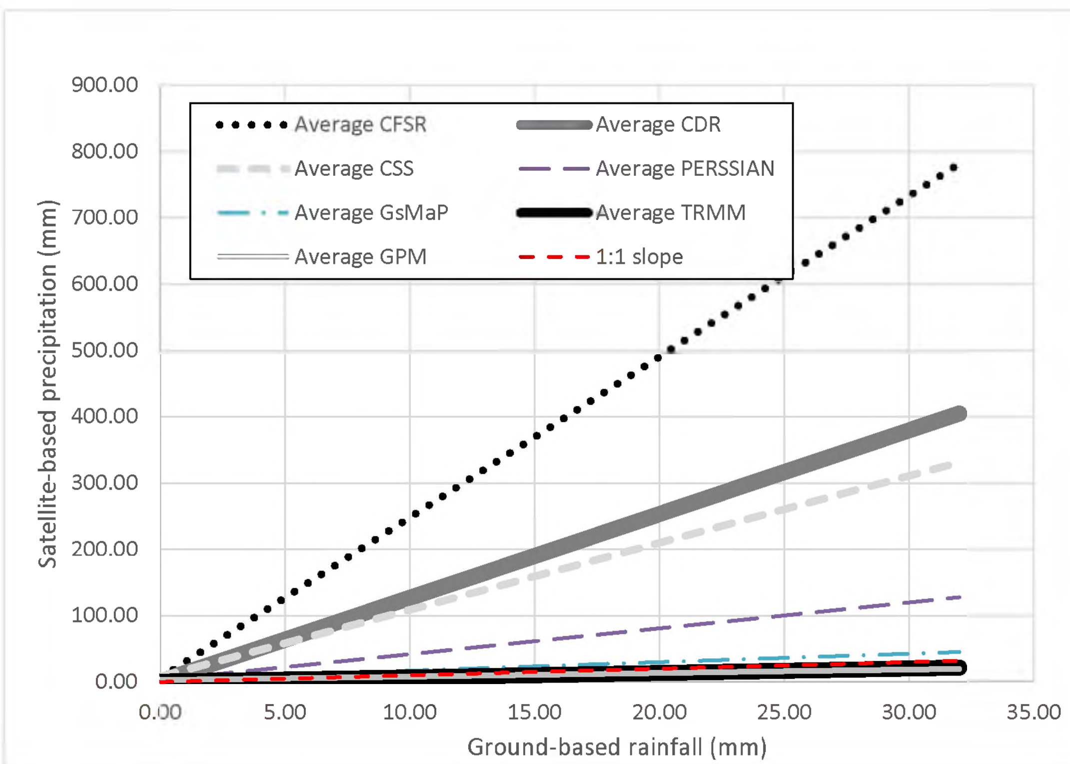

Figure 10. Categories of satellite monthly forecasting for prediction analysis.

Table 4. Linear correlation parameters between rain gauge measurements and satellite-based estimates of precipitation.

Satellite rainfall data	slope	intercept	$I_{1:1}$	R^2
CFSR Daily	20.83	0.29	-0.01	0.2
CFSR Biweekly	25.89	1.76	-0.07	0.48
CFSR Monthly	24.24	5.49	-0.24	0.53
CDR Daily	5.11	0.25	-0.06	0.04
CDR Biweekly	9.38	1.72	-0.21	0.15
CDR Monthly	12.62	0.78	-0.07	0.27
CSS Daily	5.08	0.41	-0.10	0.11
CSS Biweekly	8.40	4.29	-0.58	0.44
CSS Monthly	10.10	7.79	-0.86	0.56
PERSIANN Daily	2.35	0.14	-0.11	0.13
PERSIANN Biweekly	3.50	1.52	-0.61	0.40
PERSIANN Monthly	3.90	2.94	-1.02	0.46
GSMaP Daily	0.90	0.40	-14.91	0.21
GSMaP Biweekly	1.29	1.78	-14.91	0.36

Table 4. Linear correlation parameters between rain gauge measurements and satellite-based estimates of precipitation. (Cont.).

GSMaP Monthly	1.28	4.19	-14.91	0.49
TRMM Daily	0.55	0.01	0.02	0.35
TRMM Biweekly	0.65	-1.03	0.02	0.74
TRMM Monthly	0.66	0.50	0.02	0.72
GPM Daily	0.44	0.15	2.65	0.19
GPM Biweekly	0.53	1.23	2.65	0.35
GPM Monthly	0.53	2.86	2.65	0.44

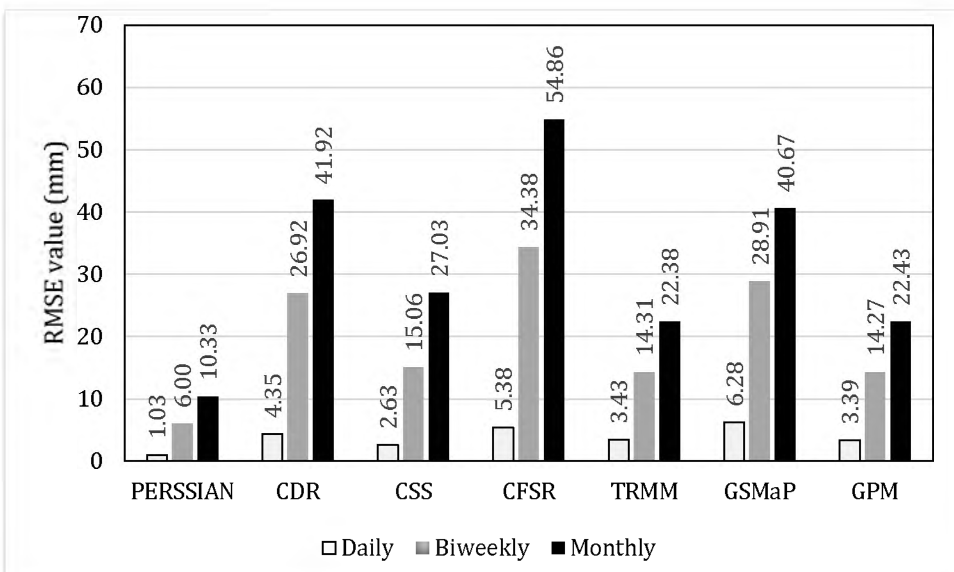

Figure 11. RMSE results for several satellite-based products in the study area.

precipitation will count as no error (if the satellite data match the rain gauge for these days.) absolute value of error of 3.5 mm for the daily data, 0.5 mm for the biweekly data, and 0.4 mm for the monthly data. Since this is an arid climate, there are many days with no rainfall, and the contribution of these days may result in a very low average error.

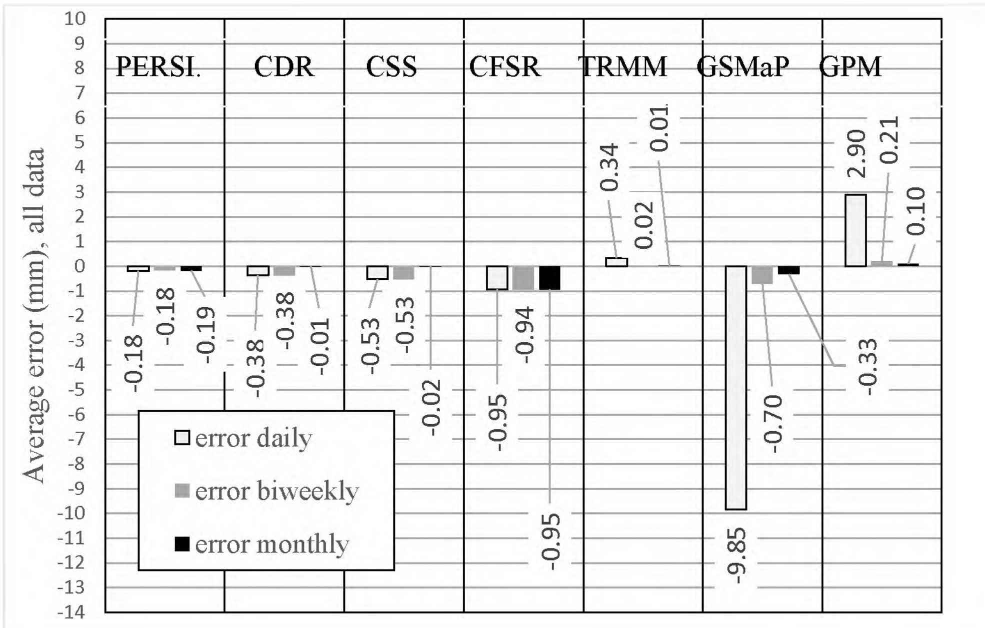

Figure 12. Average error of satellite estimates, all data included.

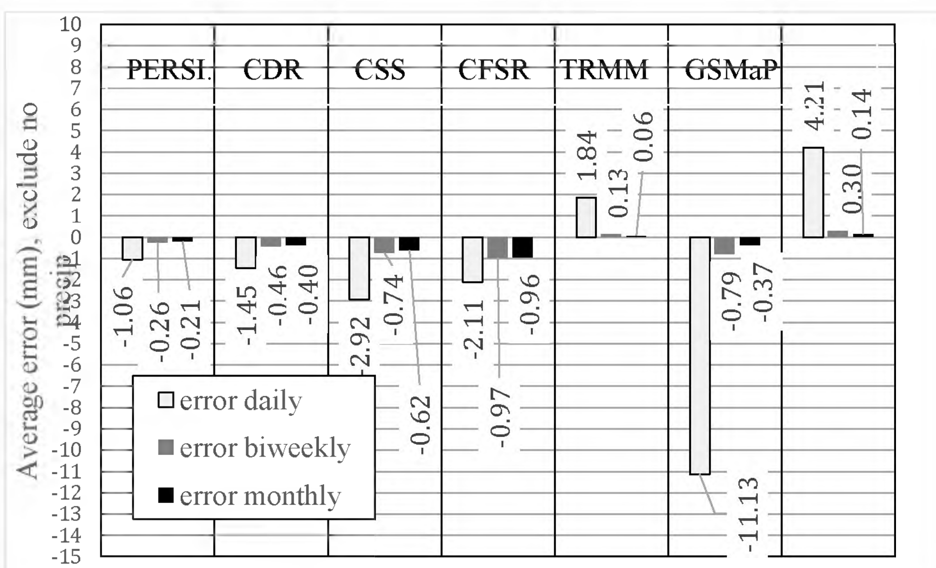

Figure 13. Average error of satellite estimates, excluding days without precipitation.

better understand the error on days when rainfall occurs, the average error analysis was repeated using only days when precipitation occurred (Figure 13), it shows that different data types still have approximately the same relative accuracy when days without precipitation are removed; TRMM are still the most accurate, again followed by PERSIANN. CFSR is still the least accurate, and GSMaP is the second least accurate. For data types with intermediate accuracy, (CDR, CSS, and GPM), the relative accuracy is changed somewhat when days without precipitation are removed. As expected, the absolute value of average error is now higher for all time intervals, with an average

6. DISCUSSION

Different satellite products are produced using different technologies for both data acquisition and analysis; the resulting estimates of precipitation from these satellite products have strengths and weaknesses corresponding to their respective technologies. Estimates of precipitation from satellite data can be used most effectively when matched with applications that require accuracy in the areas of a data product's strength. For example, estimating the total amount of precipitation an area receives as input to a water storage design may require greater accuracy in actual precipitation amounts, but not be as sensitive to the timing of precipitation. Other applications, such as dryland agriculture or predicting peak discharge during flooding events, may require greater accuracy in the timing of precipitation. In the discussion below, different satellite data products are evaluated with respect to their accuracy in both timing and magnitude of precipitation.

Both contingency analysis and methods that evaluate error based on daily estimates of precipitation could be used to analyze which satellite data products provide the most accurate information regarding the timing of precipitation. For this data set, contingency analysis showed that most data products predicted whether precipitation occurred or not reasonably well; only CFSR data performed poorly in this regard. Contingency analysis is therefore not the most useful metric for determining which satellite data product is the most accurate for measuring the timing of precipitation. When assessments of daily error are considered, the PERSIANN data set had the lowest average error (both including and omitting days with no precipitation) and the lowest RMSE. However, the PERSIANN data had a relatively lower Pearson correlation coefficient. The Pearson correlation coefficient is more affected by extreme events than the other parameters evaluated here; the low RMSE and average errors but also low Pearson correlation coefficient may indicate that the PERSIANN data set captures daily precipitation values fairly well, but does not accurately measure the magnitudes of extreme events. The TRMM data have fairly low average error and RMSE and also have a high Pearson correlation efficient, so the TRMM data product would also be a good choice when the timing of precipitation is important. GSMaP data, although the best in terms of contingency analysis, have the highest average error and RMSE. Thus, GSMaP data are for determining whether precipitation has occured, but the estimates of precipitation magnitude are poor. This finding is consistent with other studies, where both GSMaP and GPM were effective at capturing storm events based on contingency analysis, but performed poorly in measuring rainfall quantity (Fu, Q. et. al., 2011). The inaccuracy in measuring rainfall quantity for these data products could be related to the algorithm used to obtain rainfall estimates based on satellite data acquisition, which has been found to be sensitive to ground elevation and climate (Nig, S. et. al.,2017, Wang, H., & Yong, B., 2020).

If the magnitude of precipitation is more important than the precise timing of the precipitation event, the bi-weekly and monthly data may be more useful than daily data. In these data sets, errors of a few hours in the timing of precipitation are not very significant. Contingency analysis does not apply to these time intervals. For the bi-weekly data, both PERSIANN and TRMM data products perform fairly well for average error and RMSE analyses. TRMM data also have a relatively high correlation coefficient, but this parameter is lower for the PERSIANN data, suggesting that considering the PERSIANN data over a longer time interval does not eliminate the weakness in predicting extreme events that was observed in the daily data. For the monthly data, TRMM data have lower average error and a higher correlation coefficient than other satellite products; the PERSIANN data set is better than TRMM only in the RMSE calculation for monthly data. Thus, while both PERSIANN and TRMM data products might be able to provide high quality data for longer-term estimates of precipitation magnitude, TRMM is probably preferred. The least acceptable data set for longer-term magnitude analysis was CFSR, which had high average error and high RMSE for both time intervals considered, although the Pearson correlation coefficient was not especially low. These results suggest that CFSR is sensitive to extremes in precipitation but may contain too much noise to be a reliable estimator.

Although one would ideally be able to access the satellite data product most suitable to a given application, not all satellite data sets cover all areas or are available for all time periods. Also, even if the optimal data set is available, Figures 8, 10 show that most satellite products are either extreme-biased or average-biased. The correction to satellite precipitation estimates given by Equation 4 and Table 4 could be used to increase the accuracy of satellite-based estimates of precipitation. The increased accuracy could be especially useful for data sets that have relatively high Pearson correlation coefficients when compared to rain gauge data, but which had intermediate RMSE or average error values (such as the CSS or CFSR data sets), as the proposed correction could help reduce systematic bias.

7. CONCLUSIONS

This study assessed the accuracy of seven types of satellite-based rainfall data to determine which provided the best estimates of precipitation over a mid-latitude arid area. Several different techniques were used as measures of accuracy, including contingency analysis, forecasting, linear correlation, average error, and RMSE. Accuracy was also considered over three different time intervals (daily, biweekly, and monthly). Accuracy was shown to vary as a function of time interval, so the optimal data set should be chosen based on the needs of a specific application. However, this study showed that for most time intervals considered, the TRMM data appear to be the most robust data set. The TRMM data had the highest correlation with the ground-based data (regression analysis) and had very low forecasting bias. They also had relatively low RMSE and average error. However, the PERSIANN data seemed to perform better on a daily basis and was similar to the TRMM data on a bi-weekly basis, so this data set could also be a strong choice.

Other studies have also shown TRMM data to be a fairly accurate data product. Duan et al., (2016) evaluated eight different satellite data products in Italy and found TRMM and CMORPH_BLD were the most accurate data types. Derin and Yilmaz (2014) evaluated four data types in a study in Turkey and found the TRMM data to have the best performance. However, others studies (Fengrui and Xi, 2016) have found other data sets to be more accurate than TRMM. Some studies (Fuka et al., (2014), Zhu et al., 2016, Liu et al., (2016), Worqlul et al., (2017) have had successful precipitation estimation from CDR and CFSR data; these data types also performed fairly well in this study, but were not consistently good estimates of precipitation as the CDR data had lower correlation with rain gage measurements and the CFSR data had higher average error and performed poorly in contingency analysis. These data types may work better in a more humid climate, such as in the studies listed above.

The results of this research provide guidance on which satellite-based data types might provide the most accurate precipitation estimates in mid-latitude, arid areas with few ground-based measurements. Additionally, the forecasting analysis and Equation 4 provide a method for correcting different data types. This may lead to better inputs into hydrological models and better management of arid lands.

ACKNOWLEDGEMENT

The authors acknowledge the Ministry of Higher Education and Scientific Research (Iraq) to fund this project. The authors express their gratitude to the National Aeronautics and Space Administration (NASA) to make satellite-based precipitation products available to scientists, which has been used in this research, including: Global

Precipitation Measurement (GPM), Multi-satellite Precipitation Analysis (TRMM 3B42). The authors express their gratitude to all the organizations that are responsible for providing weather data, namely, NOAA's National Centers for Environmental Prediction (NCEP) for CFSR, Center for Hydrometeorology and Remote Sensing for PERSIANN-CDR data, and Japan Aerospace Exploration Agency (JAXA) for GSMaP data.

REFERENCES

Abbott, M. B., & Refsgaard, J. C. (2012). *Distributed Hydrological Modelling*. Springer Science & Business Media.

Adler, R. F., Huffman, G. J., Chang, A., Ferraro, R., Xie, P.-P., Janowiak, J., Rudolf, B., Schneider, U., Curtis, S., Bolvin, D., Gruber, A., Susskind, J., Arkin, P., & Nelkin, E. (2003). The Version-2 Global Precipitation Climatology Project (GPCP) Monthly Precipitation Analysis (1979–Present). *Journal of Hydrometeorology*, *4*(6), 1147–1167.

AghaKouchak, A., Mehran, A., Norouzi, H., & Behrangi, A. (2012). Systematic and random error components in satellite precipitation data sets. *Geophysical Research Letters*, *39*(9). https://doi.org/10.1029/2012GL051592

AghaKouchak, A., Nasrollahi, N., Li, J., Imam, B., & Sorooshian, S. (2011). Geometrical Characterization of Precipitation Patterns. *Journal of Hydrometeorology*, *12*(2), 274–285.

Arkin, P. A. (1979). The Relationship between Fractional Coverage of High Cloud and Rainfall Accumulations during GATE over the B-Scale Array. *Monthly Weather Review*, *107*(10), 1382–1387.

Arkin, P. A., & Ardanuy, P. E. (1989). Estimating Climatic-Scale Precipitation from Space: A Review. *Journal of Climate*, *2*(11), 1229–1238.

Arkin, P. A., & Meisner, B. N. (1987). The Relationship between Large-Scale Convective Rainfall and Cold Cloud over the Western Hemisphere during 1982-84. *Monthly Weather Review*, *115*(1), 51–74.

Artan, G., Gadain, H., Smith, J. L., Asante, K., Bandaragoda, C. J., & Verdin, J. P. (2007). Adequacy of satellite derived rainfall data for stream flow modeling. *Natural Hazards*, *43*(2), 167–185.

Ashouri, H., Hsu, K.-L., Sorooshian, S., Braithwaite, D. K., Knapp, K. R., Cecil, L. D., Nelson, B. R., & Prat, O. P. (2015). PERSIANN-CDR: Daily Precipitation Climate Data Record

Behrangi, A., Khakbaz, B., Jaw, T. C., AghaKouchak, A., Hsu, K., & Sorooshian, S. (2011). Hydrologic evaluation of satellite precipitation products over a mid-size basin. *Journal of Hydrology*, *397*(3), 225–237.

Bellerby, T. J., & Sun, J. (2005). Probabilistic and Ensemble Representations of the Uncertainty in an IR/Microwave Satellite Precipitation Product. *Journal of Hydrometeorology*, *6*(6), 1032–1044.

Bharti, V., & Singh, C. (2015). Evaluation of error in TRMM 3B42V7 precipitation estimates over the Himalayan region. *Journal of Geophysical Research, D: Atmospheres*, *120*(24), 12458–12473.

Blacutt, L. A., Herdies, D. L., de Gonçalves, L. G. G., Vila, D. A., & Andrade, M. (2015). Precipitation comparison for the CFSR, MERRA, TRMM3B42 and Combined Scheme datasets in Bolivia. *Atmospheric Research*, *163*, 117–131.

Carrey, D. M. (2011). *Water recycling and water management*. http://agris.fao.org/agris-search/search.do?recordID=US201300002142

Chen, F., & Li, X. (2016). Evaluation of IMERG and TRMM 3B43 Monthly Precipitation Products over Mainland China. *Remote Sensing*, *8*(6), 472.

Derin, Y., & Yilmaz, K. K. (2014). Evaluation of Multiple Satellite-Based Precipitation Products Over Complex Topography. *Journal of Hydrometeorology*, *15*(4), 1498–1516.

Duan, Z., Liu, J., Tuo, Y., Chiogna, G., & Disse, M. (2016). Evaluation of eight high spatial resolution gridded precipitation products in Adige Basin (Italy) at multiple temporal and spatial scales. *The Science of the Total Environment*, *573*, 1536–1553.

Ebert, E. E. (2005). Satellite vs. model rainfall—Which one to use. *Fifth Int. Scientific Conf. on the Global Energy and Water Cycle*.

Ebert, E. E., Janowiak, J. E., & Kidd, C. (2007). Comparison of Near-Real-Time Precipitation Estimates from Satellite Observations and Numerical Models. *Bulletin of the American Meteorological Society*, *88*(1), 47–64.

Fuka, D. R., Walter, M. T., MacAlister, C., Degaetano, A. T., Steenhuis, T. S., & Easton, Z. M. (2014). Using the Climate Forecast System Reanalysis as weather input data for watershed models. *Hydrological Processes*, *28*(22), 5613–5623.

Fu, Q., Ruan, R., & Liu, Y. (2011). Accuracy assessment of global satellite mapping of precipitation (GSMaP) product over Poyang Lake Basin, China. *Procedia Environmental Sciences*, *10*, 2265-2271.

Gao, J., Tang, G., & Hong, Y. (2017). Similarities and Improvements of GPM Dual-Frequency Precipitation Radar (DPR) upon TRMM Precipitation Radar (PR) in Global Precipitation Rate Estimation, Type Classification and Vertical Profiling. *Remote Sensing*, *9*(11), 1142.

Gourley, J. J., Hong, Y., Flamig, Z. L., Wang, J., Vergara, H., & Anagnostou, E. N. (2011). Hydrologic evaluation of rainfall estimates from radar, satellite, gauge, and combinations on Ft. Cobb basin, Oklahoma. *Journal of Hydrometeorology*, *12*(5), 973–988.

Hijmans, R. J., & van Etten, J. (n.d.). Raster: Geographic data analysis and modeling [Internet]. 2016. In *Available*. Available.

Hong, Y., Alder, R. F., Hossain, F., Curtis, S., & Huffman, G. J. (2007). Estimate gridded and time variant runoff curve numbers using satelliteremote sensing and geospatial data. *Water Resources Research*, *43*, 285–294.

Hong, Y., Hsu, K.-L., Sorooshian, S., & Gao, X. (2004). Precipitation Estimation from Remotely Sensed Imagery Using an Artificial Neural Network Cloud Classification System. *Journal of Applied Meteorology*, *43*(12), 1834–1853.

Hou, A. Y., Kakar, R. K., Neeck, S., Azarbarzin, A. A., Kummerow, C. D., Kojima, M., Oki, R., Nakamura, K., & Iguchi, T. (2014). The Global Precipitation Measurement Mission. *Bulletin of the American Meteorological Society*, *95*(5), 701–722.

Hsu, K.-L., Gao, X., Sorooshian, S., & Gupta, H. V. (1997). Precipitation Estimation from Remotely Sensed Information Using Artificial Neural Networks. *Journal of Applied Meteorology*, *36*(9), 1176–1190.

Hsu, K.-L., Gupta, H. V., Gao, X., & Sorooshian, S. (1999). Estimation of physical variables from multichannel remotely sensed imagery using a neural network: Application to rainfall estimation. *Water Resources Research*, *35*(5), 1605–1618.

Hsu, K.-L., Gupta, H. V., Gao, X., & Sorooshian, S. (2000). Rainfall Estimation from Satellite Imagery. In R. S. Govindaraju & A. R. Rao (Eds.), *Artificial Neural Networks in Hydrology* (pp. 209–234). Springer Netherlands.

Hsu, K.-L., Gupta, H. V., Gao, X., Sorooshian, S., & Imam, B. (2002). Self-organizing linear output map (SOLO): An artificial neural network suitable for hydrologic modeling and analysis. *Water Resources Research*, *38*(12), 38–31.

Huffman, G. J. (2006). Satellite-Based Estimation of Precipitation Using Microwave Sensors. *Encyclopedia of Hydrological Sciences*. https://onlinelibrary.wiley.com/doi/abs/10.1002/0470848944.hsa055

Huffman, G. J., Bolvin, D. T., Nelkin, E. J., Wolff, D. B., Adler, R. F., Gu, G., Hong, Y., Bowman, K. P., & Stocker, E. F. (2007). The TRMM Multisatellite Precipitation Analysis (TMPA): Quasi-Global, Multiyear, Combined-Sensor Precipitation Estimates at Fine Scales. *Journal of Hydrometeorology*, *8*(1), 38–55.

Iglesias, A., & Garrote, L. (2015). Adaptation strategies for agricultural water management under climate change in Europe. *Agricultural Water Management*, *155*, 113–124.

Kottek, M., Grieser, J., Beck, C., Rudolf, B., & Rubel, F. (2006). *World map of the Köppen-Geiger climate classification updated. Meteorol Z: 259--263.*

Lakshmi, V. (2014). *Remote Sensing of the Terrestrial Water Cycle*. John Wiley & Sons.

Liu, X., Yang, T., Hsu, K., Liu, C., & Sorooshian, S. (2017). Evaluating the streamflow simulation capability of PERSIANN-CDR daily rainfall products in two river basins on the Tibetan Plateau. *Hydrology and Earth System Sciences*. https://www.osti.gov/biblio/1366534

Manz, B., Buytaert, W., Zulkafli, Z., Lavado, W., Willems, B., Robles, L. A., & Rodríguez-Sánchez, J.-P. (2016). High-resolution satellite-gauge merged precipitation climatologies of the Tropical Andes. *Journal of Geophysical Research, D: Atmospheres*, *121*(3), 1190–1207.

Miao, C., Ashouri, H., Hsu, K.-L., Sorooshian, S., & Duan, Q. (2015). Evaluation of the PERSIANN-CDR Daily Rainfall Estimates in Capturing the Behavior of Extreme Precipitation Events over China. *Journal of Hydrometeorology*, *16*(3), 1387–1396.

Ning, S., Song, F., Udmale, P., Jin, J., Thapa, B. R., & Ishidaira, H. (2017). Error analysis and evaluation of the latest GSMaP and IMERG precipitation products over Eastern China. *Advances in Meteorology*, *2017*.

Nguyen, P., Sellars, S., Thorstensen, A., Tao, Y., Ashouri, H., Braithwaite, D., Hsu, K., & Sorooshian, S. (2014). Satellites track precipitation of super typhoon Haiyan. *Eos, Transactions, American Geophysical Union* , *95*(16), 133–135.

Nguyen, P., Thorstensen, A., Sorooshian, S., Hsu, K., & AghaKouchak, A. (2015). Flood Forecasting and Inundation Mapping Using HiResFlood-UCI and Near-Real-Time Satellite Precipitation Data: The 2008 Iowa Flood. *Journal of Hydrometeorology*, *16*(3), 1171–1183.

Nijssen, B., Lettenmaier, D. P., Liang, X., Wetzel, S. W., & Wood, E. F. (1997). Streamflow simulation for continental-scale river basins. *Water Resources Research*, *33*(4), 711–724.

Peel, M. C., Finlayson, B. L., & McMahon, T. A. (2007). World map of the Köppen-Geiger climate classification updated. Hydrol Earth Syst Sci, 11, 1633-1644.

Pfeifroth, U., Mueller, R., & Ahrens, B. (2013). Evaluation of Satellite-Based and Reanalysis Precipitation Data in the Tropical Pacific. *Journal of Applied Meteorology and Climatology*, *52*(3), 634–644.

Plate, E. J. (2002). Flood risk and flood management. Journal of Hydrology, 267(1-2), 2-11.

Ruckstuhl, C., & Norris, J. R. (2009). How do aerosol histories affect solar “dimming” and “brightening” over Europe?: IPCC-AR4 models versus observations. *Journal of Geophysical Research, D: Atmospheres*, *114*(D10). https://agupubs.onlinelibrary.wiley.com/doi/abs/10.1029/2008JD011066@10.1002/(ISSN)2169-8996.DIMBRIGHT1

Saha, S. (2014). Coauthors, 2010: NCEP Climate Forecast System Reanalysis (CFSR) 6-hourly products, January 1979 to December 2010. *Research Data Archive at the National Center for Atmospheric Research, Computational and Information Systems Laboratory, Accessed*, *31*.

Sawunyama, T., & Hughes, D. A. (2008). Application of satellite-derived rainfall estimates to extend water resource simulation modelling in South Africa. *Water SA*, *34*(1), 1–10.

Scheel, M. L. M., Rohrer, M., Huggel, C., Santos Villar, D., Silvestre, E., & Huffman, G. J. (2011). Evaluation of TRMM Multi-satellite Precipitation Analysis (TMPA) performance in the Central Andes region and its dependency on spatial and temporal resolution. *Hydrology and Earth System Sciences*, *15*(8), 2649–2663.

Setiawati, M. D., Miura, F., & Others. (2016). Evaluation of GSMaP Daily Rainfall Satellite Data for Flood Monitoring: Case Study—Kyushu Japan. *Journal of Geoscience and Environment Protection*, *4*(12), 101.

Sharifi, E., Steinacker, R., & Saghafian, B. (2016). Assessment of GPM-IMERG and Other Precipitation Products against Gauge Data under Different Topographic and Climatic Conditions in Iran: Preliminary Results. *Remote Sensing*, *8*(2), 135.

Sikorska, A., & Seibert, J. (2015). *Importance of precipitation data quality for streamflow predictions*. 13369.

Sorooshian, S., Gao, X., Hsu, K., Maddox, R. A., Hong, Y., Gupta, H. V., & Imam, B. (2002). Diurnal Variability of Tropical Rainfall Retrieved from Combined GOES and TRMM Satellite Information. *Journal of Climate*, *15*(9), 983–1001.

Sorooshian, S., Hsu, K.-L., Gao, X., Gupta, H. V., Imam, B., & Braithwaite, D. (2000). Evaluation of PERSIANN System Satellite-Based Estimates of Tropical Rainfall. *Bulletin of the American Meteorological Society*, *81*(9), 2035–2046.

Sorooshian, S., Lawford, R., Try, P., Rossow, W., Roads, J., Polcher, J., Sommeria, G., & Schiffer, R. (2005). Water and energy cycles: Investigating the links. *World Meteorological Organization Bulletin*, *54*(2), 58–64.

Sorooshian, S., Nguyen, P., Sellars, S., Braithwaite, D., AghaKouchak, A., & Hsu, K. (2014). Satellite-based remote sensing estimation of precipitation for early warning systems. *Extreme Natural Hazards, Disaster Risks and Societal Implications*, *1*, 99.

Stisen, S., & Sandholt, I. (2010). Evaluation of remote-sensing-based rainfall products through predictive capability in hydrological runoff modelling. *Hydrological Processes: An International Journal*, *24*(7), 879–891.

Tang, G., Zeng, Z., Long, D., Guo, X., Yong, B., Zhang, W., & Hong, Y. (2016). Statistical and Hydrological Comparisons between TRMM and GPM Level-3 Products over a Midlatitude Basin: Is Day-1 IMERG a Good Successor for TMPA 3B42V7? *Journal of Hydrometeorology*, *17*(1), 121–137.

Tang, Q., Gao, H., Lu, H., & Lettenmaier, D. P. (2009). Remote sensing: hydrology. *Progress in Physical Geography: Earth and Environment*, *33*(4), 490–509.

Tapiador, F. J., Turk, F. J., Petersen, W., Hou, A. Y., García-Ortega, E., Machado, L. A. T., Angelis, C. F., Salio, P., Kidd, C., Huffman, G. J., & de Castro, M. (2012). Global precipitation measurement: Methods, datasets and applications. *Atmospheric Research*, *104-105*, 70–97.

Taylor, J. (1997). *Introduction to Error Analysis, the Study of Uncertainties in Physical Measurements, 2nd Edition*. adsabs.harvard.edu.

Tian, Y., Peters-Lidard, C. D., & Eylander, J. B. (2010). Real-Time Bias Reduction for Satellite-Based Precipitation Estimates. *Journal of Hydrometeorology*, *11*(6), 1275–1285.

Turk, F. J., Arkin, P., Ebert, E. E., & Sapiano, M. R. P. (2008). EVALUATING HIGH-RESOLUTION PRECIPITATION PRODUCTS. *Bulletin of the American Meteorological Society*, *89*(12), 1911–1916.

Ushio, T., Sasashige, K., Kubota, T., Shige, S., Okamoto, K. 'ichi, Aonashi, K., Inoue, T., Takahashi, N., Iguchi, T., Kachi, M., Oki, R., Morimoto, T., & Kawasaki, Z.-I. (2009). A Kalman Filter Approach to the Global Satellite Mapping of Precipitation (GSMaP) from Combined Passive Microwave and Infrared Radiometric Data. *気象集誌. 第2輯*, *87A*, 137–151.

Vrugt, J. A., Gupta, H. V., Nualláin, B., & Bouten, W. (2006). Real-Time Data Assimilation for Operational Ensemble Streamflow Forecasting. *Journal of Hydrometeorology*, *7*(3), 548–565.

Wang, H., & Yong, B. (2020). Quasi-Global Evaluation of IMERG and GSMaP Precipitation Products over Land Using Gauge Observations. Water, 12(1), 243.

Worqlul, A. W., Yen, H., Collick, A. S., Tilahun, S. A., Langan, S., & Steenhuis, T. S. (2017). Evaluation of CFSR, TMPA 3B42 and ground-based rainfall data as input for hydrological models, in data-scarce regions: The upper Blue Nile Basin, Ethiopia. *Catena*, *152*, 242–251.

Zambrano-Bigiarini, M., Nauditt, A., Birkel, C., Verbist, K., & Ribbe, L. (2017). Temporal and spatial evaluation of satellite-based rainfall estimates across the complex topographical and climatic gradients of Chile. *Hydrology and Earth System Sciences*, *21*(2), 1295.

Zhiyong, M., Lianshou, C., & Xiangde, X. (2002). Recent progress on tropical cyclone research in China. *Advances in Atmospheric Sciences*, *19*(1), 103–110.

Zhu, Q., Xuan, W., Liu, L., & Xu, Y.-P. (2016). Evaluation and hydrological application of precipitation estimates derived from PERSIANN-CDR, TRMM 3B42V7, and NCEP-CFSR over humid regions in China. *Hydrological Processes*, *30*(17), 3061–3083.

II. HYDROLOGICAL ANALYSIS OF AN UNGAUGED WATERSHED USING REMOTE SENSING TECHNIQUES

Majid S. Mohamod[1, 2] and Katherine Grote[1]

Department of Geosciences and Geological and Petroleum Engineering, Missouri University of Science and Technology, McNutt Hall, 1400 N. Bishop Ave, Rolla, MO 65401, USA,

College of Science, University of Tikrit, Salahdin, Iraq

ABSTRACT

Historical records of stream discharge are needed to develop water management strategies for flood control or water storage, but these data are not available for many watersheds. In this work, historical records of precipitation from satellite data are used with a hydrological model to generate simulated stream discharge measurements. The study is performed in the ungauged Hatra watershed in northwestern Iraq using precipitation records from 1977 to 2014. The hydrological model was developed using the Soil Water Assessment Tool (SWAT), and the model was calibrated using stream discharge measurements collected at the mouth of the watershed. No reliable ground-based precipitation records were available, so three types of satellite-based data (TRMM 3B42 v07, PERSIANN-CDR, and CFSR) were used as input to the model, and calibration was performed for each data set using the SWAT-CUP sensitivity analysis method. Calibration metrics (Nash-Sutcliffe efficiency, coefficient of determination, and percent bias) showed that the CSFR data produced a model that best matched the measured output on a temporal basis, but TRMM data provided a cumulative discharge volume that was most similar to that measured. The CFSR data were used to simulate

discharge over the study period, and these discharge measurements were used to develop tools for water management, such as flood recurrence intervals and duration curves. Analysis of these tools showed that the Hatra watershed has highly variable discharge on both a daily and annual basis. Discharge is usually quite low (or zero), but high magnitude flood events significantly raise the average discharge. This pattern indicates that water management in this watershed will be challenging. Flood control structures may be needed for low frequency but high magnitude events, while significant water storage will be needed to provide water during the majority of the year. The tools developed in this study can be used to design structures or strategies for better water management in this region.

1. INTRODUCTION

Understanding stream discharge variability is an essential component of many aspects of water management, from delineating floodplains or designing flood control structures to selecting groundwater recharge locations. To understand the hydrologic variability, measurements of stream discharge with time are needed. Unfortunately, these measurements are not available for most streams. The lack of data is especially problematic in arid and semiarid areas, where precipitation and surface runoff can vary greatly in time and space (Wheater, Mathias, & Li, 2010; Ribot, Magalhães, & Panagides, 2005; Watson & Zinyowera, 1998), and factors such as sparse populations, limited economic resources, and infrequent hydrological events make collecting data difficult (Wheater et al., 2010). Subsequently, many arid and semiarid areas have very limited hydrological data (Wheater, Sorooshian, & Sharma, 2007). The lack of data limits the success of hydrological models needed for effective water management (Kavetski, Kuczera, & Franks, 2006).

When ground-based hydrological measurements are not available, remote sensing data can be used to provide some types of hydrological information (Tang, Gao, Lu, & Lettenmaier, 2009; Schmugge, Kustas, Ritchie, Jackson, & Rango, 2002; Pietroniro, & Prowse, 2002.). Remote sensing has been used extensively to estimate precipitation, and numerous studies have compared remotely sensed estimates of precipitation with ground-based measurements (Habib et al., 2009; Kubota et al., 2009; Levizzani et al., 2002; Jamandre et al., 2013). Remote sensing data are advantageous because they cover large areas that cannot always be accessed from the ground, and some types of remote sensing data have been acquired over long periods of time. For example, the Earth Resources Technology Satellite (ERTS-1 or Landsat-1) was first successfully launched was on July 23, 1972, and is presently still operating, making Landsat data acquisition the longest continuous Earth-monitoring data set (Irons, et al., 2012; Serbina & Miller, 2014). Accordingly, Landsat provides vital data needed for hydrological modeling, such as land use/land cover information.

Remotely-sensed estimates of precipitation can be used as inputs to hydrological models that calculate other parameters, such as surface runoff, infiltration, evapotranspiration, and stream discharge (Collischonn et al., 2008; Zubieta et al., 2017; Beck et. al, 2020; Cohen Liechti et al., 2012; Bitew et al., 2012). Several different hydrological models are available, but one of the most commonly applied is the Soil Water Assessment Tool (SWAT), developed by United States Department of Agriculture (USDA) – Agricultural Research Service (ARS). Devia, Ganasri, and Dwarakish (2015) have examined the performance of various hydrological models, and they concluded that the SWAT model could obtain good hydrological predictions, even with limited calibration. In addition, several studies have shown the capability of SWAT to predict hydrological parameters in regions with sparse data (Nyeko, 2015; Näschen et al., 2018, Suliman et. al., 2015; Wagner et. sl., 2013; Srinivasan et. al., 2010; Noori & Kalin, 2016; Rafiei Emam et al., 2017) and at scales ranging *from* catchment to continental scales (Abbaspour et al., 2015; Jayakrishnan, Srinivasan, Santhi, & Arnold, 2005). Although all model predictions have some error and uncertainty due to the avoidable simplification of physical processes during modeling (Rivas-Tabares, Tarquis, Willaarts, & De Miguel, 2019), models still offer a valuable method for making hydrological predictions in areas with poor data availability.

Although satellite-based data are essential inputs to hydrological models, the accuracy of these data depends on many factors (Povey & Grainger, 2015) and can vary with changing atmospheric conditions (Tian et al., 2009). Accordingly, it is important to calibrate and validate the satellite-based estimates when using these data as input into hydrological models. To calibrate and validate a hydrological model, observational data are needed. However, the majority of watersheds worldwide are ungauged, so ground-based observational data are not readily available (Blöschl, Sivapalan, Wagener, Viglione, & Savenije, 2013). Therefore, methods to calibrate ungauged basins, such as regionalization, have been developed (Deckers, 2006). Regionalization assumes that the properties of adjacent watersheds are similar; if data are available to calibrate model parameters for one basin, regionalization then applies those same parameters to another basin with similar hydrological properties (Hrachowitz et al., 2013). Gitau and Chaubey

(2010) applied the method of regionalization to gauged and ungauged watersheds using the SWAT Model within watersheds in Arkansas, USA and were able to obtain satisfactory estimates of discharge in the ungauged watershed. Other researchers also estimated hydrological parameters in ungauged basins. Ang & Oeurng (2018) used the SWAT model and regionalization to simulate the streamflow of ungauged Tonlesap Lake basin in Cambodia. They calibrated their model on a daily and monthly basis over a 10 year time period (2001-2010) using discharge from a gauged basin, then used the hydrological parameters on the adjacent ungauged basin. They concluded that SWAT model is very powerful tool to estimate the streamflow of ungauged watersheds.

Another method of calibration for hydrological models that can be used if no surface-based measurements are available is to use satellite-based data. Ha et al. (2018) successfully examined the capability of using remotely sensed evapotranspiration (ET) and leaf area index (LAI) data to calibrate the SWAT model for a watershed in Vietnam. The SUFI-2 model was used for auto calibration mode in SWAT-CUP (Abbaspour et al., 2012) to compare the ET and LAI produced by the SWAT model with the same inputs from satellite-based data. After calibrating the model with these data sets, the predicted discharge compared well with that measured at the mouth of the watershed. A similar study published by Milzow, Krogh, & Bauer-Gottwein (2011) used a combination of remotely sensed data (SAR surface soil moisture, satellite radar altimetry, and GRACE total storage) to calibrate a SWAT model to estimate the surface runoff of a poorly gauged catchment in South Africa. In this study, the surface soil moisture and river stage measurements were acquired through the Envisat satellite, and total water storage changes were estimated through the Gravity Recovery and Climate Experiment

(GRACE) satellite. The SWAT model was calibrated using these data through the generalized likelihood uncertainty estimation (GLUE) method. The predicted results show good model performance on monthly and daily scales, with acceptable uncertainty.

In the study performed here, remotely sensed datasets were used as input into a SWAT model to estimate the historical surface runoff in poorly gauged watershed in northwestern Iraq. Few rain gauges are available in the study area, so satellite-based precipitation data were used as input to the SWAT model. Because of the uncertainty of satellite-based products, the model was calibrated using stream discharge measurements acquired over a 3-monmth period to develop appropriate model input values for temporarily constant variables. This calibrated model was then used with historical records of precipitation from 1982 to 2014 to simulate stream discharge over this time interval. These stream discharge measurements were used to better understand the temporal variability streamflow in this region and to develop hydrological tools such as a duration curve and flood frequency analysis. These tools can be used to better prepare for floods during the brief rainy season that supplies most of the surface water in this region and for groundwater recharge or water storage projects that will provide a more consistent source of water during the lengthy dry season.

2. MATERIAL AND METHODS

The study area is located in northwestern Iraq, in the Hatra sub-watershed, which is within the larger Jezira watershed. The Jezira region is located east of Syria, west of the Tharthar Valley, north of the Euphrates River and south of the Sinjar Mountains (Figure 1). The climate in this region is similar to that of the southwestern United States, with hot and arid summers, cooler winters, and moderate springs and falls. The average monthly rainfall during the wet season ranges between 20 and 50 mm (Figure 2). Most of this precipitation occurs in the northern part of the study area, and approximately 90% of the annual precipitation occurs between November and April, with the greatest concentration of precipitation occurring between December and March. The remainder of the year is dry, especially the during hottest months of June, July, and August, with average temperatures about 32°C (Figure 3 and 4) (National Centers for Environmental Information, 2015).

2.1. DEVELOPMENT OF A HYDROLOGICAL MODEL

The SWAT model is a well-established hydrological model that has been utilized for over 30 years by a variety of researchers (Gassman, Reyes, Green, & Arnold, 2007). The SWAT model requires four sets of inputs: a digital elevation model (DEM), land use/land cover, soil parameters, and weather data. The SWAT model can be used on daily and monthly scales, and uses an ArcGIS interface for the input data (Winchell, Srinivasan, Di Luzio, & Arnold, 2013). SWAT divides the area being modeled into hydrological response units (HRUs), where each HRU is a unique unit in the watershed having a distinctive hydrological property such as soil type, slope, and land cover. To estimate the total runoff of the watershed, the SWAT model estimates the surface runoff of each of the HRUs separately, which increases the model's accuracy (Neitsch, Arnold, Kiniry, & Williams, 2011). (Equation 1) (Neitsch et al., 2011):

$$SWt = SWo + \sum_{i=1}^{t} (\mathrm{R_{day}} - \mathrm{Q_{surf}} - \mathrm{Ea} - \mathrm{w_{seep}} - \mathrm{Q_{gw}}) \qquad \text{Equation (1)}$$

where SWt is the final soil water content; i designates the time period unit of the model, *SWo* is the initial soil water content; t is the time; R_{day} is the total precipitation; Q_{surf} is the total surface runoff; E_a is the total evapotranspiration, w_{seep} is the water that flows through the shallow soil to greater depths in the vadose zone; and Q_{gw} is the water that enters an aquifer and is lost to groundwater flow.

In order to delineate the watershed and sub-watersheds, a digital elevation model (DEM) is the first input required in the SWAT model. Elevation data were clipped from the ALOS World 3D - 30m (AW3D30), with the original data provided by JAXA (Tadono et al., 2014, 2016; Takaku & Tadono, 2017; Takaku, Tadono, & Tsutsui, 2014; Takaku, Tadono, Tsutsui, & Ichikawa, 2016). AW3D30 elevation data were chosen based on the recommendation of Santillan, Makinano-Santillan, and Makinano (2016), who found that these data were more accurate than the SRTM-30m or ASTER GDEM Version 2 DEMs. Using the DEM, the watershed area was determined to be 5353.65 km^2, with a minimum, maximum, and mean ground elevation of 157 m, 1370 m, and 290 m, respectively.

The study area was divided into 33 sub-basins. The DEM was also used to calculate the slope at each point in the watershed, and five categories of slope (0-2%, 2-5%, 5-10%, 10-15% and >15%) were generated. The next SWAT input is land use/land cover. The land cover (LC) information was obtained from the Climate Change Initiative (CCI) (Santoro et al., 2017), founded by the European Space Agency (ESA) to assist in managing and further understanding the changes in global climate. The CCI-LC project has provided global land cover maps for each year from 1992 until 2015 (Santoro et al., 2017), each with a spatial resolution of 300 m.

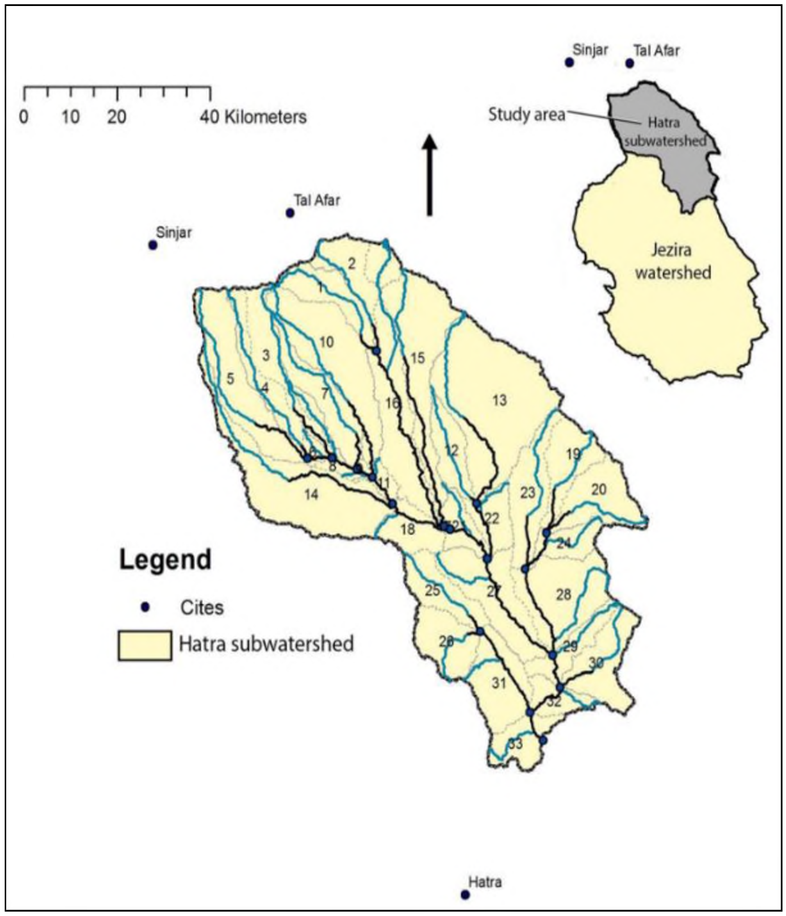

Figure 1. Geographical location of the study area.

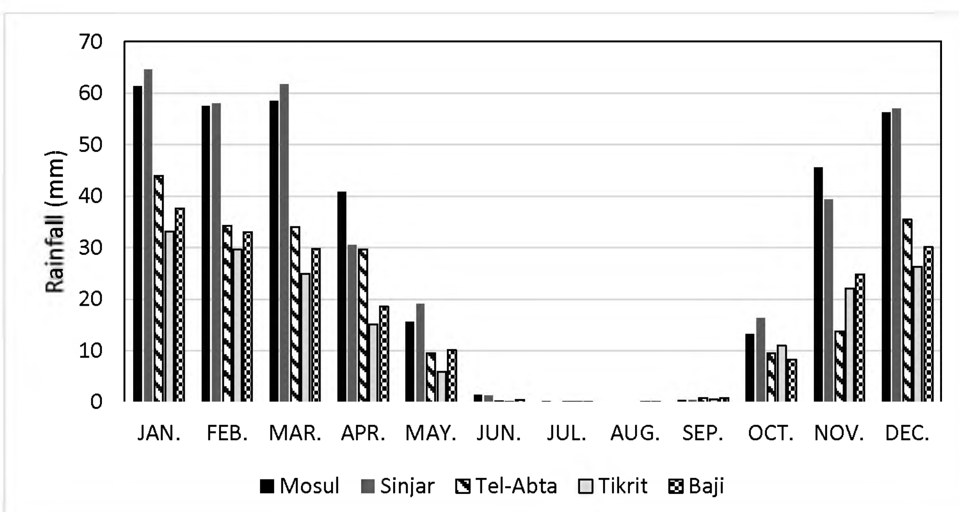

Figure 2. Average monthly rainfall (1981-2011) of the study area.

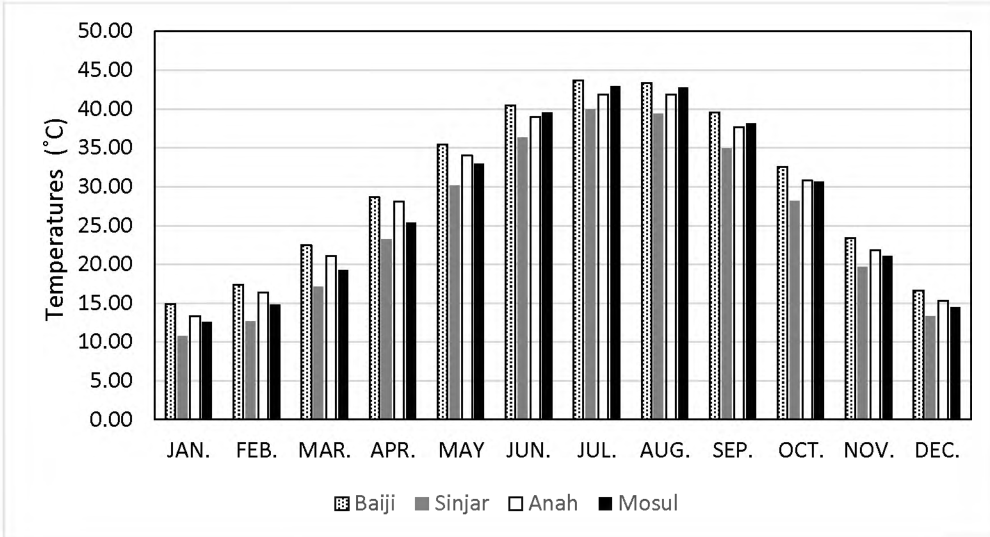

Figure 3. Average maximum temperatures of the Jezira area.

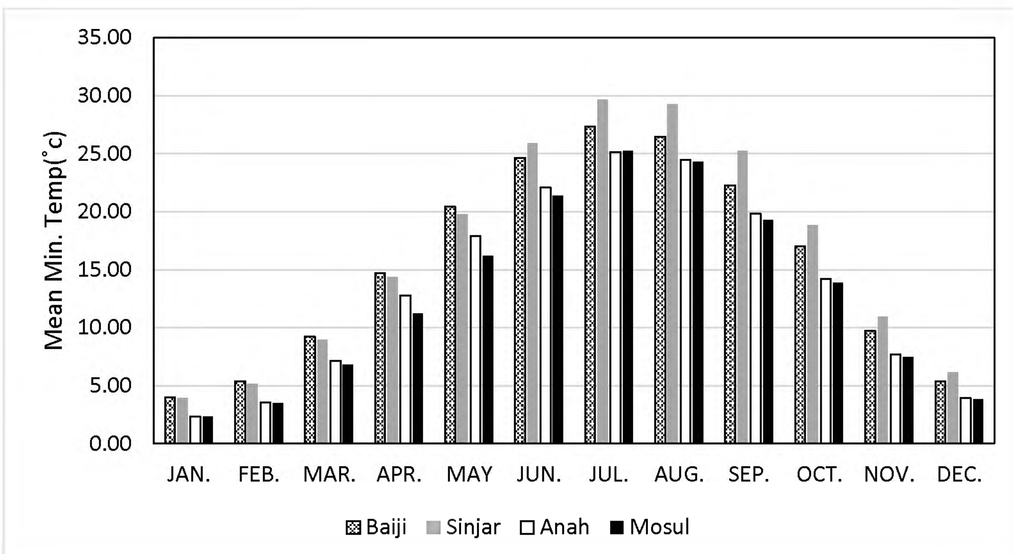

Figure 4. Average minimum temperatures of the Jezira area.

The predominant land cover of the study area is bare ground, largely due to the arid climate. There are also significant areas of irrigated cropland and small sections covered by sparse vegetation (trees, shrubs, and herbaceous plants with less than 15% as pasture/hay) and sparse herbaceous cover (less than 15% of land covered with vegetation) (Figure 5).

Soil properties are also an important input to SWAT. The soil map was extracted from the Food and Agriculture Organization (FAO) Harmonized World Soil Database v 1.2, with 30 arc-second database spatial resolution at a 1:5,000,000 scale (Nachtergaele et al., 2009, 2010). The Harmonized World Soil Database classifies soil according to soil texture. The Hatra sub-watershed's soil is predominantly comprised of three soil types: Calcic Xerosols, Gypsic Xerosols, and Gypsic Yermosols (Figure 6), which are classified as clay loam, clay loam, and loam, respectively. An infiltration capacity must be assigned for each soil classification; for the soils in the study area, the infiltration capacity is relatively low (infiltration is less than or equal to 0.10 cm per hour) for all soil types, so runoff of precipitation is expected to be high (NRCS, 2009).

HRUs are generated on the basis of differing soil, land use/land cover, and slope characteristics. Based on the preceding inputs, the Hatra sub-watershed was divided into 86 HRUs. The average area of each HRU in this study area was approximately 100 km^2.

The preceding model inputs are temporally constant for this study. The last input, precipitation, varies greatly with time and is input as a time series of rainfall. This input is especially important for the SWAT model, as it is the main dynamic variable (Chaplot et al., 2005; Masih et al., 2011). Precipitation data have historically been severely limited in the Hatra sub-watershed, as few very ground-based measurements are available. Therefore, satellite-based rainfall data with large spatial coverage and a long temporal record was chosen to provide precipitation input instead of using very limited rain gauge data. Different satellite-based precipitation data sets are available for this region, and the algorithms and inputs used to estimate precipitation based on satellite data differ for each data set. Thus, the precipitation input varies depending on which data set is chosen. For this study, the Tropical Rainfall Measuring Mission (TRMM 3B42 V7), 3.2. Precipitation Estimation from Remotely Sensed Information using Artificial Neural Networks (PERSIANN-CDR), and 3.1. Climate Forecast System Reanalysis (CFSR) data sets were available for the time period of the study, so the model was created three times, once with each data set. Table 1 shows the sources for all SWAT model input data.

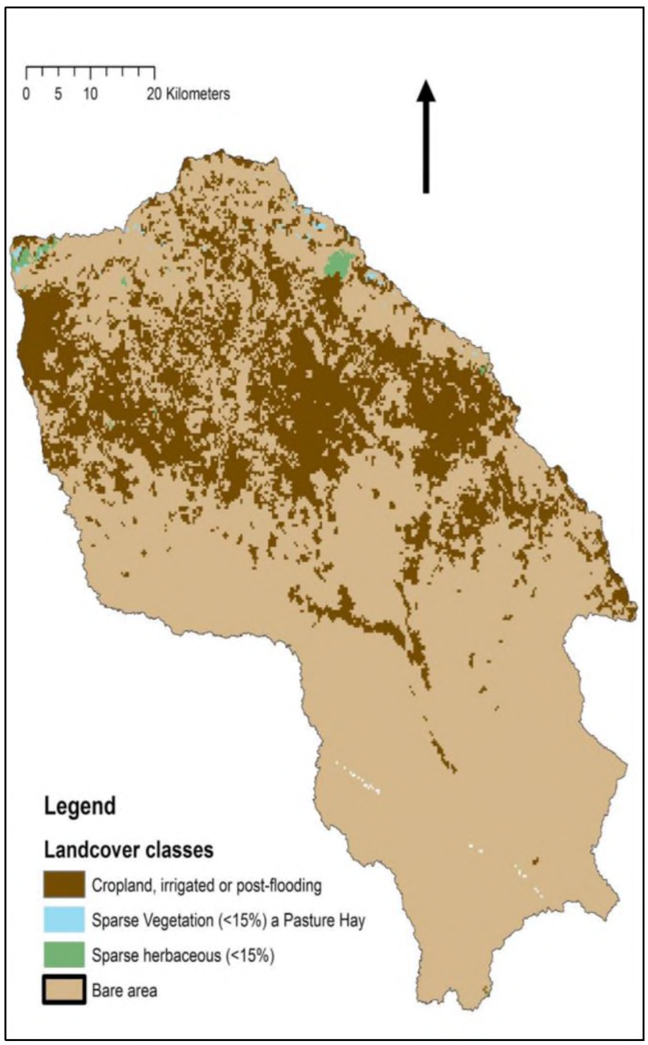

Figure 5. Land cover characteristics derived from the CCI-LC project.

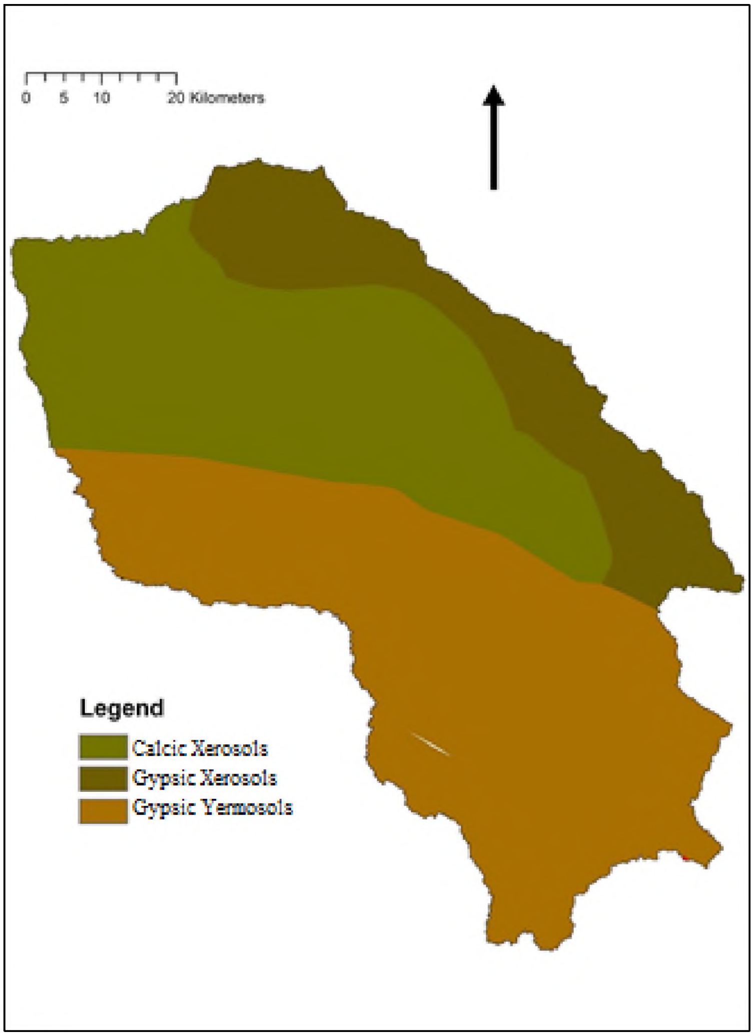

Figure 6. Study area soil map.

2.2. MODEL CALIBRATION

Many hydrological variables are used in the SWAT simulation that are not directly input by the user. Some of these variables are determined by manipulation of the input data (i.e., slopes are calculated based on the input DEM). Other variables are set at initial default values. The first type of model calibration, passive calibration, is performed automatically in the SWAT code. During passive calibration, the SWAT output is evaluated based on expected results for comparable input parameters, and some default values are modified within the program. For this project, passive calibration was performed using five years of precipitation data acquired between 1977 and 1983.

Table 1. Summary of the data sources for the SWAT model inputs.

Data Type	**Resolution**	**Source**
Digital Elevation Model AW3D30	30 m	Japan Aerospace Exploration Agency (JAXA) http://www.eorc.jaxa.jp/ALOS/en/aw3d30/index.htm
CCI Land Cover	300 m	European Space Agency (ESA) http://maps.elie.ucl.ac.be/CCI/viewer/index.php http://maps.elie.ucl.ac.be/CCI/viewer/download.php#usertool
Harmonized World Soil Database v 1.2	30 arc-second raster	Food and Agriculture Organization (FAO) http://www.fao.org/soils-portal/soil-survey/soil-maps-and-databases/harmonized-world-soil-database-v12/en/
Climate Forecast System Reanalysis (CFSR)	0.25 degree	Global Weather Data for SWAT https://globalweather.tamu.edu/

Table 1. Summary of the data sources for the SWAT model inputs (Cont.).

Precipitation Estimation PERSIANN-CDR	**0.25 degree**	**CHRS Data Portal http://chrsdata.eng.uci.edu/**
Tropical Rainfall Measuring Mission (TRMM) 3B42 V7	0.25 degree	Giovanni https://giovanni.gsfc.nasa.gov/giovanni/

The next, more intensive phase of calibration will be referred to as manual calibration. For manual calibration, the simulated stream discharge was output at the mouth of the Hatra sub-watershed. This simulated discharge was compared to discharge measurements conducted acquired at this location by Salih, Abdulrahman, and Saleh (2017) from Nov. 10, 2012 until February 12, 2013. Selected parameters were then modified to reduce the difference between the simulated and measured discharges.

To determine which parameters should be modified to calibrate the SWAT model, a global sensitivity analysis was performed using the SUFI-2 algorithm (Abbaspour et al., 2004, 2007), which was integrated with the SWAT-CUP software (Abbaspour et al., 2012). The sensitivity analysis calculated a statistical p-value for each hydrological parameter. Small values of p are associated with highly sensitive hydrological models, so small changes in these inputs can results in large changes in output. Parameters with a sensitivity analysis p-value of 0.05 or less are considered to have a large impact on the model (Abbaspour, 2007). Sensitivity analysis of this model showed that the model was sensitive to eight parameters that were taken into consideration in the SWAT manual calibration. These parameters, in order of decreasing sensitivity, were the SCS runoff curve number, channel width-depth ratio, specific yield of the shallow aquifer, surface runoff lag time, calibration coefficient used to control the impact of the storage time constant for normal flow, baseflow alpha factor for bank storage, groundwater delay, and the calibration coefficient used to control the impact of the storage time constant for low flow.

2.3. EVALUATION OF MODEL ACCURACY

Model calibration was performed for each of the three satellite-based precipitation data sets. Three metrics were used to compare the accuracy of the different precipitation data sets. The first metric was the Nash-Sutcliffe model efficiency coefficient (NSE):

$$NSE = 1 - \left[\frac{\sum_{i=1}^{n}\left(Y_i^{obs} - Y_i^{sim}\right)^2}{\sum_{i=1}^{n}\left(Y_i^{obs} - Y_{obs}^{mean}\right)^2}\right] \qquad \text{Equation (2)}$$

where Y_i^{obs} is the observed variable, Y_i^{sim} is the simulated variable and Y^{mean} $\bar{O}$ is the mean of the observed variable (Nash and Sutcliffe, 1970) . The NSE is particularly useful for evaluating the quality of a modeled prediction over a period of time and is often applied to hydrological models (Mohammed-Ali et al., 2020). An NSE value of 1 represents a model that perfectly predicts the observed condition. A value of zero indicates that the model will predict the mean value of the observed events, while negative values indicate that a model’s predictions are less accurate than assuming the mean value occurs at all times, which is generally viewed as unacceptable. Models that generate NSE values between 0 and 1.0 are generally viewed as acceptable (Golmohammadi et al., 2014).

The second metric for assessing model accuracy was the coefficient of determination (R^2), which describes the degree of linear relationship between the simulated and observed data (Moriasi et al., 2007). Perfect linear agreement between simulated and observed data results in an R^2 of 1, while no correlation results in a value of 0. R^2 values larger than 0.5 are usually considered acceptable (Santhi et al., 2001; Van Liew et al., 2003)

The third metric was the percent bias (PBIAS) (Equation 3), which measures the tendency of the simulated data to either over- or underestimate the observed data and uses the same variables as the Nash-Sutcliffe model (Gupta, Sorooshian, & Yapo, 1999).

$$PBIAS = \left[\frac{\sum_{i=1}^{n}\left(Y_i^{obs} - Y_i^{sim}\right) * (100)}{\sum_{i=1}^{n}\left(Y_i^{obs}\right)}\right] \qquad \text{Equation (3)}$$

A positive value for the PBIAS indicates that the simulation underestimates the actual value, while a negative value indicates overestimation; a value of 0 indicates no bias.

3. RESULTS AND DISCUSSION

3.1. MODEL ACCURACY

Model accuracy was evaluated for the TRMM, CFSR, and CDR data sets. The model was separately calibrated for each of these data sets, as described above. Table 2 shows the metrics used to evaluate model accuracy for each precipitation data set. This table shows that the model is difficult to calibrate; none of the precipitation data sets have metrics that show a fully acceptable model, and all data sets have a positive PBIAS value, indicating that the models underestimate the actual discharge. The CFSR data set produces the best results and has a relatively low NSE value, but the R^2 is less than 0.5. The TRMM data set produces a negative NSE value, indicating that the model performance is worse than predicting the average discharge, and the R^2 is low. When CDR-based estimates of precipitation are used, the NSE value is slightly negative and the underestimation bias is high, and the correlation with the measured discharge data was so poor that no R^2 value could be established.

Table 2. NSE, PBIAS, and R2 of the three satellite-based rainfall data.

Data set	NSE	PBIAS	R^2
CFSR	0.20	51.9	0.28
TRMM	-1.09	35.74	0.012
CDR	-0.13	100	N/A

Multiple factors may be responsible for the relatively poor model performance. First, the field-based discharge measurements available for calibration are very limited (short term period); a longer time period would greatly facilitate more accurate calibration. Secondly, discharge estimates were obtained using stage measurements and a rating curve, so some inaccuracy exists in the discharge estimates used for calibration.

A third reason could be the "flashy" nature of surface water in this region; discharge was often zero unless a precipitation event had recently occurred. This further reduces the discharge measurements available for understanding watershed properties.

Figure 7 shows the stream discharge estimates for each of the precipitation data sets, as well as the measured discharge. This figure shows that modeled results are often less than those measured in the field (as also evaluated with the PBIAS), and that the timing of discharge often differs between the simulated and measured responses. This latter result is especially interesting, as low NSE and R^2 values can be generated if the timing of discharge differs between modeled and simulated results, but the volumes of water discharged may be more accurate than these metrics would indicate.

This is important if the simulated results are used for applications where the exact date of occurrence is less important than annual totals or discharge magnitudes, such as flood prediction or water storage projects. When the total discharge over the calibration period is considered, the gauge-based measured discharge was 8.5 x 10^7 m^3, while the discharge for the CFSR, CDR, and TRMM data sets were 5.7 x 10^7 m^3, 2.0 x 10^3 m^3, 7.6 x 10^7 m^3, respectively. While the CDR data set is obviously unsuitable, the CFSR and

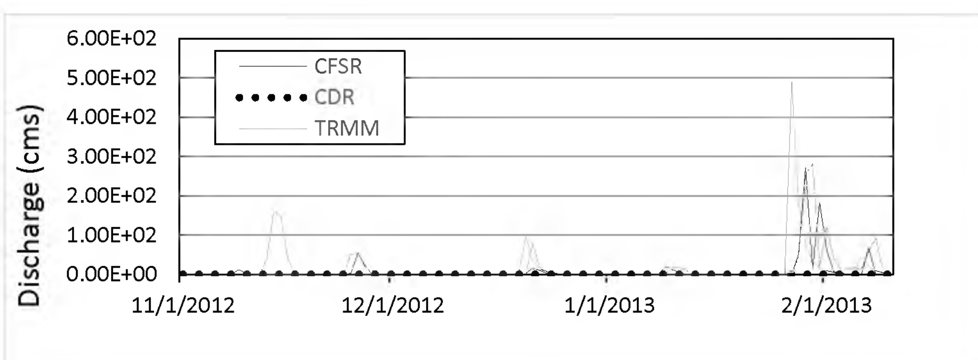

Figure 7. Simulated and measured discharge values for the calibration period.

TRMM estimates are more reasonable than standard time-based metrics might indicate. The percent error for the cumulative discharge for the TRMM and CFSR data sets were 9% and 34% respectively, which indicates that TRMM data might provide a suitable estimate of total discharge but may be less accurate about the specific dates of discharge.

3.2. HISTORICAL SIMULATED DISCHARGE

Water management projects need long-term measurements of parameters such as discharge. Although these measurements do not exist for many watersheds, satellite-based estimates of precipitation are sometimes available. To provide estimates of discharge that could be used in water management projects, simulated discharge estimates were created for the time period for which satellite-based estimates of precipitation were available. For the study area, this time period is 1977 to 2014, but since the first five years were needed for passive model calibration, the simulation period is from 1982 to 2014. Based on the analysis of simulation accuracy, the CFSR were considered to provide the best estimates of discharge with the SWAT model. Accordingly, historical discharge measurements were made over the Hatra sub-watershed from 1982 to 2014 using the CFSR data for the precipitation input. The simulated discharge over this time period is shown in Figure 8.

As shown in the previous figure, discharge in the Hatra watershed can vary significantly from year to year. Most years have relatively modest discharge, but large storm events occur in a few years. To better understand the probability of storm events, and subsequent floods, a flood frequency analysis was done using the largest discharge measurement from each year and employing the Weibull method. The probability of a discharge of a given magnitude or greater is given by p

$$p = 100 * [m / (n + 1)] \qquad \text{Equation (4)}$$

where and n and m are the number of years of data and the rank of the discharge in any one year, respectively. The flood probability graph is shown in Figure 9. While maximum discharge recurrence analysis is important for flood control planning, the average daily discharge is more useful for water supply planning. A histogram showing the distribution of the average simulated daily discharge measurements are shown in Figure 10. This figure shows that the "flashy" nature of the stream observed during the calibration period is typical for this watershed, as most of the time the discharge is very low or zero, and even moderate discharge values occur infrequently.

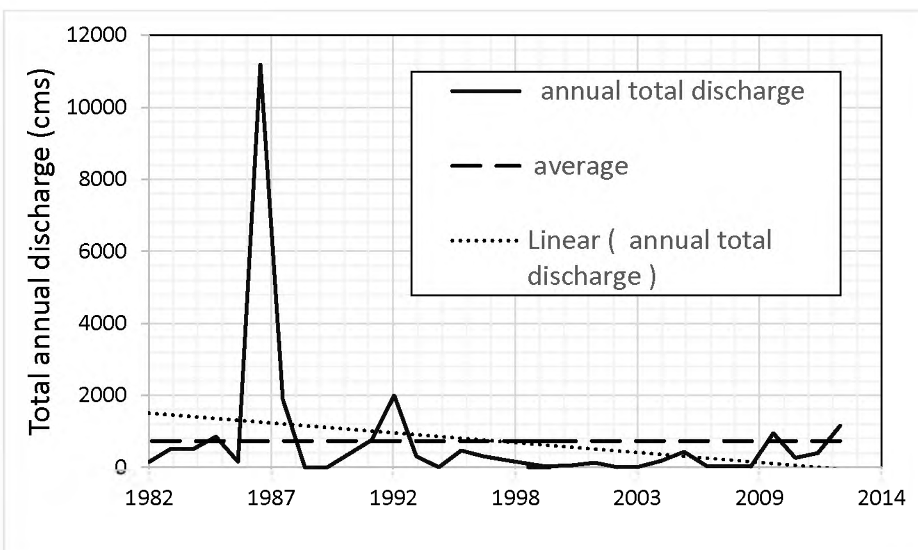

Figure 8. Simulated discharge over the Hatra watershed from 1982-2014.

The simulated daily discharge measurements were also used to create a duration curve of the average discharge in the Hatra watershed (Figure 11). Duration curves are especially useful for water supply planning projects such as aquifer recharge, since they provide more statistical detail than histograms. To construct a daily duration curve that was representative of the entire period of simulated data, a duration curve was calculated for each of the 32 years of the study period, again using the Weibull method. A final duration curve was then constructed by averaging the discharge for each probability in the single-year duration curves. The resulting duration curve provides an average discharge/probability that is more presentative of this watershed than the curves constructed using only one year's worth of data.

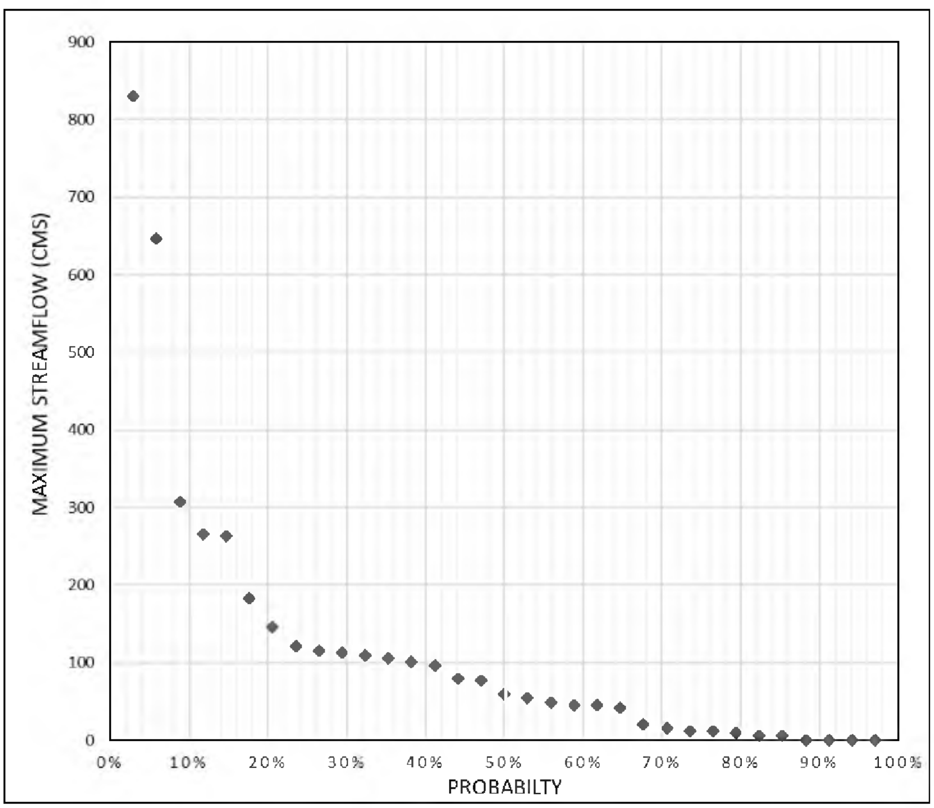

Figure 9. Flood probability curve for the Hatra watershed.

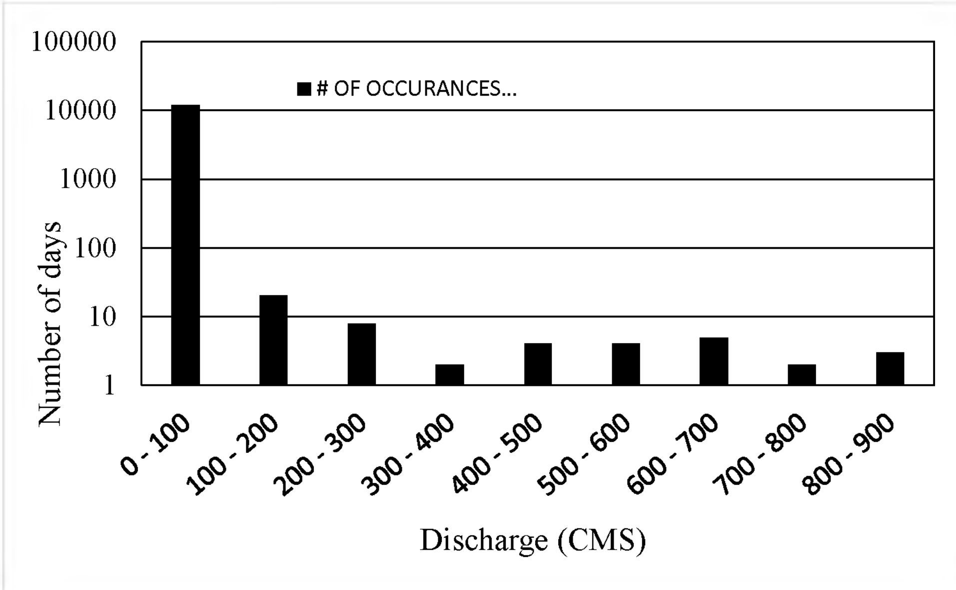

Figure 10. Histogram of simulated discharge for the Hatra watershed outlet, 1982-2014.

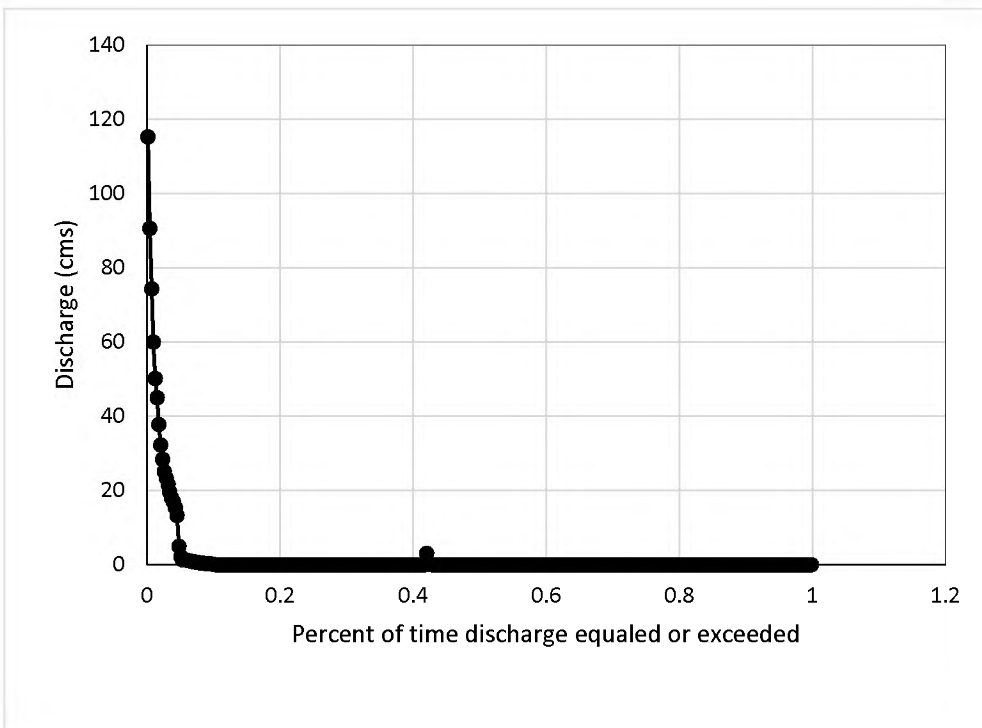

Figure 11. Duration curve using simulated discharge for the Hatra watershed outlet, 1982-2014.

4. CONCLUSIONS

Historical records of stream discharge are needed to develop water management strategies, but these data are not available for most watersheds. This research used historical precipitation records and the SWAT hydrological model to generate a simulated discharge record from 1982 to 2014 for an ungauged watershed in northwest Iraq. Calibration of the hydrological model was difficult, as the period of time when measured discharge was available was quite limited, but sensitivity analysis, applied using the SWAT-CUP (Abbaspour et al., 2012 method, assisted with calibration. Calibration was done using three different precipitation records (CFSR, TRMM, and CDR), and the calibration metrics (Nash-Sutcliffe efficiency, coefficient of determination, and percent bias) showed that output achieved using the CFSR data best matched the measured discharge measurements, although the TRMM data better represented the actual volume discharged. These CFSR data were then used to simulate discharge over the study period, and these discharge measurements were used to develop tools for water management, such as flood recurrence intervals and duration curves.

The results of this study can be used for future engineering projects for water management, such as flood control and aquifer storage projects. The historical discharge record is highly variable on an annual basis (Figure 8); discharge for most years is quite low, but high magnitude flood events in a few years significantly raise the average discharge. This pattern indicates that water management in this watershed will be challenging. Flood control structures may be needed for low frequency but high magnitude events (Figure 9), but average discharge will be low. A duration curve of average flow throughout a year (Figure 11) shows that the discharge is also highly variable on a daily basis, with most discharge occurring in less than 15% of the year. As the primary water problem in this area is water shortage, the duration curve shows that significant structures will be needed to conserve water from large but infrequent precipitation events; the volumes that might be captured can be calculated from the discharge-duration curve.

The hydrological model used here could be improved by better calibration and more accurate inputs. Reliable ground measurements of precipitation would be helpful for assessing the accuracy of the satellite-based precipitation input. Longer term monitoring of discharge at the watershed outlet would also improve calibration. A better-calibrated hydrological model would provide more reliable discharge estimates, but even with the limited data available, the simulated discharge measurements are a useful preliminary tool for water management in this region.

ACKNOWLEDGEMENTS

The authors acknowledge the Ministry of Higher Education and Scientific Research (Iraq) for their financial support. We appreciate the efforts of the Earth Observation Research Center of the Japan Aerospace Exploration Agency for freely providing the ALOS World 3D - 30m (AW3D30) DEM file, and the authors greatly acknowledge all the organizations that were responsible for providing weather data, namely, NOAA’s National Centers for Environmental Prediction (NCEP) for CFSR, Center for Hydrometeorology and Remote Sensing for PERSIANN-CDR data, and the TRMM’s research community. We are also highly appreciative of the European Space Agency (ESA) for providing land use and land cover data free of charge (Climate Change

Initiative - CCI) and also the Food and Agriculture Organization of the United Nations for the Harmonized World Soil Database. The efforts of the SWAT as well as the SWAT-CUP developers are also highly appreciated for making these models and software available to international users.

REFERENCES

Abbaspour, K. C. (2007). User manual for SWAT-CUP, SWAT calibration and uncertainty analysis programs. Swiss Federal Institute of Aquatic Science and Technology, Eawag, Duebendorf, Switzerland, 93.

Abbaspour, K. C., Rouholahnejad, E., Vaghefi, S., Srinivasan, R., Yang, H., & Kløve, B. (2015). A continental-scale hydrology and water quality model for Europe: Calibration and uncertainty of a high-resolution large-scale SWAT model. Journal of Hydrology. https://doi.org/10.1016/j.jhydrol.2015.03.027.

Ahmed Suliman, A. H., Jajarmizadeh, M., Harun, S., & Darus, I. Z. M. (2015). Comparison of Semi-Distributed, GIS-Based Hydrological Models for the Prediction of Streamflow in a Large Catchment. Water Resources Management, 29(9), 3095–3110.

Ang, R., & Oeurng, C. (2018). Simulating streamflow in an ungauged catchment of Tonlesap Lake Basin in Cambodia using Soil and Water Assessment Tool (SWAT) model. Water Science. https://doi.org/10.1016/j.wsj.2017.12.002.

Blöschl, G., Sivapalan, M., Wagener, T., Viglione, A., & Savenije, H. (2013). Runoff Prediction in Ungauged Basins: Synthesis across Processes, Places and Scales. Cambridge University Press.

Deckers, D. (2006). Predicting discharge at ungauged catchments: parameter estimation through the method of regionalisation. University of Twente.

Devia, G. K., Ganasri, B. P., & Dwarakish, G. S. (2015). A Review on Hydrological Models. Aquatic Procedia, 4, 1001–1007.

Gassman, P. W., Reyes, M. R., Green, C. H., & Arnold, J. G. (2007). The soil and water assessment tool: historical development, applications, and future research directions. Transactions of the ASABE, 50(4), 1211–1250.

Gitau, M. W., & Chaubey, I. (2010). Regionalization of SWAT Model Parameters for Use in Ungauged Watersheds. Water. https://doi.org/10.3390/w2040849.

Golmohammadi, G., Prasher, S., Madani, A., & Rudra, R. (2014). Evaluating three hydrological distributed watershed models: MIKE-SHE, APEX, SWAT. Hydrology, 1(1), 20-39.

Gupta, H. V., Sorooshian, S., & Yapo, P. O. (1999). Status of automatic calibration for hydrologic models: Comparison with multilevel expert calibration. Journal of Hydrologic Engineering. Retrieved from https://ascelibrary.org/doi/abs/10.1061/(ASCE)1084-0699(1999)4:2(135).

Ha, L., Bastiaanssen, W., van Griensven, A., van Dijk, A., & Senay, G. (2018). Calibration of Spatially Distributed Hydrological Processes and Model Parameters in SWAT Using Remote Sensing Data and an Auto-Calibration Procedure: A Case Study in a Vietnamese River Basin. Water. https://doi.org/10.3390/w10020212.

Hargreaves, G. H. (1975). Moisture availability and crop production. Transactions of the ASAE. American Society of Agricultural Engineers, 18(5), 980–0984.

Hrachowitz, M., Savenije, H. H. G., Blöschl, G., McDonnell, J. J., Sivapalan, M., Pomeroy, J. W., … Others. (2013). A decade of Predictions in Ungauged Basins (PUB)—a review. Hydrological Sciences Journal, 58(6), 1198–1255.

Irons, J. R., Dwyer, J. L., & Barsi, J. A. (2012). The next Landsat satellite: The Landsat Data Continuity Mission. Remote Sensing of Environment, 122, 11–21.

Jayakrishnan, R., Srinivasan, R., Santhi, C., & Arnold, J. G. (2005). Advances in the application of the SWAT model for water resources management. Hydrological Processes, 19(3), 749–762.

Kavetski, D., Kuczera, G., & Franks, S. W. (2006). Bayesian analysis of input uncertainty in hydrological modeling: 1. Theory. Water Resources Research. https://doi.org/10.1029/2005wr004368.

Liang, S., Li, X., & Wang, J. (2012). Advanced Remote Sensing: Terrestrial Information Extraction and Applications. Academic Press.

Milzow, C., Krogh, P. E., & Bauer-Gottwein, P. (2011). Combining satellite radar altimetry, SAR surface soil moisture and GRACE total storage changes for hydrological model calibration in a large poorly gauged catchment. Hydrology and Earth System Sciences. https://doi.org/10.5194/hess-15-1729-2011.

Mohammed-Ali, W., C. Mendoza, and R.R. Holmes Jr. (2020), Influence of hydropower outflow characteristics on riverbank stability: case of the Lower Osage River (Missouri, USA). Hydrological Sciences Journal, 2020.

Montanari, A., Young, G., Savenije, H. H. G., Hughes, D., Wagener, T., Ren, L. L., … Belyaev, V. (2013). “Panta Rhei—Everything Flows”: Change in hydrology and society—The IAHS Scientific Decade 2013–2022. Hydrological Sciences Journal. https://doi.org/10.1080/02626667.2013.809088.

Moriasi, D. N., Arnold, J. G., Van Liew, M. W., Bingner, R. L., Harmel, R. D., & Veith, T. L. (2007). Model Evaluation Guidelines for Systematic Quantification of Accuracy in Watershed Simulations. Transactions of the ASABE. https://doi.org/10.13031/2013.23153.

National Centers for Environmental Information (2010 – 2016): Local Climatological Data (LCD). Retrieved August 21, 2016, from https://www.ncdc.noaa.gov/cdo-web/datatools/lcd.

Nachtergaele, F., van Velthuizen, H., Verelst, L., Batjes, N., Dijkshoorn, K., van Engelen, V., … Others. (2009). Harmonized world soil database. ISRIC: Wageningen, The Netherlands. Retrieved from https://library.wur.nl/WebQuery/file/isric/fulltext/isricu_t4bb310b7_001.pdf.

Nachtergaele, F., van Velthuizen, H., Verelst, L., Batjes, N. H., Dijkshoorn, K., van Engelen, V. W. P., … Montanarela, L. (2010). The harmonized world soil database. In Proceedings of the 19th World Congress of Soil Science, Soil Solutions for a Changing World, Brisbane, Australia, 1-6 August 2010 (pp. 34–37).

Näschen, K., Diekkrüger, B., Leemhuis, C., Steinbach, S., Seregina, L. S., Thonfeld, F., & Van der Linden, R. (2018). Hydrological Modeling in Data-Scarce Catchments: The Kilombero Floodplain in Tanzania. WATER, 10(5), 599.

Neitsch, S. L., Arnold, J. G., Kiniry, J. R., & Williams, J. R. (2011). Soil and water assessment tool theoretical documentation version 2009. Texas Water Resources Institute.

Noori, N., & Kalin, L. (2016). Coupling SWAT and ANN models for enhanced daily streamflow prediction. Journal of Hydrology, 533, 141–151.

Nrcs, U. (2009). Chapter 7: Hydrologic Soil Groups. Part 630 Hydrology-National Engineering Handbook.

Nyeko, M. (2015). Hydrologic Modelling of Data Scarce Basin with SWAT Model: Capabilities and Limitations. Water Resources Management. https://doi.org/10.1007/s11269-014-0828-3.

Pietroniro, A., & Prowse, T. D. (n.d.). Applications of remote sensing in hydrology. Hydrological Processes, 16(6), 1537–1541.

Povey, A. C., & Grainger, R. G. (2015). Known and unknown unknowns: uncertainty estimation in satellite remote sensing. Atmospheric Measurement Techniques, 8(11). Retrieved from https://ora.ox.ac.uk/objects/uuid:c93ab516-794b-4913-9495-457a94ac86e5.

Rafiei Emam, A., Kappas, M., Linh, N. H. K., & Renchin, T. (2017). Hydrological Modeling and Runoff Mitigation in an Ungauged Basin of Central Vietnam Using SWAT Model. Hydrology, 4(1), 16.

Ribot, J. C., Magalhães, A. R., & Panagides, S. (2005). Climate Variability, Climate Change and Social Vulnerability in the Semi-arid Tropics. Cambridge University Press.

Rivas-Tabares, D., Tarquis, A. M., Willaarts, B., & De Miguel, Á. (2019). An accurate evaluation of water availability in sub-arid Mediterranean watersheds through SWAT: Cega-Eresma-Adaja. Agricultural Water Management. https://doi.org/10.1016/j.agwat.2018.09.012

Roy, S., & Mistri, B. (2013). Estimation of Peak Flood Discharge for an Ungauged River: A Case Study of the Kunur River, West Bengal. Geography Journal. https://doi.org/10.1155/2013/214140

Salih, A. M., Abdulrahman, O. R., & Saleh, S. A. (2017). Innovated Method to Estimate the Water Income in the Section of Tharthar Valley near the Site of Hatra Proposed Dam. Tikrit Journal of Pure Science, 22(6), 88–102.

Santillan, J. R., Makinano-Santillan, M., & Makinano, R. M. (2016). Vertical accuracy assessment of ALOS World 3D - 30M Digital Elevation Model over northeastern Mindanao, Philippines. 2016 IEEE International Geoscience and Remote Sensing Symposium (IGARSS). https://doi.org/10.1109/igarss.2016.7730400

Santhi, C., Arnold, J. G., Williams, J. R., Dugas, W. A., Srinivasan, R., & Hauck, L. M. (2001). Validation of the swat model on a large rwer basin with point and nonpoint sources 1. JAWRA Journal of the American Water Resources Association, 37(5), 1169-1188.

Santoro, M., Kirches, G., Wevers, J., Boettcher, M., Brockmann, C., Lamarche, C., & Defourny, P. (2017). Land Cover CCI: Product User Guide Version 2.0. Retrieved from h ttp://maps. elie. ucl. ac. be/CCI/viewer/download/ESACCI-LC ….

Schmugge, T. J., Kustas, W. P., Ritchie, J. C., Jackson, T. J., & Rango, A. (2002). Remote sensing in hydrology. Advances in Water Resources, 25(8), 1367–1385.

Serbina, L. O., & Miller, H. M. (2014). Landsat and water: Case studies of the uses and benefits of Landsat imagery in water resources. US Department of the Interior, US Geological Survey.

Serbina, L. O., & Miller, H. M. (2014). Landsat and water: case studies of the uses and benefits of landsat imagery in water resources. Open-File Report. https://doi.org/10.3133/ofr20141108

Srinivasan, R., Zhang, X., & Arnold, J. (2010). SWAT ungauged: hydrological budget and crop yield predictions in the Upper Mississippi River Basin. Transactions of the ASABE, 53(5), 1533–1546.

Suliman, A. H. A., Jajarmizadeh, M., Harun, S., & Darus, I. Z. M. (2015). Comparison of semi-distributed, GIS-based hydrological models for the prediction of streamflow in a large catchment. Water resources management, 29(9), 3095-3110.Tadono, T., Ishida, H., Oda, F., Naito, S., Minakawa, K., & Iwamoto, H. (2014). Precise global DEM generation by ALOS PRISM. ISPRS Annals of the Photogrammetry, Remote Sensing and Spatial Information Sciences, 2(4), 71.

Tadono, T., Nagai, H., Ishida, H., Oda, F., Naito, S., Minakawa, K., & Iwamoto, H. (2016). GENERATION OF THE 30 M-MESH GLOBAL DIGITAL SURFACE MODEL BY ALOS PRISM. International Archives of the Photogrammetry, Remote Sensing & Spatial Information Sciences, 41. Retrieved from https://pdfs.semanticscholar.org/d5c2/be3e9f4533b0cd256bad47cbe308cde43229.pdf

Takaku, J., & Tadono, T. (2017). Quality updates of "AW3D" global DSM generated from ALOS PRISM. 2017 IEEE International Geoscience and Remote Sensing Symposium (IGARSS). https://doi.org/10.1109/igarss.2017.8128293

Takaku, J., Tadono, T., & Tsutsui, K. (2014). GENERATION OF HIGH RESOLUTION GLOBAL DSM FROM ALOS PRISM. ISPRS Annals of Photogrammetry, Remote Sensing & Spatial Information Sciences, 2(4). Retrieved from http://www.aw3d.jp/wp/wp-content/themes/AW3DEnglish/technology/doc/pdf/technology_02.pdf

Takaku, J., Tadono, T., Tsutsui, K., & Ichikawa, M. (2016). Validation of“ AW3D” Global DSM Generated from Alos Prism. ISPRS Annals of the Photogrammetry, Remote Sensing and Spatial Information Sciences, 3, 25.

Tang, Q., Gao, H., Lu, H., & Lettenmaier, D. P. (2009). Remote sensing: hydrology. Progress in Physical Geography: Earth and Environment, 33(4), 490–509.

Tian, Y., Peters-Lidard, C. D., Eylander, J. B., Joyce, R. J., Huffman, G. J., Adler, R. F., … Zeng, J. (2009). Component analysis of errors in satellite-based precipitation estimates. Journal of Geophysical Research. https://doi.org/10.1029/2009jd011949

Van Liew, M. W., Arnold, J. G., & Garbrecht, J. D. (2003). Hydrologic simulation on agricultural watersheds: Choosing between two models. Transactions of the ASAE, 46(6), 1539.

Wagner, P. D., Kumar, S., & Schneider, K. (2013). An assessment of land use change impacts on the water resources of the Mula and Mutha Rivers catchment upstream of Pune, India. Hydrology and Earth System Sciences Discussions. https://doi.org/10.5194/hessd-10-1943-2013

Watson, R. T., & Zinyowera, M. C. Moss. RH (1996) The Regional Impacts of Climate Change: An Assessment of Vulnerability. REPORTS-SPECIAL REPORTS, Cambridge: Cambridge University Press.

Wheater, H. S., Mathias, S. A., & Li, X. (2010). Groundwater Modelling in Arid and Semi-Arid Areas. Cambridge University Press.

Wheater, H., Sorooshian, S., & Sharma, K. D. (2007). Hydrological Modelling in Arid and Semi-Arid Areas. Cambridge University Press.

Winchell, M., Srinivasan, R., Di Luzio, M., & Arnold, J. (2013). ArcSWAT (2013) interface for SWAT 2012--User’s guide. Blackland Research and Extention Center Texas Agrilife Research & Grassland.

III. DELINEATE POTENTIAL ZONES OF GROUNDWATER RECHARGE IN SEMI-ARID REGION

Majid Sueed Mohamod[1, 2] and Katherine Grote[1]

Department of Geosciences and Geological and Petroleum Engineering, Missouri University of Science and Technology, Rolla, MO, 65401

College of Science, University of Tikrit, Salahdin, Iraq

ABSTRACT

All around the world the demand for water is increasing, especially in arid and semi-arid regions. Thus, it's crucial to have a better strategy for water management. One of these strategies is to promote groundwater recharge for restoring the aquifer depletion. The successful groundwater recharge is limited by selecting the right sites or zone of groundwater recharge. The study area geology consists of clastic sedimentary rock (i.e claystone, sandstone, siltstone, and limestone) within Injana formation. Gypsum rock also existed in the area which belong to Fat'ha formation. We have used in this study, satellite data integrated by GIS tools, to indicate the favorable zones of groundwater recharge, in the Hatra subwatershed, North western Iraq. Several thematic layers were prepared for the purpose of groundwater recharge suitable zones which are: soil type, lineament feature density, stream buffering distance, depth to groundwater, the annual flow in subbasin, stream density, and the geology of the study area. Each layer has assigned to a weight based on its importance as a control factor in groundwater recharge. The weight ranged between 1 to 5, where 1 is less of an influence factor, and 5 is the most influential factor. The total score of each pixel in the study area was estimated through summing up

the overlapping of each assigned weighted thematic layer. The results show that 11% (area km2) of the study area considered as excellent zones for groundwater recharge. 21% of total area (area km2)indicated as good zone, 23% classified as moderate suitable for groundwater recharge, and finally 45% (area km^2) considered poor area. Low grade suitability could be enhanced by using some engineering project.

1. INTRODUCTION

Arid and semi-arid regions subject to cycles of high intense rainfall could cause huge floods, followed by sudden drop in precipitation which leads to droughts periodically. In addition, Water resources deficiency has created challenges globally particularly in these regions, which make the groundwater the most needed source of freshwater worldwide. Therefore, better water management in such regions are crucial and have been improving constantly,one of these practices is to promote groundwater recharge during the wet season help to increasing a longer-term groundwater supplies for later extraction during the drought seasons (Gale 2005, Dillon et al. 2009; Maliva and Missimer 2012; O'Leary et al. 2012, Russo, Fisher, and Lockwood 2015, Das and Pardeshi 2018),) One of the advantages of ground storage is limiting water losses by evaporation as well as improve groundwater quality (Russo, Fisher, and Lockwood 2015) (Ma and Spalding 1997).

Success groundwater recharge project is depending totally on how accurate the groundwater potential delineation (Ahmadi, Mahdavirad, and Bakhtiari 2017). Indicating suitable zones for groundwater recharge through traditional methods by using field testing is difficult and time consuming as groundwater is subsurface flow, it will require numerous field measurements in this matter. For these reasons, using the indirect method to locate groundwater potential zones is more efficient, which relies on analysis several satellite-derived surface features data such as soil texture, drainage pattern and density, lineament features, landuse and land cover, surficial lithology, and some satellite-based precipitation measurements (Sander et al. 1996; Nag 2005; Sener et al. 2005; Solomon and Quiel 2006;Ahmed, Jayakumar, and Salih 2008 ; Ganapuram et al. 2009; Singh et al. 2011b; Magesh et al. 2012; Mukherjee et al. 2012; Russo, Fisher, and Lockwood 2015; Russo, Fisher, and Lockwood 2015; Ahmadi, Mahdavirad, and Bakhtiari 2017;Das et al. 2017, 2018; Das and Pardeshi 2018b). Many hydrogeomorphology features can be processed and integrated into variety hydrogeomorphology thematic layers, to identify groundwater potential zones with accuracy and time-consuming efficiency, (Tiwari et al. 2017). (Bhowmick, Mukhopadhyay, and Sivakumar 2014) (Tiwari et al. 2017) (Bhowmick, Mukhopadhyay, and Sivakumar 2014)

“GIS has emerged as a useful computer tool for handling / a large volume of data, both spatial and temporal, Thus, the integrated application of RS and GIS techniques provides potentially powerful tools to study groundwater resources and design a suitable exploration plan. / analyzing water-resources systems in general and groundwater systems in particular, (Stafford 1991; Goodchild 1993).”Several studies have applied remote sensing and GIS techniques to delineate groundwater potential zones all over the world (Raj and Sinha, 1989; Champati et al., 1993; Krishnamurththyet al., 1996; Saraf and Chaudhary, 1998; Shahid et al., 2000). , Jaiswal, 2003) Solomon and Quiel 2006; Agarwal, P. K. Garg and R. D. Garg

The surficial features of the ground impact the ground infiltration rate (e.g. slope, lineament density, drainage density, soil type and surficial lithology). The subsurface flow of groundwater also is controlled by the aquifer hydrological characteristics such as permeability and porosity (Bagyaraj et al. 2013)(Das and Pardeshi 2018)

In recent years, many works have been done to identify groundwater potential zones. For example, some researchers have used multi-criteria decision analysis techniques field measurements such as Jha et al. (2010) where several thematic layers have process and integrated through ArcGIS environment (i.e. slope map, elevation data, geomorphological features, soil and geological information, depth to groundwater, annual net recharge, annual rainfall) (Machiwal, Jha, and Mal 2011) a similar method was used by (Ghayoumian et al. 2005) (Chenini, Ben Mammou, and El May 2010) (Salar, Othman, and Hasan 2018) (Mukherjee et al. 2012; Kumar et al. 2014; Machiwal and Singh 2015; Das et al. 2017), Deepesh Machiwal P. K. Singh (2015). Weighted overlay analysis Identification of Artificial Recharge Sites (Selvarani et al. 2017)(Selvarani et al. 2017; Saraf and Choudhury 1998)(Salar, Othman, and Hasan 2018)(Machiwal, Jha, and Mal 2011)(Jasrotia, Majhi, and Singh 2009)(Ghazavi, Babaei, and Erfanian 2018) Fuzzy logic studies have been done by (Tiwari et al. 2017), to determine areas most suitable for artificial recharge using GIS-based fuzzy logic approach. Another method is using the true or false Boolean logic method with several thematic layers classified, weighted and integrated in ArcGIS environment, (Riad P. et. al., 2011).

The objectives of this study is to determine zones of groundwater potential in Heather subwatershed using remote sensing and GIS techniques. Several thematic layers were prepared including the depth to groundwater, lineament feature density, stream density, the distance from the stream, geological map, soil types and the annual subasin-flow in. ArcGIS was used to integrate these data and identify the suitable zones of groundwater recharge.

2. METHODOLOGY

2.1. LOCATION AND THE GEOLOGY OF THE STUDY AREA

The study area is located near Hatra city north-west Iraq, part of Jezira watershed which we have named it by Hatra sub-watershed. Jezira watershed falls between the boundary Eurphrate river from the south and Sinjar mountains from the north, Tharthar valley from the east and Syria from the west, (Figure 1). The area climate classified as arid and semi-arid based on the Köppen climate classification. Average annual rainfall of Jezira region was calculated using the average monthly rainfall that is estimated by Iraqi Meteorological Organization and Seismology between 1982 and 2012, which varies between 150 and 500 mm.The rainiest region happens in the northern part of Hatra sub-watershed and decreases towards the southern parts of the region. The study area climate is similar to south-western USA climate such as orange county in California state, which is characterized by hot and dry summers, cool winters, and most rainfall occurs during between November and April The remaining half of the year is dry, especially the hottest months are June, July, and August, with a monthly average temperature of 32° C.

Lithology of Jezira area goes back to Neogene period which form out of two informations which are; Injana and Fat'ha formations. Fat'ha formation comprises of thick layer of gypsum with thickness of 14m overlay on top of limestone and dolomitic limestone with thickness ranges between 1.7-7m, the bottom layer is comprised of marl and mudstone with thickness of 3m (Ma'ala, 1976) When the Fat'ha formation meet the surface/expose that cause a groundwater discharge /springs, along Tharthar valley there are about 25 spring (Krasny et al., 2006) Piezometric levels indicate the water bearing horizons are hydraulically connected with each other.

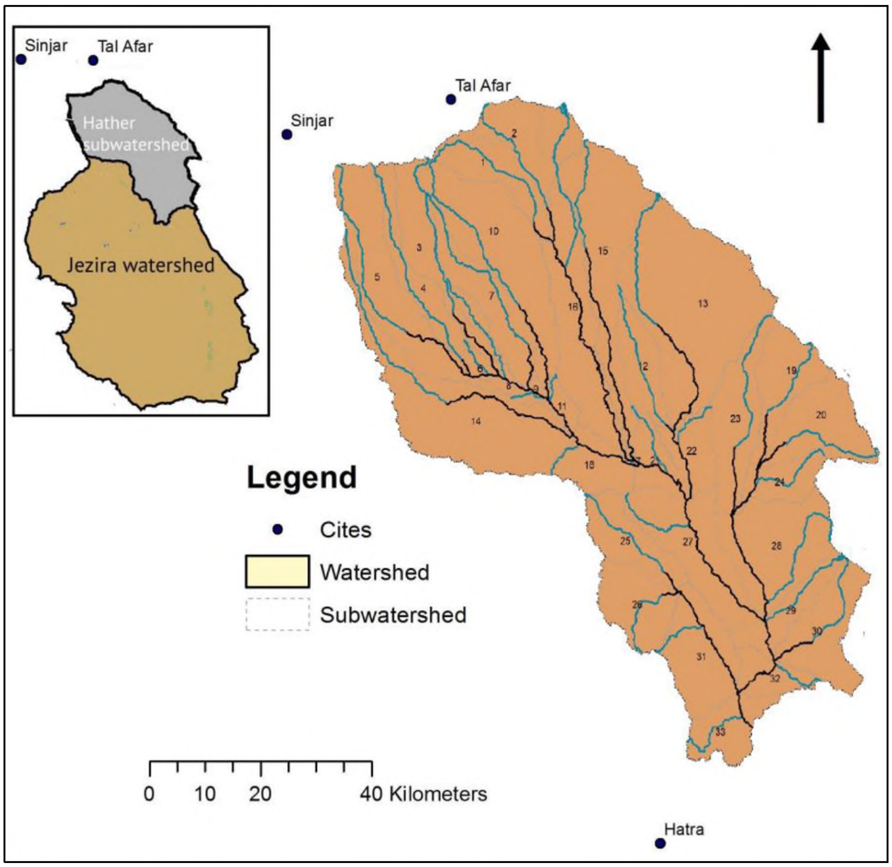

Figure 1. Geographical location of the study area.

The Injana formation comprises of sandstone, limestone, siltstone and claystone. Injana formation is exposed within the northern part of the study area as well as along Tharthar valley and the south of the region where the Tharthar Lake is located. Fat'ha formation exposed in the middle and southern areas of Jezira region.

The lithology of study area comprised of Injana, and Fat'ha formations (refer to study area lithology's section number). Injana overlay over Fat'ha formation. Choosing Injana formation as zone where the water will seep through will help to decrease the gypsum solubility due to the clastic materials of Injana formation as well as the calcium bicarbonate ion which generates due to the carbonate rocks in injana formation, all of that will increase the quality of extracted groundwater in future use.

2.2. MATERIALS AND METHODS

In order to study subsurface water through satellite data and some field measurement, there is a direct relationship between groundwater and some hydrogeomorphology features of the basin (Devi et. al., 2018) Throughout reviewing previous work in this field (Xu et. al., 2002; Nag, S. K. 2005; Dar et. al., 2010; Teixeira et. al., 2013), revealed that surface water infiltration influence by several hydrogeomorphology parameters such as length of the drainage net,, relation of the drainage net to the basin area, lithology, slope, relief aspects of the basin, land use land cover (LULC), rainfall, groundwater depth, drainage density, landform, lineament density, elevation, and topographic position index (TPI) (). We also concluded that each study area characterizes in specific potential parameters that have an effect on groundwater recharge, particularly in that area only. The hydrogeomorphology parameters were considered in this study were; the distance from the streams, vadose zone thickness, the average annual flow in in each subbain, soil texture, surficial lithology, and lineament density.

GIS techniques were employed in this study for zoning area suitable for groundwater recharge used for future projects of Hatra subwatershed. Each factor has weighted based on expert opinion to the size of influence of this factor to control groundwater recharge project. The total weight of each pixel comes by summing the overlaid/overlay weights of all factors on that pixel. A pixel with a higher total weight will appear as good zone for groundwater recharge.

The Food and Agriculture Organization (FAO) Harmonized World Soil Database v 1.2 was used to generate the soil texture map with spatial resolution of 30 arc-second (1:5 000 000 scale), (Nachtergaele et al. 2009, 2010). This database relias on the soil regional and national information combination to map soil units, (Nachtergaele et al. 2010).The soil map classified soil into particles size classes, (sand, clay, loam, etc.) coarse textured soils consist of sand sized particles, finer texture is related to clay size, while medium texture could contain silt size particles, (Nachtergaele et al. 2010).

The study area predominated by 3 soil types (Figure 2), which are; calcic xerosols, gypsic xerosols, and gypsic yemosols. The northern and southern part of the study area tend to be covered by gypsic soil, meanwhile, the middle part of region covers by calcic soil. We are trying to avoid the gypsic soil as recharge zone in the current study, despite of their high groundwater infiltration, but gypsic soil tends to be high soluble in water which give high possibility of groundwater pollution. Accordingly, the clcic soil as preferable zone of groundwater recharge. In addition, the clastic materials which coming from non-gypsiferous soil zones can help to improve the water quality because these materials would work as a coating materials to the fractures in gypsum aquifer, because gypsum rock are more soluble in clear water than water carry clastic materials (which help to reduce the soluble rate in hence increase water quality). Therefore, it has been considered the area with gypsiferous soil is not suitable for recharge in the first place.

Another factor controls surface water infiltration is lineament density especially where the main formations comprised of hard rocks, then the movement and occurrences of groundwater depends mainly on the secondary porosity and permeability which resulting from folding and fracturing etc. Therefore, the most obvious structural features that are important from the groundwater point of view are the lineaments, (Mohmood, A., 1996; Koch, M., & Mather, P. M., 1997; Subba Rao et al., 2001). Accordingly, lineament density could relate with high surface water infiltration zone, in general, a zone with distance of 300m or less from a lineament consider an acceptable zone for groundwater recharge (Krishnamurthy et al., 2000). (J. Krishnamurthy et. al., 1993)

Satellite technology has been improved for the last three decades, now we are able to study structural geology and geomorphological features through remote sensing and geographic information system techniques, and as a very powerful tool to study groundwater . (e.g. Krishnamurthy et. al. 1996; Sander 1996; Saraf and Choudhury 1998). The lineament density of study area were prepared from the available 1:100,000 lineament thematic map, (Figure 3) (Shamaa, 2001), which was extracted using remote sensing techniques.

Lineament density represents the total length of lineaments in a unit area (Yeh et. al., 2016). Generally, three distinctive lineament feature directions which are 260°, 45° and 0° are presented in the study area. We had assigned more weight on higher density lineament density, as higher density lineament zones are favorable region for groundwater recharge. Lineament density map was prepared using ArcGIS and classified into four classes (Figure 4).

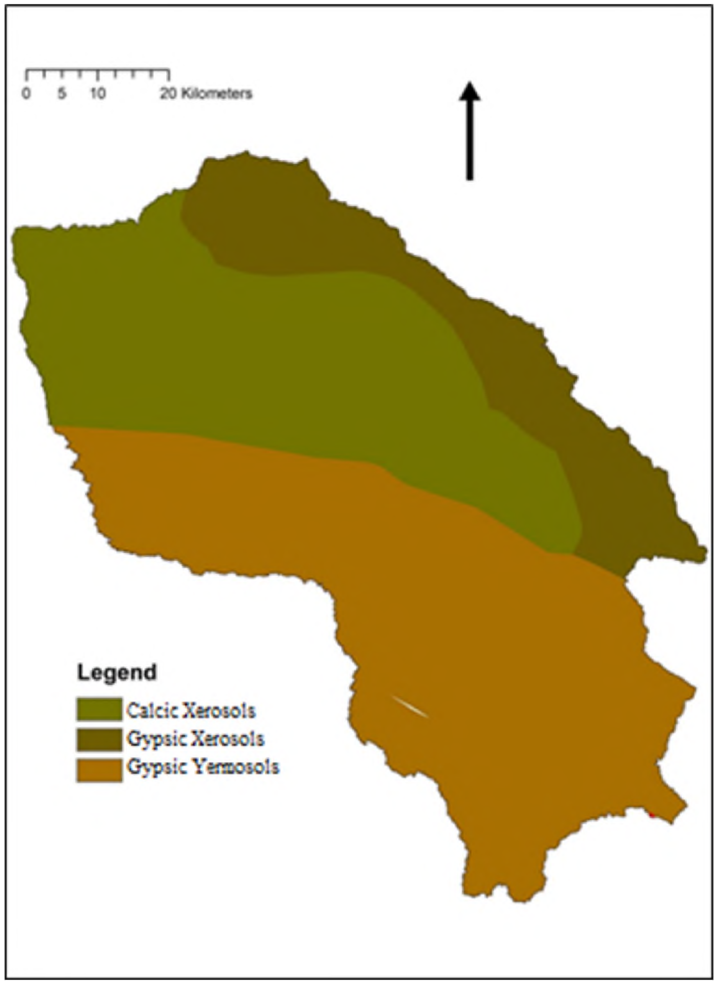

Figure 2. The soil map of Hatra subwatershed.

Another factor considered in this study, the depth to groundwater. This information was collected by (Al-Jiburi, 2004 a and b). Groundwater table level is ranging between 10-49m . ArcGIS was used to generate grids of depth to groundwater thematic layer. It has noticed that the deepest groundwater table is in the center of the study area (Figure 5). We had also used the annual average surface water flow of each

HRU. The water flow in data was generated using SWAT model (Sueed and Grote, 2020) in the previous project on the same watershed.

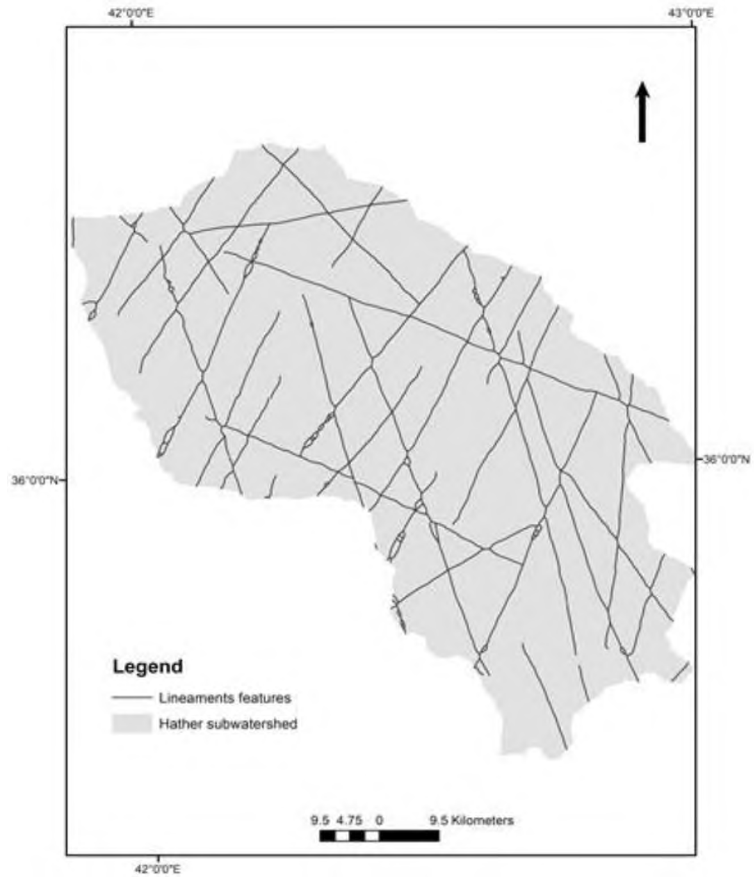

Figure 3. Study area lineament thematic map.

This parameter is important to determine the importance of groundwater recharge in particular sub-basin. However, if there are two consecutive sub-basins surface water flow from one to the other, increase groundwater infiltration in the first one will reduce the flow in surface water to the other, as a result, will decrease the groundwater recharge importance in the next sub-basin, (Figure 6).

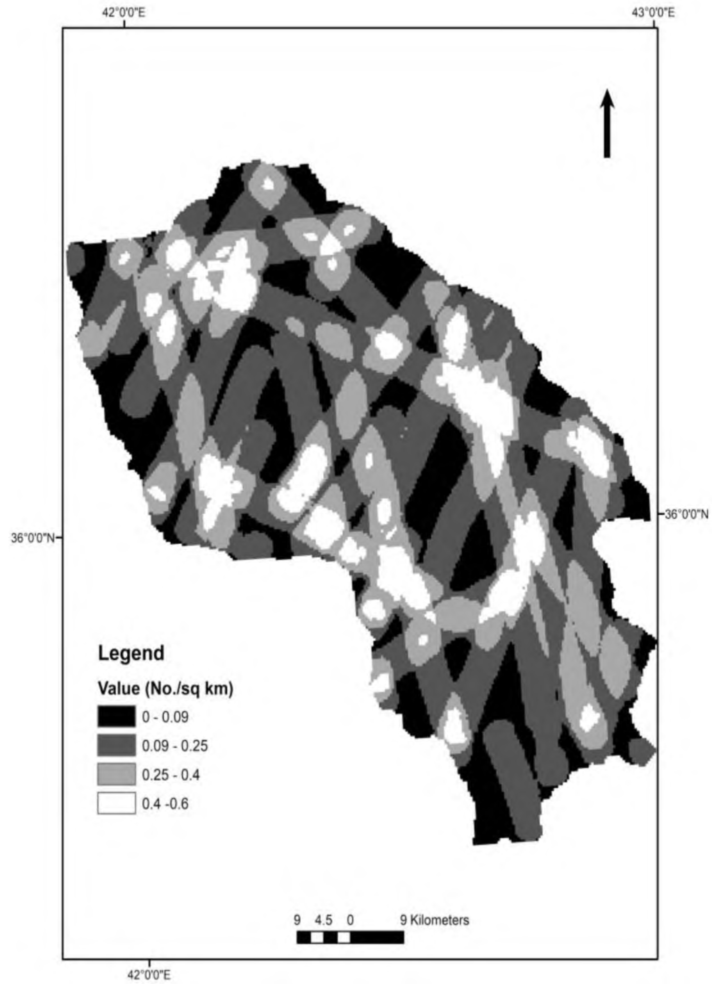

Figure 4. Lineament density map.

2.3. WEIGHTED INDEX OVERLAY ANALYSIS

Each thematic layer has converted to a raster to be treated in ArcGIS software. These rasters have been weighted based on previous studies and application of these studies to this site (Tess A. et. al., 2015; Andualem T. et. al., 2019) (Table 1). The overlaid weighted procedure is a straightforward method that was applied by using ArcGIS environment tool. Each thematic layer received a rank based on previous work in this matter as well as based on the researcher view to define the importance of each parameter. More important is the relative potential of each of these parameters.(influence of that particular feature on the hydrogeological environment of the area), thus there is no standard can be used for the thematic layer rank, rather than using human judgment in this matter, (Krishnamurthy et al., 1996; Saraf and Choudhary, 1998; Saraf and Chowdhury, 1998). Five range levels were used for the thematic layers where 1 indicates (assigned as) less important and 5 is the most important. The overall weight come by summing all overlaid rank levels.

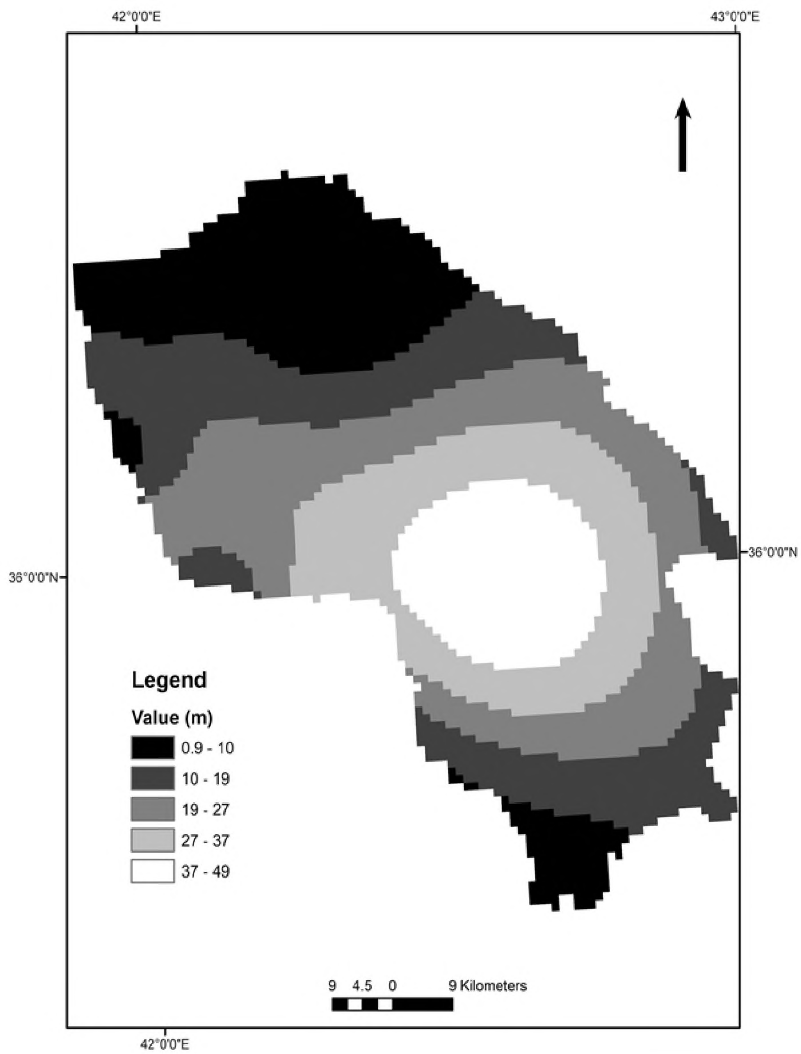

Figure 5. Water table level map.

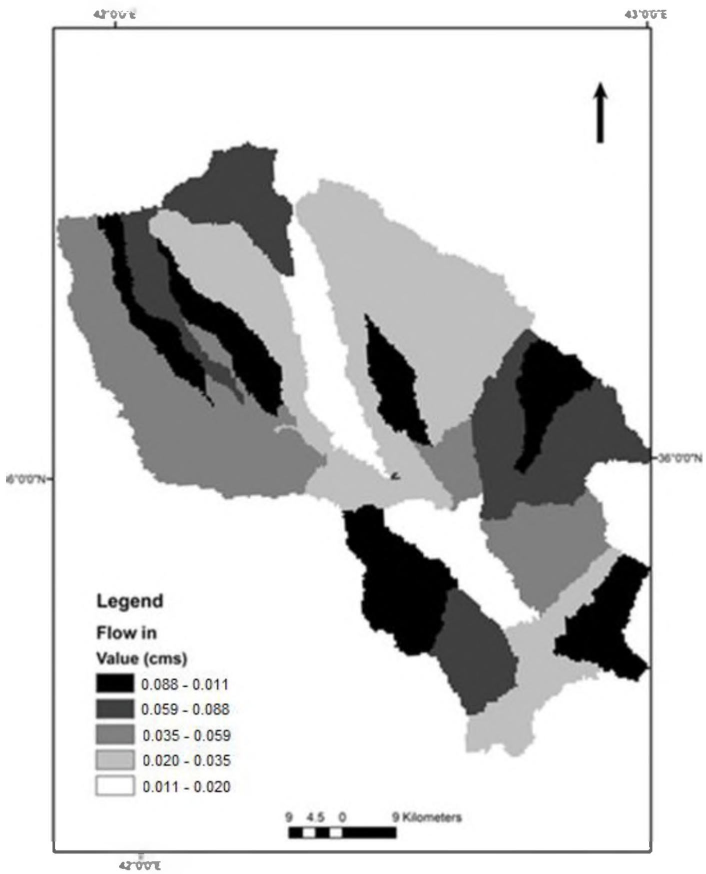

Figure 6. Annual average surface water flow.

Table 1. Hematic layer relative weight.

Factor	Description	Relative weight
Soil type	Soil type will control the groundwater quality in the area. A higher weighting was given to clastic soil, than gypsic soil due to the possiblie contamination the latter can cause.	Clastic soil: 5 Gypsiferous soil: 1

Table 1. Hematic layer relative weight (Cont.)

Lineaments density	A higher density if lineaments means higher possible groundwater infiltration. Therefore, a high lineament density is favorable for artificial groundwater recharge.	Low density (0-0.37 km^{-1}): 1 Moderate density (0.37-1.08 km^{-1}): 2 High density (1.08-2.96 km^{-1}): 3 Jasim and Mallikarjuna (2011), Dar et al.(2010)
Formation Lithology	We prefer infiltration into the Injana formation to change the chemistry of the water to carbonate, which will reduce the gypsum solubility.	Injana formation: 5 Fat'ha Formation: 3
Depth to Groundwater	Greater depth to groundwater could have room for more infiltration.	Class 5 (37-49m) Class 4 (27-37m) Class3 (19-27m) Class 2 (10-19m) Class1 (1-10m)
FlowIn	Annual water budget is the main factor in this study.	Flow 20-30 cubic meter: 5 Flow 20 -0: 1

Table 1. Hematic layer relative weight (Cont.)

Distance from stream	It's important to locate the engineering project of groundwater recharge on the stream, to avoid the private property and it's more efficient in terms of water collection	500 m: 3 1000 m: 2 5000 m: 1

3. RESULT AND DISCUSSION

Six hydrogeomorphology were applied in this study which are; lineament density, stream buffering, average annual subbasin flow in, vadose zone thickness, soil texture, surficial lithology. These parameters have weighed from one to five based on their expected impact on groundwater recharge. One is less impact and five is the most impact parameter on groundwater recharge. These parameters have been integrated in ArcGIS environment to generate a final suitability map. Higher total weight means a more suitable area for groundwater recharge than other regions (which indicates a higher groundwater potential over an increasing value of/had a higher groundwater potential). Lineament density classified into four ranges, (0-0.09, 0.09-0.25, 0.25-0.4, 0.4-0.6 km./sq km) higher value of lineament density is favorable zone for groundwater recharge. The depth to groundwater is grouped into five levels (0.9-10, 10-19, 19-27, 27-37, 37-49 m), higher depth gives higher storage for groundwater. Annual stream discharge of subbians of the Hatra subwatershed have been estimated by Majid and Grote (2020). High flowin has located in the middle of the study area which ranges between 143 to 241 cms. In terms of the surficial lithology and soil texture, the clastic sediments of injana formation and study area's soil are preferred as groundwater zone. The slope parameter was dismissed in this study, because 96% of the study area has slope ranges between 0-5 degrees.

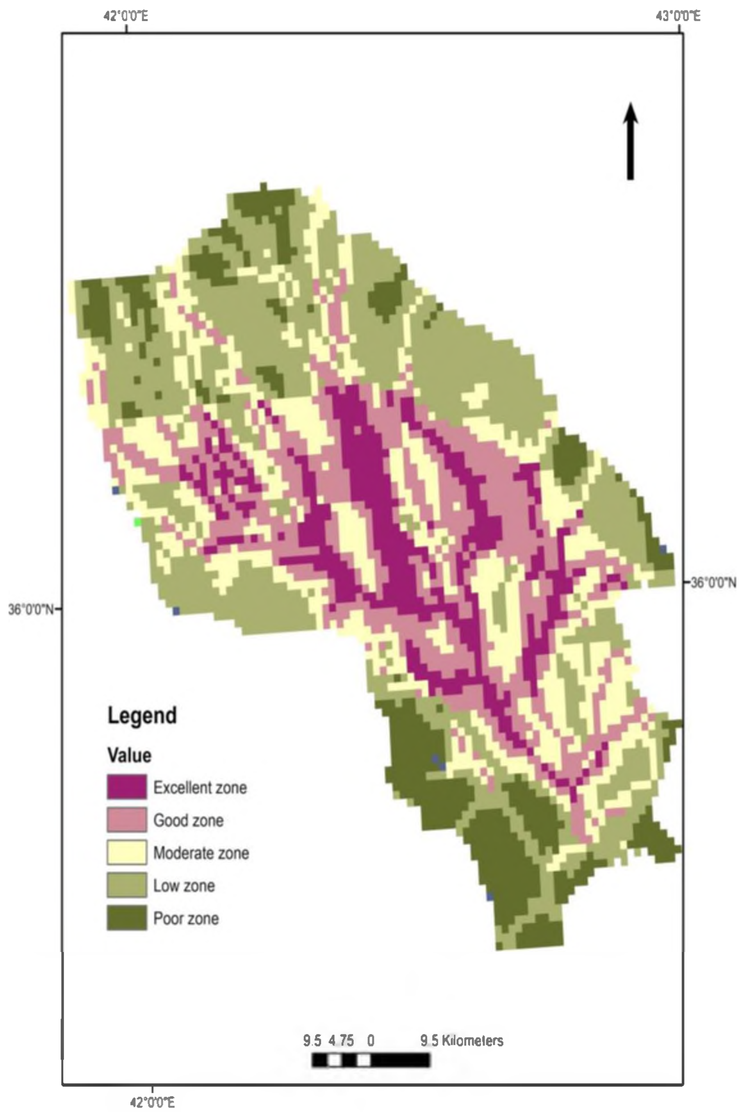

Figure 7. Groundwater recharge zone suitability map.

The suitability map has been generated by integrating these important hydrogeomorphology factors. The results of groundwater recharge suitability zones (Figure 7) have been classified into five grades; Excellent, Good, Moderate, Low, and Poor zones. The results indicate that 11% of the study area classify as an excellent zone of groundwater recharge, which demonstrate as promising region for groundwater recharge, which has dark purple color, it is characterized by high lineament density, short buffering distance, receives high annual surface water, has higher thickness of vadose zone, and has preferable soil and rock materials. An area of 21% classified as good zones of groundwater recharge. Soil, lineament density, and annual water flow-in in the basin, all played a role to reduce the suitability for this region. The analytical results show that 23% of the study area has a grade of moderate suitability. The main factor affecting this zone is the distance from the main channel. In this study valleys are always a favorable zone for groundwater recharge as unused land or own by locals, also they are excellent areas to collect surface water. About 45% of the land range between low to poor zones for water recharge purposes.

4. CONCLUSIONS

In regard to the (purposes of) groundwater investigations, it's recommended to start indicating groundwater recharge zones as an initial step before completion of groundwater subsurface exploration (Shaban 2003). We had demonstrated in current study a delineation of groundwater recharge potential (The current study carries out an analysis of groundwater potential of Jazira area.) by using hydromorphology thematic layers were extracted from satellites which indirectly affect the groundwater recharge (e.g. surficial lithology, soil type, drainage, lineament features), in addition to some field data, all together was integrated with GIS environment in Hatra subwatershed in north-western Iraq. The overly weighted method was operated to classify the regions into five classes ranging from excellent to poor zones for this purpose. The Geographic Information System has proven in this study as an effective method to handle multiple data sets and allows them to correlate spatially and better decision-making water management.

ACKNOWLEDGMENTS

The authors acknowledge the Ministry of Higher Education and Scientific Research (Iraq) for their financial support. We appreciate the efforts of TRMM's research community, Center for Hydrometeorology and Remote Sensing for PERSIANN-CDR data, and NOAA's National Centers for Environmental Prediction (NCEP) for CFSR. We are also highly appreciative of the SWAT model community to make this model accessible for research. We also think the Food and Agriculture Organization of the United Nations for the Harmonized World Soil Database.

REFERENCES

Ahmadi, M. M., Mahdavirad, H., & Bakhtiari, B. (2017). Multi-criteria analysis of site selection for groundwater recharge with treated municipal wastewater. *Water Science and Technology*, *76*(4), 909-919.

Ahmed, S., Jayakumar, R., & Salih, A. (Eds.). (2008). *Groundwater dynamics in hard rock aquifers: sustainable management and optimal monitoring network design*. Springer Science & Business Media.

Al-Jiburi, H.K.S., (2004a) Hydrogeological and hydrochemical study of Sur Quadrangle, sheet NI-37-4, scale 1: 250 000. GEOSURV, int. rep. no. 2866.

Al-Jiburi, H.K.S., (2004b) Hydrogeological and hydrochemical study of Al-Qaiyara Quadrangle, sheet NI-38-1, scale 1: 250 000. GEOSURV, int. rep. no. 2877.

Bagyaraj, M., Ramkumar, T., Venkatramanan, S., & Gurugnanam, B. (2013). Application of remote sensing and GIS analysis for identifying groundwater potential zone in parts of Kodaikanal Taluk, South India. *Frontiers of Earth Science*, *7*(1), 65-75.Bhowmick, Prasenjit, S. Mukhopadhyay, and V. Sivakumar. 2014. "A Review on GIS Based Fuzzy and Boolean Logic Modelling Approach to Identify the Suitable Sites for Artificial Recharge of Groundwater." *Scholars Journal of Engineering and Technology* 2: 316–19.

Chenini, I., Mammou, A. B., & El May, M. (2010). Groundwater recharge zone mapping using GIS-based multi-criteria analysis: a case study in Central Tunisia (Maknassy Basin). *Water resources management*, *24*(5), 921-939.

Das, S., & Pardeshi, S. D. (2018). Integration of different influencing factors in GIS to delineate groundwater potential areas using IF and FR techniques: a study of Pravara basin, Maharashtra, India. *Applied Water Science*, *8*(7), 197.

Dar, M. A., Sankar, K., & Dar, I. A. (2010). Groundwater prospects evaluation-based on hydrogeomorphological mapping: a case study in Kancheepuram district, Tamil Nadu. Journal of the Indian Society of Remote Sensing, 38(2), 333-343.

Devi, P. S., Srinivasulu, S., & Raju, K. K. (2001). Hydrogeomorphological and groundwater prospects of the Pageru river basin by using remote sensing data. Environmental Geology, 40(9), 1088-1094.

Gale, I. (Ed.). (2005). *Strategies for Managed Aquifer Recharge (MAR) in semi-arid areas*. UNESCO.

Koch, M., & Mather, P. M. (1997). Lineament mapping for groundwater resource assessment: a comparison of digital Synthetic Aperture Radar (SAR) imagery and stereoscopic Large Format Camera (LFC) photographs in the Red Sea Hills, Sudan. International Journal of Remote Sensing, 18(7), 1465-1482.

Salgarello, M., Visconti, G., & Barone-Adesi, L. (2013). Interlocking circumareolar suture with undyed polyamide thread: a personal experience. *Aesthetic plastic surgery*, *37*(5), 1061-1062.

Ghazavi, R., Babaei, S., & Erfanian, M. (2018). Recharge wells site selection for artificial groundwater recharge in an urban area using fuzzy logic technique. *Water Resources Management*, *32*(12), 3821-3834.

Jasrotia, A. S., Majhi, A., & Singh, S. (2009). Water balance approach for rainwater harvesting using remote sensing and GIS techniques, Jammu Himalaya, India. *Water resources management*, *23*(14), 3035-3055.

Machiwal, D., Jha, M. K., & Mal, B. C. (2011). Assessment of groundwater potential in a semi-arid region of India using remote sensing, GIS and MCDM techniques. *Water resources management*, *25*(5), 1359-1386.

Ma, L., & Spalding, R. F. (1997). EFFECTS OF ARTIFICIAL RECHARGE ON GROUND WATER QUALITY AND AQUIFER STORAGE RECOVERY 1. *JAWRA Journal of the American Water Resources Association*, *33*(3), 561-572.

Ma, X., Feng, Q., Su, Y., Yu, T., & Deo, R. C. (2018). Characteristics of ecosystem water use efficiency in a desert riparian forest. *Environmental Earth Sciences*, *77*(10), 358.

Mahmood, A. (1996). Lineaments as groundwater exploration guides in hard-rock terranes of arid regions. Canadian journal of remote sensing, 22(1), 108-116.

Mockus, V., Werner, J., Woodward, D. E., Nielsen, R., Dobos, R., Hjelmfelt, A., & CC, H. (2009). Part 630 Hydrology National Engineering Handbook: Chapter 7: Hydrologic soil groups. *US Department of Agriculture: Natural Resources Conservation Service*.

Nachtergaele, F., van Velthuizen, H., Verelst, L., Batjes, N. H., Dijkshoorn, K., van Engelen, V. W. P., ... & Montanarela, L. (2010). The harmonized world soil database. In *Proceedings of the 19th World Congress of Soil Science, Soil Solutions for a Changing World, Brisbane, Australia, 1-6 August 2010* (pp. 34-37).

Nachtergaele, Freddy, Harrij van Velthuizen, Luc Verelst, Niels Batjes, Koos Dijkshoorn, Vincent van Engelen, Guenther Fischer, et al. (2009). "Harmonized World Soil Database." *ISRIC: Wageningen, The Netherlands*. https://library.wur.nl/WebQuery/file/isric/fulltext/isricu_t4bb310b7_001.pdf.

Nag, S. K. (2005). Application of lineament density and hydrogeomorphology to delineate groundwater potential zones of Baghmundi block in Purulia district, West Bengal. Journal of the Indian Society of Remote Sensing, 33(4), 521.

Russo, T. A., Fisher, A. T., & Lockwood, B. S. (2015). Assessment of managed aquifer recharge site suitability using a GIS and modeling. *Groundwater*, *53*(3), 389-400.

Saraf, A. K., & Choudhury, P. R. (1998). Integrated remote sensing and GIS for groundwater exploration and identification of artificial recharge sites. *International journal of Remote sensing*, *19*(10), 1825-1841.

Sueed, M. Grote, K. (2020): I. Evaluation of The Accuracy of Different Satellite-Based Estimates of Precipitation in A Semi-Arid Climate. Manuscript submitted for publication.

Selvarani, A. G., Maheswaran, G., & Elangovan, K. (2017). Identification of artificial recharge sites for Noyyal River Basin using GIS and remote sensing. *Journal of the Indian Society of Remote Sensing*, *45*(1), 67-77.

Teixeira, J., Chaminé, H. I., Carvalho, J. M., Pérez-Alberti, A., & Rocha, F. (2013). Hydrogeomorphological mapping as a tool in groundwater exploration. Journal of Maps, 9(2), 263-273.

Tiwari, A. K., Lavy, M., Amanzio, G., De Maio, M., Singh, P. K., & Mahato, M. K. (2017). Identification of artificial groundwater recharging zone using a GIS-based fuzzy logic approach: a case study in a coal mine area of the Damodar Valley, India. *Applied Water Science*, *7*(8), 4513-4524.

Xu, Y., Titus, R., Holness, S. D., Zhang, J., & Van Tonder, G. J. (2002). A hydrogeomorphological approach to quantification of groundwater discharge to streams in South Africa. Water SA, 28(4), 375-380.

SECTION

2. CONCLUSIONS AND RECOMMENDATIONS

2.1. CONCLUSIONS

The main goal of this study is to make water management studies possible in a region where there is lack of ground hydrological measurements, by using remote sensing integrated with computer modeling. The following is a summary of research findings:

1. Satellite-based rainfall estimates are a powerful tool, due to the spatial and temporal coverage, as well as the time and cost efficiency. However, there is an uncertainty corresponding with such data. The size of data validation varies depending on which application the data uses.
2. Satellite-based rainfall estimates show more uncertainty daily, and an increase in accuracy on a monthly basis, due to the under-forecasting events neutralize the over-forecasting events which results in decreases of the error magnitude. Accordingly, using satellite-based rainfall estimates to obtain hydrological data in the long run (e.g. annual watershed discharge) is more reliable.
3. SWAT model has the capability to obtain hydrological parameters of a watershed in high accuracy. In addition, the model is open source, and has a support community which makes this model suitable for use worldwide.
4. Overlying methods of hydrological thematic layers through integrating ground and satellite data in GIS environment, is a very important method to target protentional hydrological features efficiently.

5. Overall, the water management strategy is possible in arid and semi-arid regions by using remote sensing data, and by understanding the hydrological conditions of the watershed to be able to set up the computer model properly.

2.2. RECOMMENDATIONS

Satellite-based methods integrated with computer models and GIS software have been applied to substitute the ground-based hydrological measurements in the purpose of water management. Several ideas and recommendations were discovered during the research journey, which include:

- Further studying to generate a high-resolution global map of uncertainty probability for satellite-based precipitation estimates.
- Accuracy analysis and performance enhancement of hydrological satellite-based data such as: relative soil moisture, groundwater table level through GRACE satellite, and surface water altimetry data. In addition, extracting high resolution surface water boundaries to be correlated with groundwater table variations.
- Prepare SWAT model inputs globally to have more consistent results by researchers, as well as to maximize the model performance.

REFERENCES

Wheater, H. S., Mathias, S. A., & Li, X. (2010). Groundwater Modelling in Arid and Semi-Arid Areas. Cambridge University Press.

Ribot, J. C., Magalhães, A. R., & Panagides, S. (2005). Climate Variability, Climate Change and Social Vulnerability in the Semi-arid Tropics. Cambridge University Press.

Wheater, H., Sorooshian, S., & Sharma, K. D. (2007). Hydrological Modelling in Arid and Semi-Arid Areas. Cambridge University Press.

Kavetski, D., Kuczera, G., & Franks, S. W. (2006). Bayesian analysis of input uncertainty in hydrological modeling: 1. Theory. Water Resources Research. https://doi.org/10.1029/2005wr004368

Tang, Q., Gao, H., Lu, H., & Lettenmaier, D. P. (2009). Remote sensing: hydrology. Progress in Physical Geography: Earth and Environment, 33(4), 490–509.

Schmugge, T. J., Kustas, W. P., Ritchie, J. C., Jackson, T. J., & Rango, A. (2002). Remote sensing in hydrology. Advances in Water Resources, 25(8), 1367–1385.

Pietroniro, A., & Prowse, T. D. (n.d.). Applications of remote sensing in hydrology. Hydrological Processes, 16(6), 1537–1541.

Tian, Y., Peters-Lidard, C. D., & Eylander, J. B. (2010). Real-Time Bias Reduction for Satellite-Based Precipitation Estimates. *Journal of Hydrometeorology*, *11*(6), 1275–1285.

Bellerby, T. J., & Sun, J. (2005). Probabilistic and Ensemble Representations of the Uncertainty in an IR/Microwave Satellite Precipitation Product. *Journal of Hydrometeorology*, *6*(6), 1032–1044.

Turk, F. J., Arkin, P., Ebert, E. E., & Sapiano, M. R. P. (2008). EVALUATING HIGH-RESOLUTION PRECIPITATION PRODUCTS. *Bulletin of the American Meteorological Society*, *89*(12), 1911–1916.

Ebert, E. E., Janowiak, J. E., & Kidd, C. (2007). Comparison of Near-Real-Time Precipitation Estimates from Satellite Observations and Numerical Models. *Bulletin of the American Meteorological Society*, *88*(1), 47–64.

Bharti, V., & Singh, C. (2015). Evaluation of error in TRMM 3B42V7 precipitation estimates over the Himalayan region. *Journal of Geophysical Research, D: Atmospheres*, *120*(24), 12458–12473.

Näschen, K., Diekkrüger, B., Leemhuis, C., Steinbach, S., Seregina, L. S., Thonfeld, F., & Van der Linden, R. (2018). Hydrological Modeling in Data-Scarce Catchments: The Kilombero Floodplain in Tanzania. WATER, 10(5), 599.

Suliman, A. H., Jajarmizadeh, M., Harun, S., & Darus, I. Z. M. (2015). Comparison of Semi-Distributed, GIS-Based Hydrological Models for the Prediction of Streamflow in a Large Catchment. Water Resources Management, 29(9), 3095–3110.

Wagner, P. D., Kumar, S., & Schneider, K. (2013). An assessment of land use change impacts on the water resources of the Mula and Mutha Rivers catchment upstream of Pune, India. Hydrology and Earth System Sciences Discussions. https://doi.org/10.5194/hessd-10-1943-2013

Srinivasan, R., Zhang, X., & Arnold, J. (2010). SWAT ungauged: hydrological budget and crop yield predictions in the Upper Mississippi River Basin. Transactions of the ASABE, 53(5), 1533–1546.

Noori, N., & Kalin, L. (2016). Coupling SWAT and ANN models for enhanced daily streamflow prediction. Journal of Hydrology, 533, 141–151.

Rafiei Emam, A., Kappas, M., Linh, N. H. K., & Renchin, T. (2017). Hydrological Modeling and Runoff Mitigation in an Ungauged Basin of Central Vietnam Using SWAT Model. Hydrology, 4(1), 16.

Gale, I. (Ed.). (2005). *Strategies for Managed Aquifer Recharge (MAR) in semi-arid areas*. UNESCO.

Das, S., & Pardeshi, S. D. (2018). Integration of different influencing factors in GIS to delineate groundwater potential areas using IF and FR techniques: a study of Pravara basin, Maharashtra, India. *Applied Water Science*, *8*(7), 197.

Russo, T. A., Fisher, A. T., & Lockwood, B. S. (2015). Assessment of managed aquifer recharge site suitability using a GIS and modeling. *Groundwater*, *53*(3), 389-400.

Ma, L., & Spalding, R. F. (1997). EFFECTS OF ARTIFICIAL RECHARGE ON GROUND WATER QUALITY AND AQUIFER STORAGE RECOVERY 1. *JAWRA Journal of the American Water Resources Association*, *33*(3), 561-572.

Ahmadi, M. M., Mahdavirad, H., & Bakhtiari, B. (2017). Multi-criteria analysis of site selection for groundwater recharge with treated municipal wastewater. *Water Science and Technology*, *76*(4), 909-919.

Saraf, A. K., & Choudhury, P. R. (1998). Integrated remote sensing and GIS for groundwater exploration and identification of artificial recharge sites. *International journal of Remote sensing*, *19*(10), 1825-1841.

Adler, R. F., Huffman, G. J., Chang, A., Ferraro, R., Xie, P., & Janowiak, J. (2003). RudoLF, b. *SCHnEIdER, u., CuRTIS, S., boLvIn, d., GRubER, A., SuSSkInd, J. y ARkIn, P*, 1147-1167.

Ebert, E. E. (2005). Satellite vs. model rainfall—Which one to use. *Fifth Int. Scientific Conf. on the Global Energy and Water Cycle*.

Hong, Y., Alder, R. F., Hossain, F., Curtis, S., & Huffman, G. J. (2007). Estimate gridded and time variant runoff curve numbers using satelliteremote sensing and geospatial data. Water Resources Research, 43, 285–294.

Artan, G., Gadain, H., Smith, J. L., Asante, K., Bandaragoda, C. J., & Verdin, J. P. (2007). Adequacy of satellite derived rainfall data for stream flow modeling. *Natural Hazards*, *43*(2), 167–185.

Sawunyama, T., & Hughes, D. A. (2008). Application of satellite-derived rainfall estimates to extend water resource simulation modelling in South Africa. *Water SA*, *34*(1), 1–10.

Stisen, S., & Sandholt, I. (2010). Evaluation of remote-sensing-based rainfall products through predictive capability in hydrological runoff modelling. *Hydrological Processes: An International Journal*, *24*(7), 879–891.

Behrangi, A., Khakbaz, B., Jaw, T. C., AghaKouchak, A., Hsu, K., & Sorooshian, S. (2011). Hydrologic evaluation of satellite precipitation products over a mid-size basin. *Journal of Hydrology*, *397*(3), 225–237.

Sharifi, E., Steinacker, R., & Saghafian, B. (2016). Assessment of GPM-IMERG and Other Precipitation Products against Gauge Data under Different Topographic and Climatic Conditions in Iran: Preliminary Results. *Remote Sensing*, *8*(2), 135.

Tian, Y., Peters-Lidard, C. D., & Eylander, J. B. (2010). Real-Time Bias Reduction for Satellite-Based Precipitation Estimates. *Journal of Hydrometeorology*, *11*(6), 1275–1285.

Devia, G. K., Ganasri, B. P., & Dwarakish, G. S. (2015). A Review on Hydrological Models. Aquatic Procedia, 4, 1001–1007.

Nyeko, M. (2015). Hydrologic Modelling of Data Scarce Basin with SWAT Model: Capabilities and Limitations. Water Resources Management. https://doi.org/10.1007/s11269-014-0828-3

Ebert, E. E., Janowiak, J. E., & Kidd, C. (2007). Comparison of Near-Real-Time Precipitation Estimates from Satellite Observations and Numerical Models. *Bulletin of the American Meteorological Society*, *88*(1), 47–64.

AghaKouchak, A., Mehran, A., Norouzi, H., & Behrangi, A. (2012). Systematic and random error components in satellite precipitation data sets. *Geophysical Research Letters*, *39*(9). https://doi.org/10.1029/2012GL051592

Habib, E., Haile, A. T., Tian, Y., & Joyce, R. J. (2012). Evaluation of the high-resolution CMORPH satellite rainfall product using dense rain gauge observations and radar-based estimates. *Journal of Hydrometeorology*, *13*(6), 1784-1798.

VITA

Majid S. Mohamod was born in Tikrit, Iraq. After completing high school in Tikrit school for the distinguished, in 2005, he entered Tikrit University. He received his bachelor's degree in Geology in 2009, and his master's degree in Geological Engineering in 2013. In 2013, Majid was granted a scholarship from the Ministry of Higher Education and Scientific Research to study PhD at Missouri University of Science and Technology. His main research interests were water management and satellite hydrology. The main goal of his PhD research was to overcome the hydrological measurement shortage issues in arid and semi-arid regions. He received his PhD degree in Geological Engineering from Missouri University of Science and Technology in December 2020.